Aravind Medical Research Foundation

Aravind Medical Research Foundation is recognized as
Scientific and Industrial Research Organization (SIRO) by
the Department of Scientific and Industrial Research (DSIR),
Government of India

Much has been done, but much remains to be done… we look to the future with renewed strength to continue the mission of providing quality eye care and hope that some of what we have learned will be useful to other eye care workers around the world.

G. Venkataswamy

MISSION

To eliminate needless blindness by providing evidence through research and evolving methods to translate existing evidence and knowledge into effective action.

RESEARCH IN OPHTHALMIC SCIENCES

Dr. G. Venkataswamy Eye Research Institute

Annual Report 2017 - 2018

ARAVIND MEDICAL RESEARCH FOUNDATION

BOARD OF MANAGEMENT

Dr. P. Namperumalsamy, MS, FAMS

Dr. G. Natchiar, MS, DO

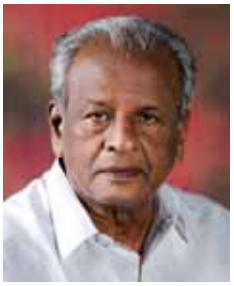

Er. G. Srinivasan, BE, MS

Mr. R.D. Thulasiraj, MBA

Dr. S.R. Krishnadas, DO., DNB

Dr. R. Kim, DO., DNB

Dr.N.Venkatesh Prajna DO., DNB., FRCophth

Dr. S. Aravind, MS, MBA

CLINICIAN-SCIENTISTS

Dr. P. Vijayalakshmi, MS
Professor of Paediatric Ophthalmology

Dr. S.R. Krishnadas, DO., DNB
Professor of Ophthalmology

Dr. SR. Rathinam, MNAMS, PH.D
Professor of Ophthalmology & HOD - Uvea Services

Dr. Haripriya Aravind, MS
HOD - IOL & Cataract Services

Dr. R. Kim, DO., DNB
Professor of Ophthalmology & Chief Medical Officer

Dr. N. Venkatesh Prajna DO., DNB., FRCophth
Professor of Ophthalmology & HOD - Cornea Services

Dr. Usha Kim, DO, DNB
Professor of Ophthalmology & HOD - Orbit, Oculoplasty & Ocular Oncology Services

Dr. Lalitha Prajna, MD., DNB
HOD - Microbiology

Dr. R. Santhi, MD (Pathology)
Pathologist

Dr. R. Sharmila, DNB
Medical Consultant
Glaucoma Services

ARAVIND MEDICAL RESEARCH FOUNDATION

FACULTY

PROF. K. DHARMALINGAM
Director - Research

PROF. VR. MUTHUKKARUPPAN
Advisor-Research

DR. P. SUNDARESAN
Senior Scientist
Molecular Genetics

DR. C. GOWRI PRIYA
Scientist, Immunology &
Stem Cell Biology

DR. S. SENTHILKUMARI
Scientist, Ocular Pharmacology

DR. A. VANNIARAJAN
Scientist, Molecular Genetics

DR. J. JEYA MAHESHWARI
Scientist, Proteomics

DR. D. BHARANIDHARAN
Scientist, Bioinformatics

DR.O.G.RAMPRASAD
Scientist, Proteomics

RESEARCH ADVISORY COMMITTEE

Chairman

Dr. P. Namperumalsamy
Chairman – Emeritus
Aravind Eye Care System
1, Anna Nagar, Madurai - 625020

Member-Secretary

Prof. K. Dharmalingam
Director - Research
Aravind Medical Research Foundation
1, Anna Nagar, Madurai - 625020

Members

Prof. VR. Muthukkaruppan
Advisor-Research
Aravind Medical Research Foundation
1, Anna Nagar, Madurai - 625020

Prof. S. Murty Srinivasula
Professor , School of Biology
Indian Institute of Science Education and Research,
Thiruvananthapuram,
CET Campus, Engineering College P.O.
Thiruvananthapuram – 695016, Kerala

Dr. Ch. Mohan Rao
Director
Centre for Cellular & Molecular Biology, Uppal Road,
Hyderabad - 500007

Prof. Anuranjan Anand
Faculty
Human Genetic lab
Jawaharlal Nehru Centre for Advanced Scientific Research
Jakkur, Bangalore - 560064

Prof. S.Karuthapandian
Professor & Head
Department of Biotechnology
Alagappa University
Karaikudi

Dr. R. Kim
Chief Medical Officer
Aravind Eye Hospital
No.1, Anna Nagar, Madurai - 625020

Dr. N. Venkatesh Prajna
Chief - Medical Education
Aravind Eye Care System
1, Anna Nagar, Madurai - 625020

INSTITUTIONAL ETHICS COMMITTEE (IEC)

Chairman

Prof. R. Venkataratnam m.a., ph.d
Senior Prof.of Sociology (Retired)
Madurai Kamaraj University, Madurai

Member-Secretary

Dr. R. Sharmila, dnb
Medical Officer, Glaucoma Clinic
Aravind Eye Hospital, Madurai

Members

Dr. C. Srinivasan m.sc.,ph.d
UGC Emeritus Professor
New No. 2/249 (Old No 2/172)
7th Street, Kalvinagar, Rajambadi, Madurai - 625021

Dr. T.S. Chandrasekaran ms, do
Ophthalmologist,
No.6, N.M.R.Subbaraman Road,
Chokkikulam North, Madurai

Mr. M. Senthilkumar m.a., b.l
Advocate
Plot No.32, Sindanayalar Nagar
Senthamil Nagar, Karuppayoorani East, Madurai

Mr. R. Raja Govindasamy m.a., m.a (usa)
Former Principal, Thiagarajar College
169-1, 2nd Cross Street, I Main Road, Gomathipuram,
Madurai - 625020

Dr. S. Sabhesan dpm, mnams, ph.d
Consultant – Psychiatrist, Apollo Specialty Hospitals
Lake view Road, K.K.Nagar, Madurai

Dr. A. Amirtha Mekhala bds, mph, mfdsrcps
Private Practice - Dental Services
208 Karpaga Nagar 8th Street, K.Pudur, Madurai - 625007

Mrs. Premalatha Panneerselvam m.a., m.ed
Secretary
Mahatma Montessori Matriculation Hr.Sec.School
Madurai

Dr.J.R.Vijayalakshmi md (Pharmacology)
Professor of Pharmacology
CSI college of Dental Sciences, Madurai

Mr. ARM. Ganesh b.com., llb
Advocate
D-3/4, First Cross Street
K.K.Nagar west, Madurai - 625020

Dr. Lalitha Prajna dnb
Chief - Microbiology
Aravind Eye Hospital, Madurai - 625020

CONTENTS

FOREWORD

Research programmes at Aravind Medical Research Foundation, the research arm of Aravind Eye Care System, continue to do well this year as well. Basic objective of Aravind Eye Care System is delivering affordable health care to the needy people. The objective of the research arm is to explore ways and means to deal with eye diseases of importance to India.

AECS is the major supporter of our research efforts and their help has allowed us to explore newer areas of research. This year, one of our well-wishers, Shri Dilip Sanghvi of Sun Pharma has funded the purchase of a multi- channel laser scanner (Typhoon Scanner, GE Health Care) to do quantitative proteomics. This addition will go a long way in helping the research efforts of the proteomics community at AMRF. DBT, Government of India continues to be our major supporter of research programmes. Our Ph.D students have done well after their training at AMRF and many have gone abroad for further studies.

AMRF is doing its best in basic research, and this year a new Indo-UK program funded by the government of United Kingdom will allow us to validate a predictive biomarker panel for Diabetic Retinopathy. In order to achieve excellence in all these areas we are now looking for new faculty who will be joining us in this venture.

Dr. P. Namperumalsamy
President, AMRF

INTRODUCTION

Investigations focusing on the ocular surface have resulted in discoveries which are shifting the paradigms of ocular immunology. The role of ocular surface microbiome in health and disease has been proven some time ago. Surprisingly perturbation of gut microbiome has been shown to affect the ocular surface health. This Gut-Eye axis is lot more complex since the immune effector cells differentiated in the gut can reach the retinal layer and initiate immune response. Demonstration of the core microbiome in the paucibacillary ocular surface microbiota is another landmark. The persistence of commensals residing in the ocular surface, in spite of the presence of antimicrobial defense mechanisms such as antimicrobial peptides, mucins, neutrophil NETs, indicate the importance of the commensals in shaping immune response. Another emerging paradigm in these studies is the novel role of gamma-delta T-cells in initiating IL-17 dependent T- cell response and the role of toll like receptors in suppressing inflammation upon engagement with bacterial pathogen associated molecular patterns (PAMP) in epithelial cells and B and T cells. This clarifies the long-standing issue of how the commensals fail to induce inflammatory response even though they carry the same PAMPs.

Proteome changes in time and space, a holy grail of proteomics community, is being addressed using a set of experimental approaches called cell-selective proteomics of complex biological systems. These approaches will undoubtedly be a hot topic for immediate future research since global proteomic analysis is of limited value in heterogeneous environment.

With emerging paradigms challenging the long-held concepts in science, much more needs to be done to understand the dynamics involved in the physiology and pathology of the eye.

Efforts at AMRF continue with emphasis on translational research that would enable early screening, diagnosis and prognosis of eye diseases such as Retinoblastoma and Diabetic Retinopathy. An equal emphasis is placed on understanding the disease pathogenesis as in fungal keratitis and the more complex Glaucoma. A comprehensive approach is currently employed at AMRF involving collaborations within and outside the Institute to understand the pathogenesis as well as to address the challenges in managing priority eye diseases, particularly Glaucoma and Diabetic Retinopathy.

Prof. K. Dharmalingam
Director - Research

MOLECULAR GENETICS

The Department of Molecular genetics has been working on various eye diseases and performed targeted and whole exome sequencing to identify candidate genes in two large South Indian families with primary open angle glaucoma (POAG). Based on the data, panel of genetic variations were proposed which may be the candidate genes for these two families and will be functionally characterized to prove their involvement in disease pathogenesis. The team previously reported significant association of rs1015213 *(PCMTD1-ST18)* in primary angle closure glaucoma (PACG) subjects from South India. The current study also found siginficant association of this marker rs1015213 (P=0.05) in primary angle closure suspects (PACS), suggesting that this locus may confer susceptibility to a narrow angle configuration.

The team also established the localization of sulfated keratan sulfate in corneal tissue of macular corneal dystrophy (MCD) patients through histochemistry analysis which demonstrated the type II MCD as a predominant phenotype in Indian population, followed by MCD type I and IA. In addition, five genome-wide significant exfoliation syndrome (XFS)-associated loci [13q12 (*FLT1-POMP*), 11q23.3 (*TMEM136*), 6p21 (*AGPAT1*), 3p24 (*RBMS3*) and 5q23 (*SEMA6A*)] were identified which shows the association of new biological pathways for disease pathogenesis. Moreover, the differential *LOXL1-AS1* expression profile on XFS patients was observed and the prolonged induction of oxidative stress at higher concentration of H_2O_2 over B-3 human lens epithelial cells resulted with decreased expression of *LOXL1-AS1*. This suggests the involvement of the cellular stressors as one of the risk factors for the formation of exfoliation syndrome.

Whole exome sequencing approach to identify a novel candidate gene in two South Indian families with Primary Open Angle Glaucoma

Investigators : Dr. P. Sundaresan, Dr. S.R. Krishnadas, Dr. Mohideen, Dr. Ramakrishnan and Dr. D. Bharanidharan
Ph.D Scholar : Mohd Hussain Shah
Funding Agency : Indian Council of Medical Research, New Delhi

Introduction

Glaucoma is a complex disease and genetically heterogeneous; it may either caused by the combined action of many genes or caused by mutations in a single gene. Several genetic regions or loci have been reported to be associated with POAG. But only three candidate genes were reported to be as candidate genes (MYOC, OPTN and TBK1) and these candidate genes were identified through large pedigrees with positive family history that have autosomal dominant inheritance of POAG. However, mutations in these known candidate genes are responsible for small fractions of POAG cases. Therefore, the chances of identifying a candidate

gene are more in families with positive family history of POAG. Hence, additional candidate genes involved in the development of POAG are still needed to be identified through strong positive family history of POAG, which will improve our understanding towards the pathophysiological mechanism of the disease, accuracy of diagnosis and treatment regimen. In the current study, two families were recruited a single large four generation South Indian family from Kayalpattinam (KPGF) and another from Devakottai (DKF) Tamilnadu, India. 240 members from KPGF and 51 from DKF participated in this study. Based on the relationship with the proband, 20 samples have been chosen from these two South Indian families. 16 samples from the large KPGF family (9 POAG and 8 controls) and 3 samples (2 POAG and one control) from DKF family including one control outside the family for whole exome sequencing to identify a novel candidate genes associated with these two South Indian families.

Results & Conclusion

The whole exome sequencing analysis yielded an average of 62 thousands variants from each sample. After stringent filtrating by using several bioinformatics approaches, an average of 40 casual variants were identified in samples. Based on the presence of casual variants in cases, and following segregation with the phenotype, the team came up with several variants, among them, three novel heterozygous variants in three genes in KPGF (ARHGEF-40, CEP152 & FOXN2) and one gene (SOX6) in DKF family were given top priority to further validate by Sanger sequencing based on the literature survey, segregation pattern and the same variations were identified in most of the POAG cases. Based on the data of 20 samples, panels of genetic variations were proposed for these two South Indian families. The team is in the process of screening these novel sequence variations in the entire family members of KPGF and DKF family members by Sanger sequencing to identify the gene that is responsible for POAG in these two families and will be functionally characterized to prove their involvement in disease pathogenesis.

Validating the association of the newly identified PACG risk variants in South Indian Primary Angle Closure Suspects (PACS)

Investigators : Dr. P. Sundaresan, Dr. Rengaraj Venkatesh, Dr. Srinivasan Kavitha, Dr. S.R. Krishnadas, Mr. Saravanan Vijayan
Collaborators : Dr. Chiea Chuen Khor, Dr. Tin Aung, Dr. Monisha Nongpiur, Dr. Tina Wong, Dr. Eranga Vithana
PhD Scholar : Roopam Duvesh
Funding Agency : Aravind Eye Care System

Introduction

Primary angle closure glaucoma (PACG) is a heterogeneous disorder, results from an appositional contact between peripheral iris & trabecular meshwork, making drainage angle occluded. This hinders the aqueous outflow which leads to an increase in intra ocular pressure (IOP) and thus damage to the optic nerve. It is less common than primary open angle glaucoma (POAG), though it accounts for nearly 50% of glaucoma-related blindness, especially in Asians. PACG is a complex disease with several genetic, environmental, anatomical and physiological factors involved in its pathogenesis.

The group investigates the genetic basis of PACG in South Indian patients by screening single nucleotide polymorphism (SNP) markers: rs11024102 at *PLEKHA7*, rs3753841 at *COL11A1* and rs1015213 located between *PCMTD1* and *ST18* genes, rs3816415 at EPDR1, rs1258267 at CHAT, rs736893 at GLIS3, rs7494379 at *FERMT2*, and rs3739821 mapping in between *DPM2* and FAM102A in South Indian PACG subjects for their genetic association. Among these markers studied, rs1015213 (PCMTD1-ST18; p=9.17E-05) showed significant association in South Indian subjects with PACG further replicates the previous reports (Duvesh *et al*, Invest Ophthalmol Vis Sci. 2013; Khor *et al*, Nat Genet. 2016). Furthermore, the study was also interested to validate these SNPs in primary angle closure suspects (PACS), which is an earlier stage of angle closure disease spectrum. Therefore, in collaboration with Singapore Eye Research Institute (SERI) these PACG associated SNPs were screened in South India and Chinese subjects with PACS.

Results

A total of 1397 PACS patients and 943 controls of Chinese ethnicity from Singapore and 604 PACS patients and 287 controls of South Indian ethnicity were included in this study. For genotyping, TaqMan allelic discrimination assay was performed to access the SNPs. The study observed a significant association of rs1015213 (*PCMTD1-ST18*; P=0.05) in the South Indian PACS subjects. Moreover, meta-analysis across both the ethnicities showed significant evidence of association for *PCMTD1-ST18* (OR, 1.55; 95% CI, 1.18-2.04; P = 0.002).

The association of the PACG loci with PACS status suggests that the locus may confer susceptibility to a narrow angle configuration. Further research is needed to characterize the genetic variants involved in disease progression from PACS to PACG.

Histochemical analysis of Macular Corneal Dystrophy patients with CHST6 gene mutations

Investigators : Dr. P. Sundaresan, Dr. N.V. Prajna, Dr. V. Lumbini
Ph.D Scholar : M. Durga
Funding Agency : Aravind Eye Care System, DST-INSPIRE.

Introduction

Macular Corneal Dystrophy (MCD) is an autosomal recessive inherited disorder caused by mutations in the CHST6 gene (carbohydrate sulfotransferase-6). It is responsible for encoding the enzyme corneal N-acetyl glucosamine-6-O sulfotransferase(C-GlcNAc-6-ST) which is essential for the sulfation of keratan sulfate. MCD is subdivided into three immunophenotypes, MCD types I, IA and II, based on the reactivity of serum and corneal tissue to an antibody that recognises sulfated keratan sulfate (KS). Histologically, the cornea in MCD is characterized by the accumulation of extracellular deposits (unsulfated keratan sulfate) in the stroma and Descemet membrane as well as by intracellular storage of similar material in the keratocytes and corneal endothelium. Alcian blue is a specific stain for sulfated and carboxylated acid mucopolysaccharide which stains the sulfated keratan sulfate. MCD is most prevalent in Iceland followed by Japan, India and Saudi Arabia. Unlike the western world, Macular Corneal Dystrophy is the most common corneal stromal dystrophy in India. The disease is highly prevalent in South Indian population as reported; it could be due to high frequency of consanguineous marriages. There is a limited study from the Indian population with regard to MCD genetics and pathogenesis. Therefore, this study was undertaken to determine the immunophenotypes of macular corneal dystrophy in Indian patients and to correlate them with mutations in the CHST6 gene. Genomic DNA was extracted from 46 patients (37 families) with MCD, 13 unaffected relatives and 50 healthy volunteers without any corneal dystrophies. In addition, 20 corneal buttons were collected from 20 MCD patients during penetrating keratoplasty (PKP) for histopathological examination. The coding region of *CHST6* was amplified by polymerase chain reaction (PCR) and sequenced by Sanger sequencing method. Cross-sections of the 10% formalin fixed, paraffin embedded corneal buttons from MCD as well as normal corneal buttons were stained with Alcian blue, hematoxylin and eosin (H&E) for detecting the sulfated keratan sulfate level.

Results

In this study, 12 different mutations were identified in 37 families, of these 2 mutations are novel and 10 mutations are reported in different ethnic populations. The novel mutations are: homozygous missense mutation (L129V), heterozygous deletion mutation

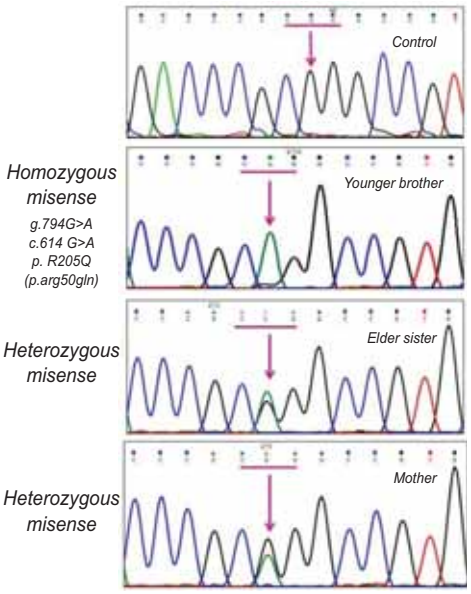

Figure: 1Shows the presence of missense mutation in MCD family 4.

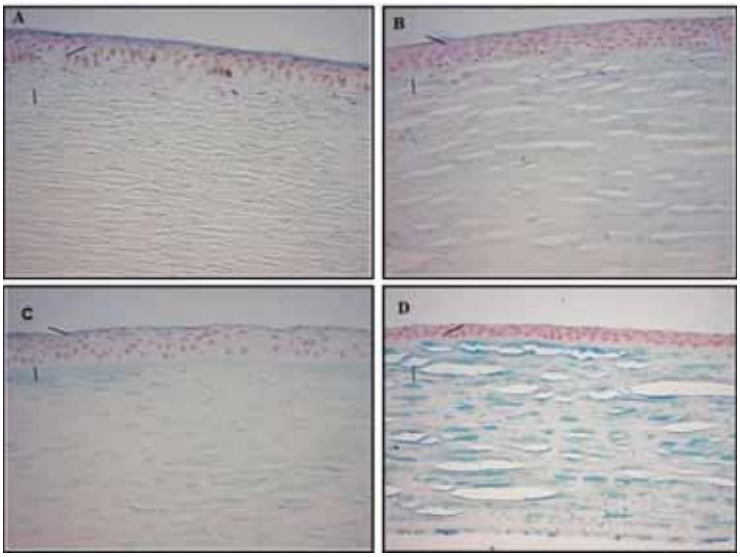

Figure: 2 Light microscopic images of representative corneas shows different immunophenotypes of MCD. (stained with Alcian blue and counterstained with Nuclear fast red). A: Cadaver cornea. B: A cornea with the absence of detectable sulfated keratan sulfate shows MCD type I (40X). C: A cornea shows with reactivity to sulfated keratan sulfate only in stromal keratocytes MCD type IA (40X). D: A cornea shows sulfated keratan sulfate detected throughout the stroma MCD type II (40X).

(L101FfsX3). Furthermore, the present study detected the absence of sulfated keratan sulfate (no Alcian blue staining) throughout the cornea in type I MCD patient (family 2) having a single homozygous missense mutation (S53L). In patients presented with type IA MCD, the team observed a low level of sulfated keratan sulfate (low Alcian blue staining) only in stromal keratocytes. This phenotype was identified in 2 patients, with a homozygous missense mutation (R205Q) present in family 4 and a homozygous deletion (Q182RfsX198) in family 8. Normal or slightly reduced sulfated keratan sulfate levels (normal Alcian blue staining) were present in the corneal stroma, keratocytes, Descemet's membrane, and endothelial cells in type II MCD patients. This type II MCD was identified in 7 patients from 7 different families (1,3,5,6,7,9,10) which was associated with the negative mutations, homozygous missense mutations (R50C, R93H), heterozygous deletion mutations (Q182RfsX198), insertion deletion mutations (p.N194_R196delinsRC). However, there was no coding region mutation was observed in 4 patients from 4 families. In this report, 2 novel mutations were identified which will add up to the list of already known mutations so far in different ethnic populations. There might be some other gene involved in those cases, which are negative for *CHST6* mutation suggesting genetic heterogeneity. Our study showed MCD type II as a predominant phenotype in the Indian population, followed by MCD type I and IA. Further immunohistochemical studies and ELISA will be performed to confirm the immunophenotypes of MCD patients.

Molecular genetics of ABCA4 gene in Stargardt disease

Investigators : Dr. P. Sundaresan, Dr. Pankaja Dhoble, Dr. KC. Lavanya
Ph.D. Scholar : R. Kadarkarai Raj
Funding Agency : Aravind Medical Research Foundation

Introduction

Stargardt disease (STGD, MIM #248200) is an autosomal recessive disease and highly heterogeneous both clinically and genetically. The prevalence rate of this disease is 1 in 10,000 globally. The onset of this disease is generally in 1-2 decades of life and less frequently in adulthood. The clinical characteristics of this disease are as follows; bilateral central visual loss, macular atrophy and yellow-white flecks at the level of the retinal pigment epithelium (RPE) at the posterior pole. Previous studies have reported the involvement of ABCA4 mutations and polymorphisms in Stargardt macular dystrophy and retina related dystrophies like age-related macular degeneration, retinitis pigmentosa, cone-rod dystrophy. ABCA4 is composed of 50 exons located in chromosome 1p13; which involved in the transport and clearance of all-transretinal aldehyde in visual cycle and it's belongs to ATP-binding cassette (ABC) transporter family. It consists of two transmembrane domains with multiple membrane-spanning segments and two cytoplasmic nucleotide-binding domains (NBDs). Several genetic studies have been performed in different ethnic populations (Northern European, German origin, Danish, Mexico and Chinese) and identified several disease causing variants. So far, there are very limited reports of this gene from Southern India. Therefore, the current study is focusing on the mutation analysis of ABCA4 gene in more number of families to further prove its involvement in South Indian population.

Results and Conclusion

Out of 50 exons only six exons were screened, including the intron exon junctions of ABCA4 gene and identified 7 different mutations in 15 unrelated probands. Among these mutations, two are novel mutations (ins/del) and rest of the five mutations are already reported in other ethnic populations. There were no sequence variations in 8 probands out of 15 probands in the six exons screened. Further, increasing the sample size and the entire coding regions of ABCA4 gene will be screened for all the samples to identify the frequency of gene mutations in South Indian population.

LOXL1-AS1 expression profile in lens epithelial cells of Pseudoexfoliation syndrome (PEX) patients and B-3 human lens epithelial cells upon induced oxidative stress

Investigators : Dr. P. Sundaresan, Dr. Haripriya Aravind
Ph.D. Scholar : Prakadeeswari Gopalakrishnan
Funding Agency : Alcon-APEX project

Introduction

Pseudoexfoliation syndrome (PEX) is a late-onset, conformational disorder of fibrillin and causes progressive elastotic degeneration. It is a recognizable cause of secondary glaucoma and irreversible blindness worldwide. The lens epithelial cells are the primary source of metabolic activity in the lens and any genetic modifications are expected to be expressed in these cells. Lens epithelial cells are the most important site for the production and

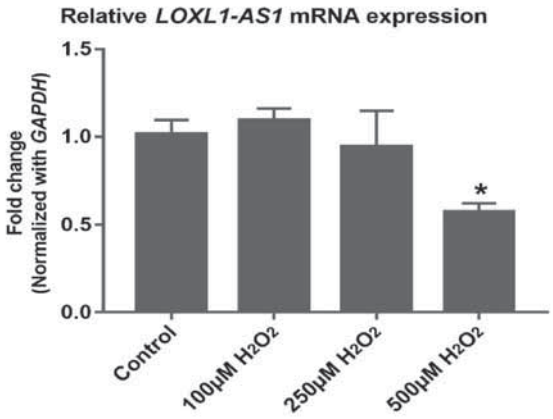

Figure: 1 Effects of ocular lens epithelial cells oxidative stressor on LOXL1-AS1 expression.

Induced oxidative stress by different concentrations of hydrogen peroxide treatment for about 48 hours. We observed a dose-dependent response of reduction in expression of LOXL1-AS1 in 500μM H_2O_2 (n=6, p = 0.0291) treated cells when compared to the untreated control cells which was also showing statistical significance. The 100μM H_2O_2 (n=6, p = 0.7967), 250μM H_2O_2 (n=6, p = 0.8993) treated cells did not show any significant difference in expression of LOXL1-AS1. The data were normalized with relative GAPDH expression and the error bars indicate the standard error of mean. P value ≤ 0.05 is considered as statistically significant.

deposition of the abnormal extracellular matrix that leads to systemic microfibrillopathy. Hauser et al showed many risk variants at *LOXL1* exon 1 / intron 1 which are strongly associated with PEX in four different ethnic populations; some were reversed in one or more populations. The intron 1 region comprises of a promoter for the long non-coding RNA (lncRNA) *LOXL1-AS1*, which is on the opposite strand of *LOXL1*. In some cases, it appears that simply the act of noncoding RNA transcription is sufficient to positively or negatively affect the expression of nearby genes (Katayama et al., 2005). Thus, the present study was undertaken to explore the gene expression of *LOXL1-AS1* in lens epithelial cells and to describe its undefined role in the pathogenesis of pseudoexfoliation syndrome. Additionally, the team was also interested to evaluate *LOXL1-AS1* gene expression of B-3 Human Lens Epithelial cells in response to induced oxidative stress. Anterior lens capsule (ALC) samples were collected from 17 PEX patients who underwent cataract surgery and the 20 cataract (without PEX) patients were used as control. Gene expression profile for *LOXL1-AS1* was analyzed by TaqMan gene expression assay. Tiny ALC tissue samples were pooled and taken for RNA extraction. B-3 Human lens epithelial cell lines (B-3 HLE cells) were used for the determining any modified *LOXL1-AS1* expression pattern in the lens epithelial cells upon induction of oxidative stress with hydrogen peroxide treatment.

Results

This current study analyzed the *LOXL1-AS1* mRNA expression profile in ALC of PEX patients, which showed increased expression in patients who had PEX-material deposition on their lens (PEX-1; p value = 0.0001) and overall anterior segment (PEX-2; p value = 0.0001) of the eye whereas it showed decreased expression in patients who had PEX-material deposition on their pupil (PEX-3; p value = 0.0133) and iris (PEX-4; p value = 0.0062) compared to control. Further, this study examined whether oxidative stress alters LOXL1-AS1 expression in the B-3 human LE cell line. Induction of oxidative stress with hydrogen peroxide treatment on B-3 human lens epithelial cell lines (B-3 HLE cells) showed a decrease LOXL1-AS1 expression pattern in 48 hours treated cells with increased concentrations of 250μM and 500μM H_2O_2 in 48 hours. However, a dose-response relationship was observed and a significant decrease in *LOXL1-AS1* expression was seen with 500μM H2O2 treatment (n=6, p = 0.0291). This study provides insights into involvement of antioxidant signaling pathway dysregulation leads to the imbalanced state of antioxidant defense mechanism and reactive oxygen species (ROS) production. This cellular stress in lens epithelial cells can lead to pathogenesis of PEX which will be further studied through primary cultures of lens epithelial cells of PEX patients to unravel the precise pathways involved in the disease.

Genetic testing of Retinoblastoma

Investigators : Dr. A. Vanniarajan,
Dr. D. Bharanidharan,
Dr. Usha Kim,
Prof. VR. Muthukkaruppan
Project Fellow : A. Aloysius Abraham
Funding agency : Aravind Eye Foundation, USA

Introduction

Retinoblastoma (RB) is a paediatric intraocular tumor arising in the retina causing loss of vision or even life. Knudson's hypothesis (1971) and conventional understanding suggest that biallelic inactivation of *RB1* gene is required for the initiation of retinoblastoma. However, the mechanisms that enable retinoblastoma cells to acquire the additional hallmarks of cancer remain elusive. Recent research had suggested that additional genetic alterations other than *RB1* inactivation are involved in the process of RB tumorigenesis. To understand the RB tumorigenesis better, it is necessary to investigate the status of genes in those regions of recurrent gains or losses in retinoblastoma tumors. High throughput technology like Next Generation Sequencing was utilized to detect the large genomic alterations in retinoblastoma.

Results

Agilent Sureselect XT customized panel covering exonic regions of 24 RB related genes and hotspots of 46 cancer related genes was used for the library preparation and sequencing was performed on Illumina Miseq platform using Miseq V2 kit. Two runs of 2x150bp paired-end sequencing with 63 samples (24 tumor and 39 blood) yielded high quality sequencing data at an average depth of 120X and 85% reads passing the phred score Q30. SNVs were detected using an established in-house bioinformatics pipeline and another tool CNVkit was used to detect the copy number variants (CNVs).

There were 33 patient samples analyzed by NGS, which included 24 tumor samples. Among the 39 blood samples, some of them were matched with tumors and additional family members are included for few patients. Pathogenic variants of *RB1* were identified in 21 patients. Large exonic deletions of *RB1* were detected in five patients. In other seven patients, the involvement of promoter methylation and other genetic changes were considered.

Other than RB1 gene variants, SNVs were found in certain tumor suppressor, checkpoint genes, repair genes like *ATM, BCOR, and CHEK2*. These variants were predicted to have deleterious effect by in-silico analysis and were speculated to have an important role in tumorigenesis. In few patients without *RB1* mutations, variants in genes like *BRCA2, E2F3* were detected which need further evaluation to elucidate their role in RB tumor formation.

Since a customized panel for RB1 and other related genes was utilized, many variants and copy number changes could be identified in almost all samples. Out of 24 tumors analyzed with CNVkit, frequent copy number gains were detected in *KIF14 (5/24), MDM4 (8/24), MYCN (10/24), DDX1 (9/24), DEK (12/24), E2F3 (15/24), OTX2 (6/24), BCOR (16/24)* and recurrent losses were identified in *TP73 (4/24), TP53 (6/24), CDH11 (9/24) and CDH13 (9/24)*. The copy number gains (Red) and losses (Blue) were mapped in the chromosomes (Fig 1).

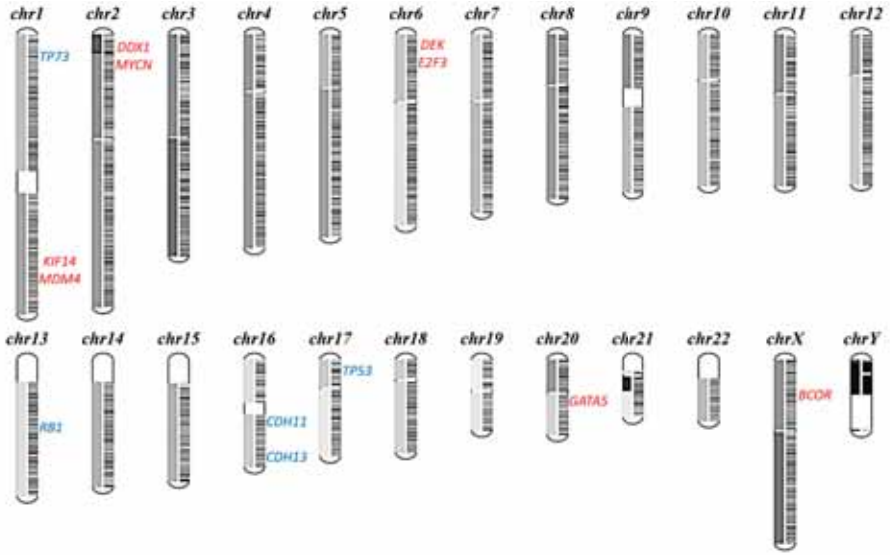

Fig 1: NGS data analysis using CNVkit showed varying levels of copy number in all 24 tumors. Genes with frequent copy number gains are named in red and those with loss are mentioned in blue.

Conclusion

Genetic testing of *RB1* gene has greatly improved the treatment and disease management of retinoblastoma patients and helped in counseling the families. A wide spectrum of *RB1* mutations like nonsense, missense, splice, exonic or whole gene deletions were identified with precision and accuracy. NGS serves as a common platform for variant detection as well as the copy number changes. Knowledge about the status of multiple candidate genes could be obtained by NGS, providing further insight into the biologic alterations underlying the progression of retinoblastoma tumor.

Transcript analysis of Retinoblastoma

Investigators : Dr. A. Vanniarajan, Dr. Usha Kim, Dr. R. Shanthi, Prof. VR. Muthukkaruppan
Project Fellow : Thirumalairaj Kannan
Funding agency : Indian Council of Medical Research

Introduction

Retinoblastoma (RB) is an intraocular childhood cancer with the incidence of 1 in 15,000 live births in India. It occurs in both heritable and non-heritable forms. Most of the heritable RB turns to be bilateral with an early onset of the disease just after birth to 2 years. In contrast, Non-heritable RB is generally unilateral with late onset of age between 2 to 5 years. Two mutational events (M1-M2) were required for the initiation of tumor. Further genetic changes (M3-Mn) were needed for the RB tumor progression. The potential candidate oncogenes and tumor suppressor genes that may be involved in tumor progression were shortlisted based on the experimental data of array CGH, NGS and microarray data of retinoblastoma tumors. The differential gene expression was optimized and analyzed by real time PCR.

Results

In order to understand the mechanism of retinoblastoma development, candidate oncogenes *(MDM2, MDM4, DEK, SYK, & SKP2)* were selected based on the earlier evidences. Initial optimization was carried out for each gene in neural retina cDNA and sequencing was performed to confirm the specific amplification of each gene (Fig 1). With the optimized conditions, the real time PCR was performed and clear amplification with a single peak in the dissociation curve was observed in the neural retina cDNA. Expression of *DEK* gene was analyzed

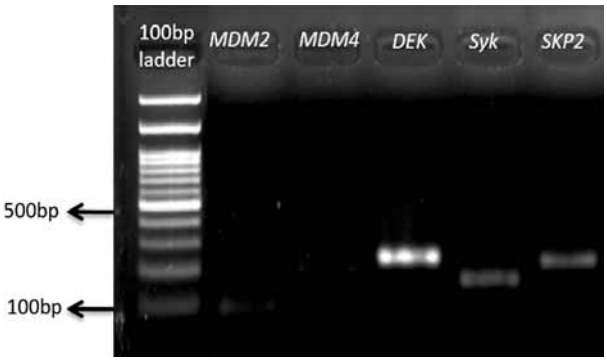

Fig 1: Amplification of candidate oncogenes with neural retina control that may be involved in retinoblastoma tumor progression

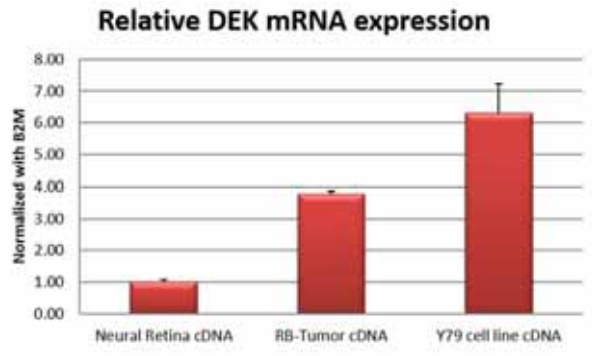

Fig 2: Increased expression of DEK in retinoblastoma tumor and cell line Y79 compared to neural retina (control)

in the tumor sample with somatic mutation in exon 8 and RB cell line Y79. In line with the published literature, quantitative real time PCR showed a 3 and 6-fold high expression of *DEK* in RB tumor and Y79 cell line respectively compared with neural retina Fig 2).

Conclusion

The potential candidate oncogenes involved in retinoblastoma gene expression were identified based on experimental evidences and literature. Further *DEK* gene was found to be differentially expressed in RB tumor and RB cell line compared to neural retina. The proband tumor has homozygous nonsense mutation in *RB1* as an initial event and the *DEK* over expression may be responsible for tumor progression. Further analysis of the other candidate oncogenes and their regulation through epigenetic mechanisms might provide new avenues in the retinoblastoma gene expression.

Understanding the molecular basis of chemoresistance in Retinoblastoma

Investigators : Dr. A. Vanniarajan, Dr. Usha Kim, Dr. R. Shanthi, Prof. VR. Muthukkaruppan

Project Fellow : T.S. Balaji

Funding : Council of Scientific and Industrial Research (Fellowship)

Introduction

Most of the retinoblastoma patients in India present with advanced disease and treatment options become limited. For reducing the tumor, chemotherapeutic drugs such as Vincristine, Etoposide and carboplatin were given as a first line of defense. Cyclosporin A (CsA) being a modulator of p-glycoprotein (ABCB1) was added to the treatment regimen for better cure rate. These ABC transporters such as ABCB1, ABCC1, ABCG2 had affinity to chemotherapeutic drugs, which might lead to the active efflux of drugs out of the cancer cells and thereby reducing the effect of chemotherapy. Hence, study of the expression of ABC transporters in the light of histological parameters might provide the nature of the cells that develop chemoresistance in retinoblastoma.

Results

The patients who underwent enucleation after chemoreduction or chemoresistance were grouped and analyzed. In group I, the eyes were either primary enucleated without any treatment or enucleated after few cycles of chemotherapy. In group II, the eyes were enucleated after multiple cycles of chemotherapy and without chemo reduction. Group I (86%) has highest well differentiated RB tumor when compared to group II (15%), whereas group II (85%) has highest poorly differentiated RB tumor when compared to group I (14%), which was statistically significant (P<0.0001) (Figure 1).

Selective ABC transporters *(ABCB1, ABCC1, ABCC3, ABCE1 & ABCG2)* were analyzed in 13 retinoblastoma (8 group I and 5 group II) eyes. Over expression of ABC transporters was found in RB eyes in group II with extensive cycle of chemotherapy

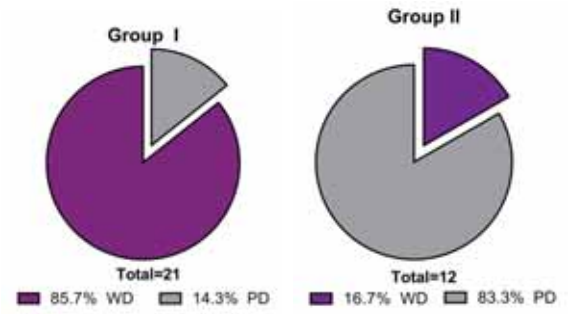

Figure 1: The differentiation pattern of the tumors in group I (primary enucleated without any treatment or enucleated after few cycles of chemotherapy) and group II (enucleated after multiple cycles of chemotherapy and without chemo reduction); WD- Well differentiated and PD-Poorly differentiated

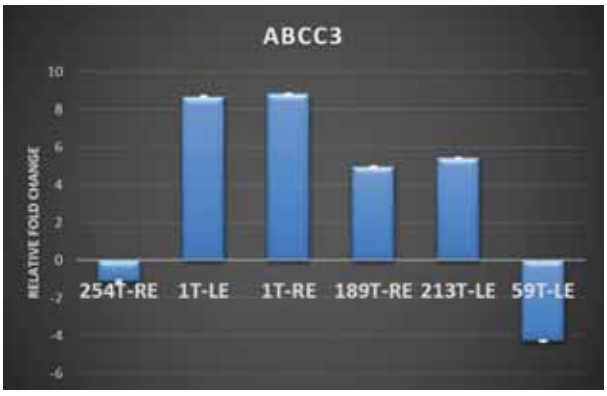

Figure 2: Increased expression of ABC transporters observed in 4 retinoblastoma tumors without chemoreduction

compared to group I with chemoreduction. Among the other transporters, *ABCC3* was found to be highly expressed in 4 samples (Figure 2)

Conclusion

There is a high correlation of the cellular pattern and chemoresistance with increased number of poorly differentiated cells more commonly seen in the tumors with no chemoreduction. Among the other drug transporters, *ABCC3* was highly expressed in RB tumors without chemoreduction. Therapeutic resistance to chemotherapy may also be due to defective apoptotic pathways, presence of cancer stem cells etc.,

Molecular characterization of tumor progression in Retinoblastoma

Investigators : Dr. A. Vanniarajan,
Dr. Usha Kim,
Dr. D. Bharanidharan,
Prof. VR. Muthukkaruppan
Research Scholar : T. Shanthini
Funding agency : DST-INSPIRE Fellowship

Introduction

In addition to the genetic events, retinoblastoma might also be caused by epigenetic factors. It is hence important to elucidate the epigenetic mechanisms like promoter methylation and miRNA regulation underlying the tumor progression of retinoblastoma. One of the epigenetic mechanisms that operate to shut off the *RB1* expression is the promoter methylation. Newer methods were developed to study the promoter methylation of *RB1*. The samples, which do not show variations or deletions in *RB1* gene, were analyzed for promoter methylation by MS-MLPA.

Results

Methylation specific-Multiplex Ligation dependent Probe Amplification is a modification of the MLPA technique, MS-MLPA allows the detection of both copy number changes and unusual methylation levels of different sequences in one simple reaction. MLPA probes for methylation quantification are similar to normal MLPA probes, except that the sequence detected by the MS-MLPA probe contains the sequence recognized by the methylation-sensitive restriction enzyme HhaI. Using this technique, promoter methylation was identified in five patients including methylation of one allele in three samples and both alleles in two samples.

Conclusion

MS-MLPA has been shown to be efficient method of analysis of the *RB1* promoter methylation. Promoter methylation had expanded the spectrum of alterations in *RB1* gene. Further confirmation of the methylation sites by bisulphite sequencing would help to distinguish partial and complete methylation.

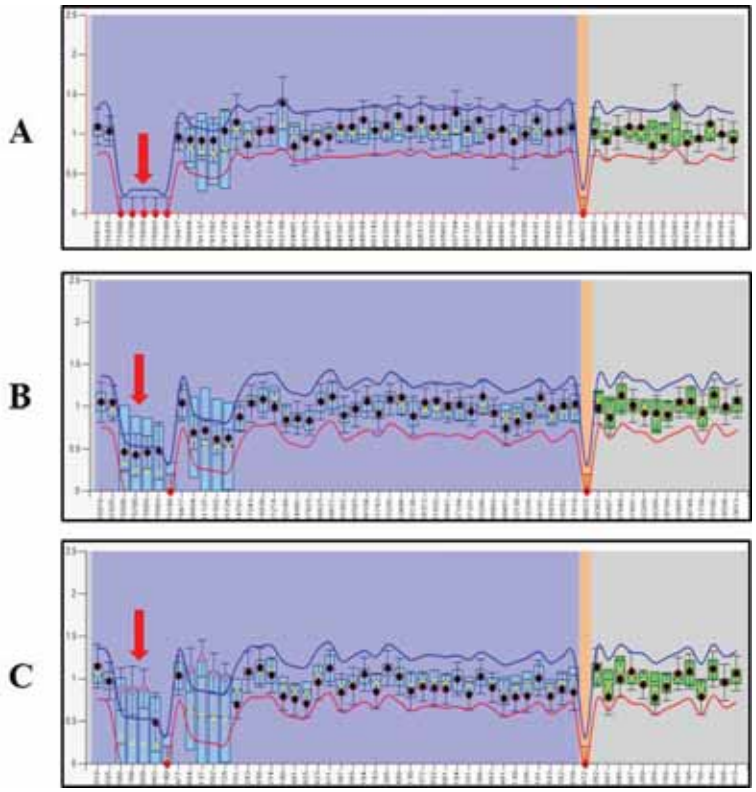

Fig: RB1 Promoter methylation analysis using MS-MLPA

A. Ratio chart of the tumor sample showing no methylation with the five probes unamplified, indicated by red arrow
B. Ratio chart of the tumor sample showing methylation of one allele with the ratio 0.5, indicated by red arrow
C. Ratio chart of the tumor sample showing methylation of both alleles with the ratio1, indicated by red arrow

STEM CELL BIOLOGY

The focus of research in this department is on understanding the basic biology of adult stem cells, specifically the human corneal epithelial stem cells and trabecular meshwork stem cells. A specific method to identify and quantify the corneal epithelial stem cells, and a two-step protocol to enrich these cells from 3-5% to 80% was established earlier. Using this enriched population, the molecular regulation of these normally quiescent stem cells in self-renewal and differentiation are being analysed. With the experience in corneal epithelial stem cells, a new project on trabecular meshwork stem cells has been initiated to identify, quantify and understand their role in ageing and glaucoma. Thus elucidating the basic biology of these adult stem cells will enable the development of better cell-based therapy for corneal surface disorders and primary open angle glaucoma.

Limbal miRNAs and their potential targets associated with the maintenance of stemness

Investigators	:	Dr. Gowri Priya Chidambaranathan
Co-Investigators	:	Dr. Bharanidharan Devarajan, Prof. VR. Muthukkaruppan Dr. N. Venkatesh Prajna
Research Scholar	:	Ms. Lavanya Kalaimani
Funding	:	Department of Biotechnology, New Delhi

Introduction

MicroRNAs (miRNA) are small non coding RNAs that act as a regulator of gene expression and are known to regulate stem cells including embryonic and induced pluripotent stem cells. Corneal epithelial stem cells (CESCs) that reside in the basal layer of the limbal epithelium maintain the homeostasis of corneal epithelium. Till date, the molecular mechanisms associated with the maintenance of stemness in CESCs are not clear due to the lack of a specific marker for their identification and hence isolation. Enrichment of these adult stem cells is essential because they co-exist together with transient amplifying cells and melanocytes in the limbal basal epithelium. The current study is of significance since a specific method to enrich these stem cells to 80% from the 3 to 5% in native population was estalished in this department by a two-step protocol i) differential enzymatic treatment to isolate the basal limbal epithelial cells followed by ii) laser capture micro dissection of cells with nucleus to cytoplasm ratio ≥ 0.7, using donor tissues obtained from Rotary Aravind International Eye Bank, Madurai (Jhansi Rani et al., 2016).

Results

miRNA expression profiling was carried out using such a highly enriched population of CESCs in comparison to central corneal epithelial cells (CCECs) by Illumina Nextseq 500 platform (Genotypic, Bangalore). Analysis of small RNA sequencing data identified 62 miRNAs to be expressed in enriched CESCs and 611 miRNAs in CCECs. hsa-miR-21-5p, hsa-miR-3168, hsa-miR-143-3p, hsa-miR-10a-5p, hsa-miR-150-5p and hsa-miR-1910-5p were highly expressed in CESCs. hsa-miR-184 and hsa-181a-5p were highly expressed in CCECs similar to other

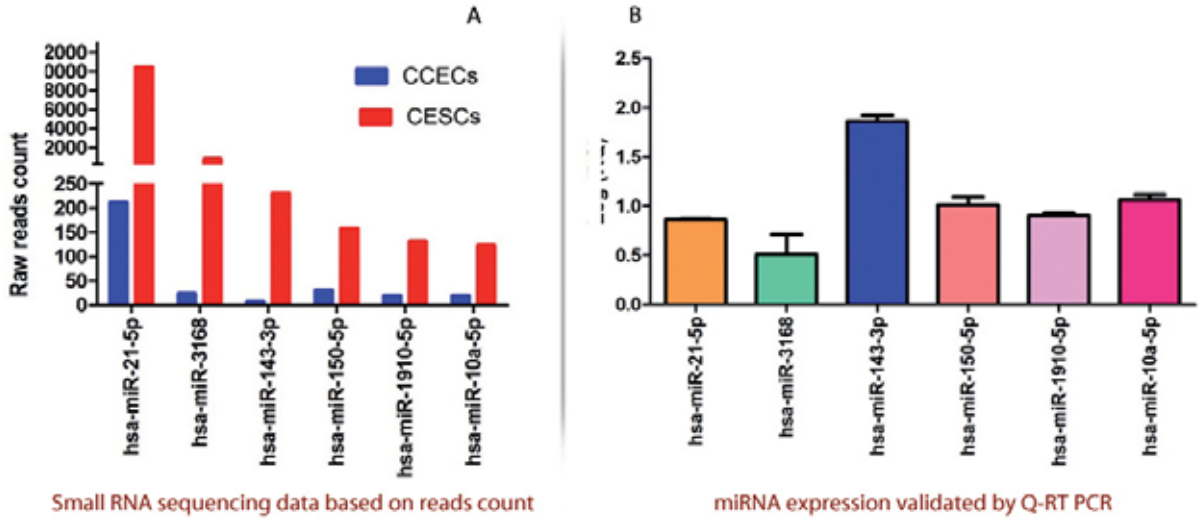

miRNAs showing significantly higher expression in CESCs. (A) Bar diagram showing the top six miRNAs that had high read counts in enriched CESCs compared to CCECs. (B) Relative microRNA expression in CESCs in comparison with CCECs by quantitative real time PCR (SYBR Green chemistry). The data are expressed as mean (n=3) and relative miRNA expression calculated by ΔΔCT method after normalization with RNU6B (housekeeping microRNA).

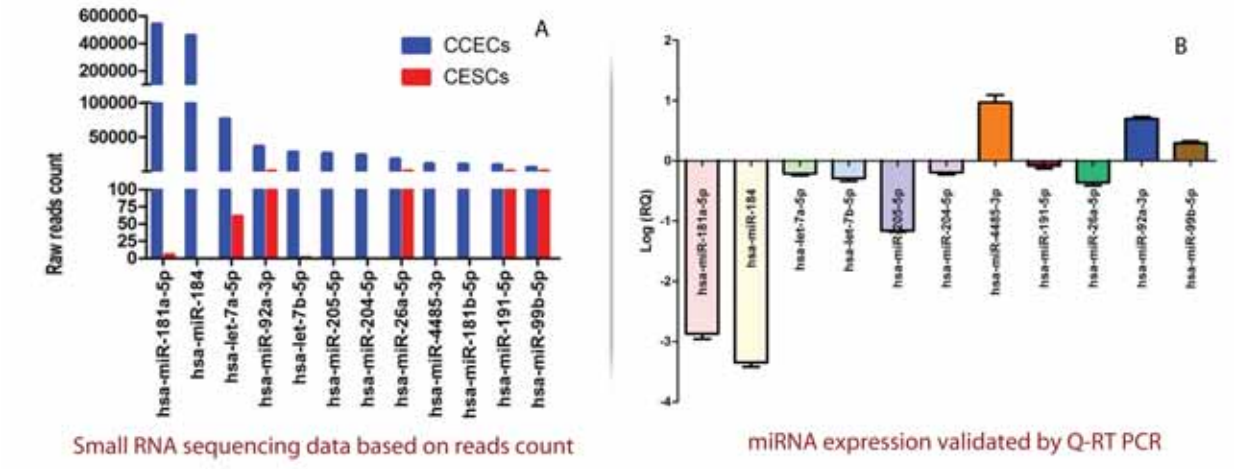

miRNAs showing significantly higher expression in CCECs. (A) Bar diagram showing the top 12 miRNAs that had high read counts in CCECs compared to enriched CSECs. (B) Relative microRNA expression in CCECs in comparison with CESCs by quantitative real time PCR (SYBR Green chemistry). The data are expressed as mean (n=3) and relative miRNA expression calculated by ΔΔCT method after normalization with RNU6B (housekeeping microRNA).

reports. The differential expression of these miRNAs was validated by quantitative real time PCR (Q-RT PCR). Two CESC specific miRNAs, hsa-miR-3168 and hsa-miR-1910-5p are reported as novel miRNAs in embryonic stem cells.

The high expression of hsa-miR-21-5p, hsa-miR-3168 and hsa-miR-143-3p in CESCs were further confirmed by miRNA locked nucleic acid in-situ hybridization (miRNA-LNA ISH). While the expression of miRNAs hsa-miR-21-5p and hsa-miR-3168 were higher in clusters of limbal basal epithelial cells compared to the corneal epithelial cells, the expression of hsa-miR-143-3p was exclusive in cluster of cells in limbal basal epithelium.

Conclusions

The miRNAs highly expressed in CESCs are reported to be associated with maintenance of other stem cells. Further studies are essential to elucidate the functional role of these miRNAs in regulating the CESCs.

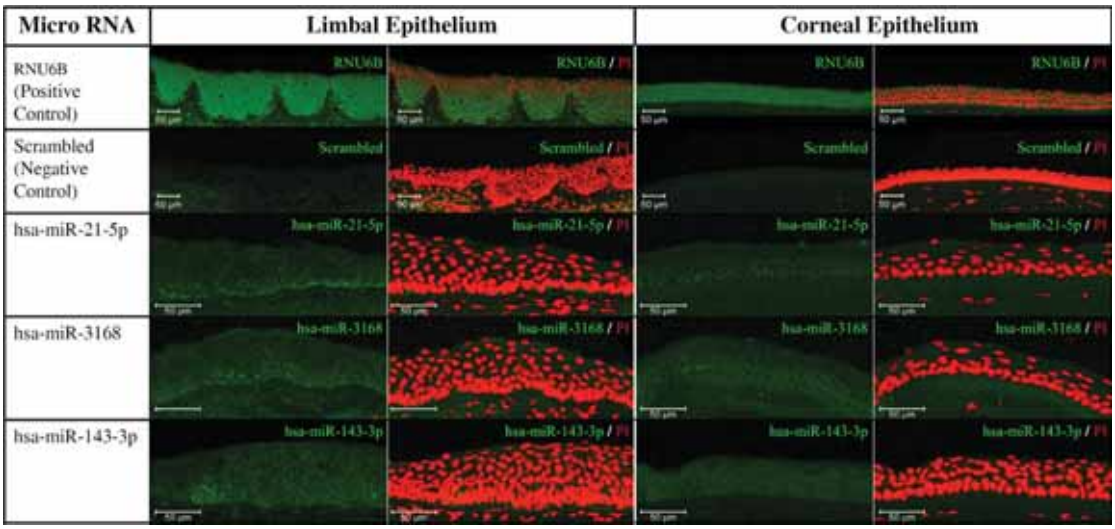

Locked nucleic acid in-situ hybridization of hsa-miR-21-5p, 3168, 143-3p in cryosections of limbal and corneal epithelium.

Expression of hsa-miR-21-5p, 143-3p, 3168 (green) was higher in clusters of limbal basal epithelial cells compared to corneal epithelial cells. Nuclei were stained with propidium iodide (PI, red). Housekeeping RNU6B was detected in all layers of epithelium both in limbus and cornea, whereas no signal was detected when hybridized with scrambled sequence. Scale bar 50µm.

Characterization and functional evaluation of trabecular meshwork stem cells in Glaucoma pathogenesis

Investigator : Dr. Gowri Priya Chidambaranathan
Co-Investigators : Dr. Senthilkumari Srinivasan; Dr. Neethu Mohan; Dr. Krishnadas Subbaiah Ramasamy; Prof. VR. Muthukkaruppan
Research Scholar : Ms. S. Yogapriya; Mr. R. Ashwin Rajkumar
Funding : Science and Engineering Research Board (SERB)

Introduction

Glaucoma is the second leading cause of blindness in the world, with primary open angle glaucoma (POAG) as the most predominant form (74%). A major risk factor for POAG is elevated intraocular pressure (IOP) caused by increased resistance to aqueous humor (AH) outflow. It has been suggested that the age and disease-related decrease of trabecular meshwork (TM) cells, abnormal accumulation of ECM materials, and the appearance of the cross-linked actin networks in the TM cells contribute to an increased resistance of the AH outflow and subsequent increase of IOP. Recent reports indicate the presence of stem cells in TM. These stem cells are believed to be located in the non-filtering anterior region of TM, in the Schwalbe's line. On culturing the TM, a population of stem cells resembling mesenchymal stem cells was identified, that exhibit the ability to home to the TM and differentiate into TM cells in vivo. The role of these trabecular meshwork stem cells (TMSCs) in maintaining the tissue homeostasis and its fate in glaucomatous condition is still not clear. Since there is a reduction in TM cells with ageing and glaucoma, it is hypothesized that TMSCs play an important role in maintaining the normal IOP and are lost significantly higher in glaucoma resulting in increase in IOP. Hence this study aims to identify the location, distribution and function of TMSCs in normal eyes (in different age groups) and glaucomatous eyes.

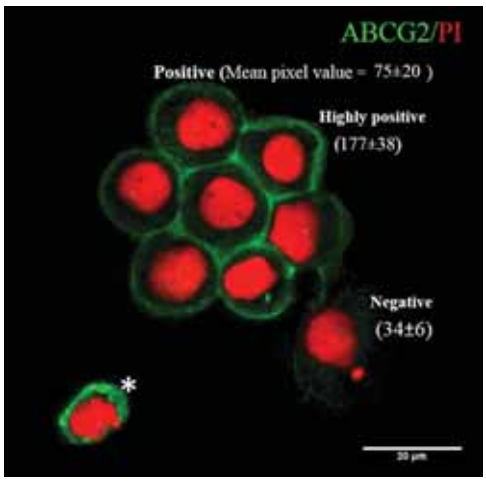

*Representative confocal image of native TM cells immunostained for ABCG2 (FITC-green), counterstained with Propidium iodide (PI-red). * Stem-like cell showing high mean pixel intensity (146) and high N/C ratio (0.755). Other cells with high pixel intensity but having low N/C ratio (<0.7) are not stem cells.*

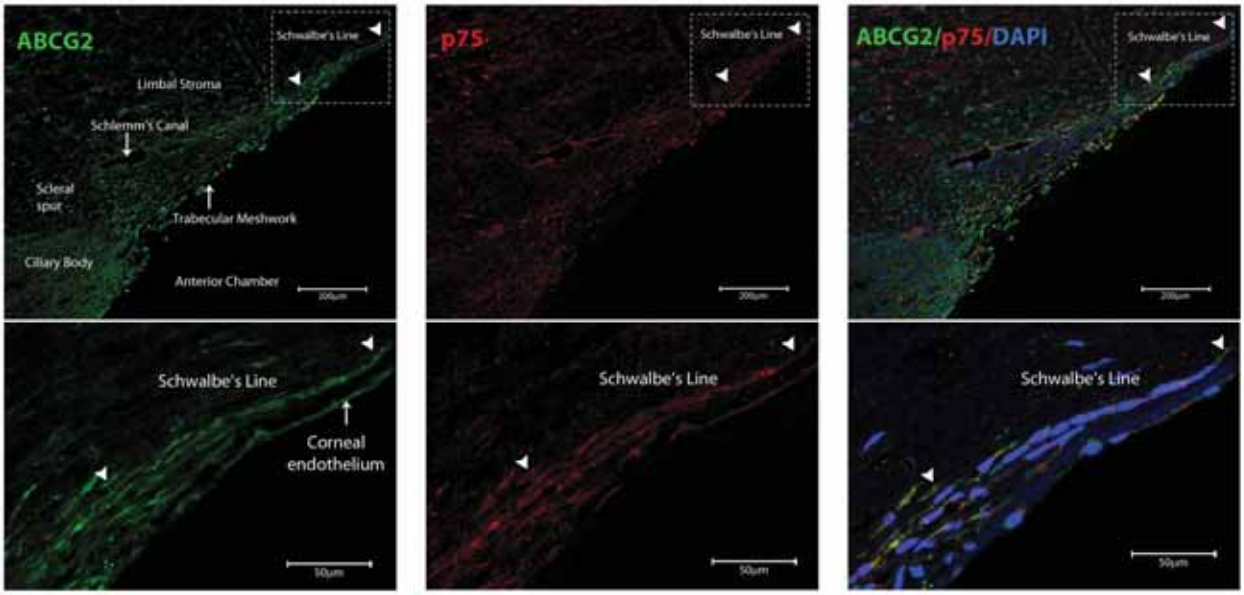

Representative confocal images of radial paraffin sections of human trabecular meshwork double immunostained for ABCG2 (FITC-green) and p75 (Alexa 633- red). Cells having high expression of both ABCG2 and p75 were present in the Schwalbe's line region. Nuclear counterstain DAPI (blue).

Results

The cytosmears of native TM cells from donor eyes (obtained from Rotary Aravind International Eye Bank) were immunostained for ABCG2 and analysed for stem cell content using two parameter analysis – high expression of ABCG2 in cells with high nuclear to cytoplasmic (N/C) ratio (which was estabilised as a specific method to identify and quantify limbal epithelial stem cells). Two parameter analysis identified 4 ± 2% TM cells as stem cells.

In order to localize these stem cells in TM and to understand the changes in TM with ageing, donor eyes of different age groups (Group I : < 30 years; Group II : 30-60 years; Group III: >60 years, N=3 each) were obtained. The anterior segment with intact iris and ciliary body were dissected from human donor tissues into quadrants. Radial paraffin sections of the quadrants were immunostained for ABCG2 (1:20) (Priya et al., 2013), an adult stem cell marker/ p75 (1:200) (Qi et al., 2008), a neural crest derived stem cell marker. Images were acquired and analysed using Leica SP8 confocal microscope.

For quantification of the stem cell content in TM, a minimum of three sections per quadrant were analysed in ImageJ. The total number of cells in the TM (including the filtering and the non-filtering regions but excluding the Schlemm's canal endothelial cells) and the cells highly positive for ABCG2 and p75 in each section were counted. The total TM cell count (Mean ± SD) from 18 sections per age group decreased significantly (rho= -0.92; p=0.0004) with increase in age.

In younger donors (<30 years) 9±3% and 11±4% of TM cells had high positivity to ABCG2 and p75 respectively. These positive cells were restricted to the Schwalbe's line region. The percentage of ABCG2 (rho= -0.79; p=0.011) and p75 (rho= -0.81; p=0.008) high positive cells decreased significantly in higher age groups.

Age Group (Years)	Total TM cell count (Mean ± SD)	Percentage of high ABCG2 positive cells (Mean ± SD)	Percentage of high p75 positive cells (Mean ± SD)
<30	134 ± 30	9 ± 3	11 ± 4
30-60	93 ± 16	7 ± 4	7 ± 6
>60	80 ± 17	5 ± 4	0 ± 1

Data on the total number of TM cells and cells expressing high levels of ABCG2 and p75 are represented as mean ± SD for the three different age groups.

A

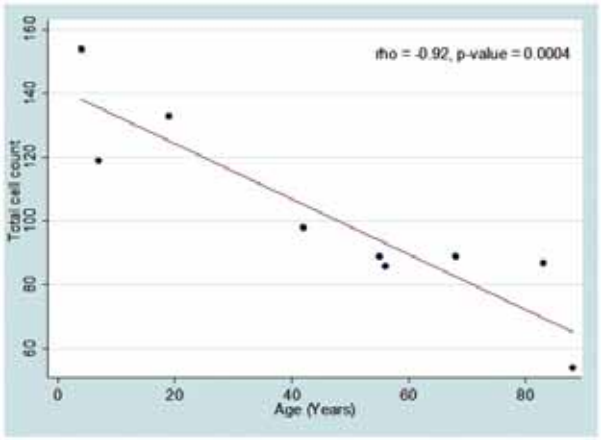

B

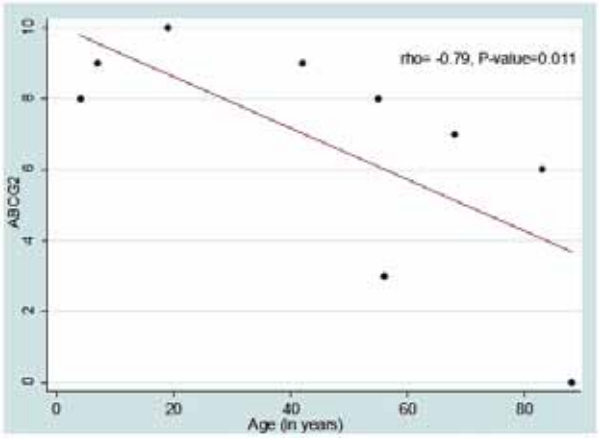

C

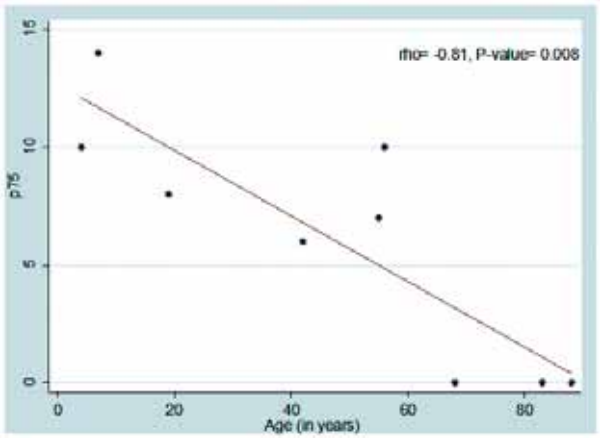

Spearman rank order correlation analysis indicated a significant negative correlation between age and the (A) TM cell counts, (B) cells expressing high ABCG2 and (C) cells expressing high p75 using Stata 14.0. P-value less than 0.05 was considered statistically significant.

Conclusion

Presence of stem-like cells in the Schwalbe's line region was observed to be significantly reduced with ageing and this reduction is associated with the loss in TM cells. Further studies are essential to understand the nature of these stem-like cells in glaucomatous condition and to elucidate their functional significance in pathogenesis.

PROTEOMICS

Fungal keratitis, Diabetic Retinopathy and Keratoconus are the three main eye disorders focused on in the department of Proteomics. Transcriptome and genome analysis are also integral part of the exploratory research. Research programs at the department are funded by government agencies, binational programmes and private corporations.

1.1 Comparative quantitative proteomics of tear using DIGE

Investigators : Prof. K. Dharmalingam, Dr. J. Jeya Maheshwari
Clinician Scientists: Dr. N. Venkatesh Prajna, Dr. Lalitha Prajna
Team Members : Mrs. K.R.P. Niranjana and Mrs. S. Nithya Lakshmi

Zinc α2 glycoprotein (ZAG), is an adipokine, secreted by normal epithelial cells. ZAG is involved in various biological processes including the regulation of melanin production and cell proliferation. Among the abundant proteins in human tear, ZAG is contributing to 12% of the total proteins.

1.1.1 Demonstration of expression levels of ZAG in mycotic keratitis patients

In a previous report by the team, the protein profile of tear was examined from keratitis patients and found that there is a difference in the level of ZAG between *Fusarium* and *A. flavus* keratitis patient tear (Ananthi et al., 2008). In *A. flavus* and *Fusarium* keratitis patients, as duration of infection increases, there was a progressive decrease in ZAG level in tear. While the ZAG level in tear decreases only two-fold in *Fusarium* infection, a four-fold decrease was observed in *A. flavus* infection. Further, based on 2D-DIGE results, it was evident that all the three proteoforms of ZAG showed a decrease during progression of *A.flavus* infection. This decrease in levels of ZAG proteoforms was also validated using western blot followed by densitometric analysis.

1.1.2 Identification of Tear Proteoforms of ZAG

In order to separate the proteoforms of ZAG, narrow range IPG Strips were used for isoelectric focusing. DIGE analysis was completed during the last report period.

1.1.3 Work done during this reporting period:

As reported earlier, ZAG gets down regulated in *A. flavus* infected keratitis patient's tear with disease progression. ZAG level in *A. flavus* infected keratitis patient's tear was analyzed using Immunoblot assay. Total of 22 patients' tear was collected from different stage of infection (Early-10; Intermediate-5; Late-7) and 6 samples from uninfected individual's tear. Tear protein concentration was estimated using Bradford method.

1.1.4 Quantitative determination of ZAG in individual samples

Tear protein concentration varies among individuals which reflects its effect on ZAG detectable range. Hence, linearity detection of ZAG in total protein

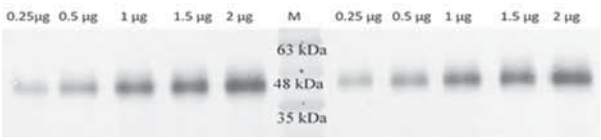

Fig1.1.4.1 Determination of Linearity of ZAG in control tear using Western blot analysis. Western blot analysis for detection of ZAG in control tear sample with increasing range of concentrations from 0.25 µg to 2 µg of total tear. Image shows the ZAG level in control tear done in replicates. Graphical representation of Densitometry analysis of mean value of ZAG band volume in blot using IQTL. From the analysis, 0.5 µg and 1 µg of tear protein were detected in linear range.

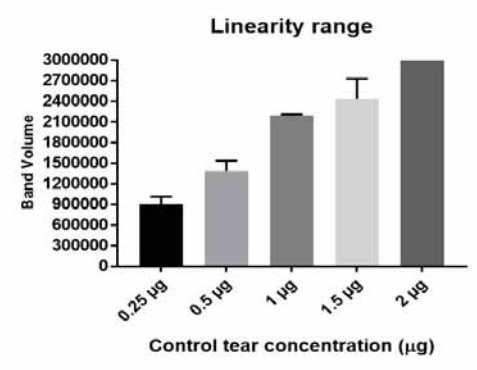

concentration of tear is an important aspect to be considered. Control tear sample was resolved in 1D-SDS PAGE with different concentrations ranging from 250 ng to 2 µg and then transferred onto a NC membrane (GE Healthcare, Uppsala, Sweden) by semidry blotting using a Pierce-fast semi dry blotter (Thermo Scientific). The membrane was processed further for the detection of ZAG. The results show that total tear protein of 500 ng and 1 µg of total tear could be used for measuring the ZAG concentration Fig1.1.4.1. Therefore, further experiments with individual tear samples used 500 ng of total tear protein.

ZAG pure protein immunoblot was used to construct a standard graph against which the experimental samples were compared Fig 1.1.4.2.

Immunoblots of individual tear samples were quantified for ZAG band volume (Fig.1.1.4.3) against the standard graph. In all samples, total tear protein used was constant. Fig. 1.1.4.3 shows the ZAG concentration in each individual sample with calculated median value. ZAG concentration in control tear sample was 68.7 ng, while in early stage the median value was 42 ng and intermediate stage was calculated to be 52 ng. The late stage of

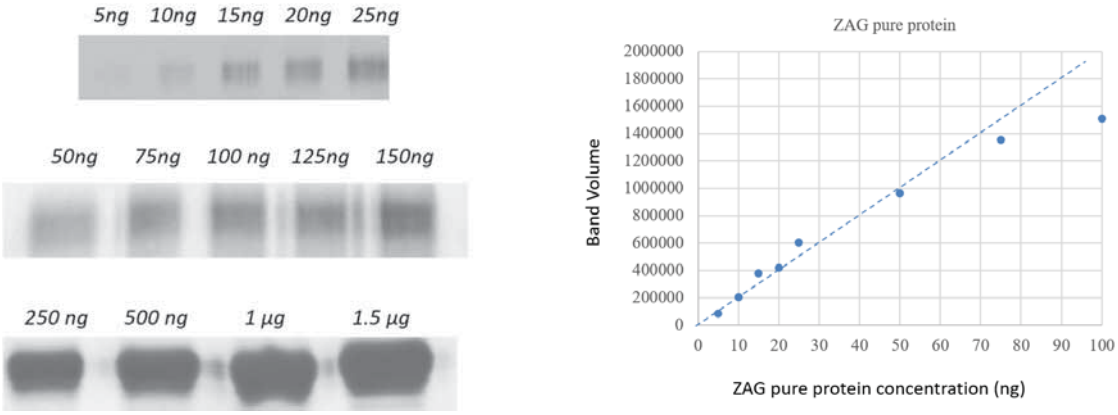

Fig 1.1.4.2 Immunoblot analysis of ZAG pure protein. Western blot analysis of different concentrations of ZAG pure protein. Densitometry analysis of the band Volume using IQTL. Graph represents the band volume (y axis) against protein concentration (x axis).

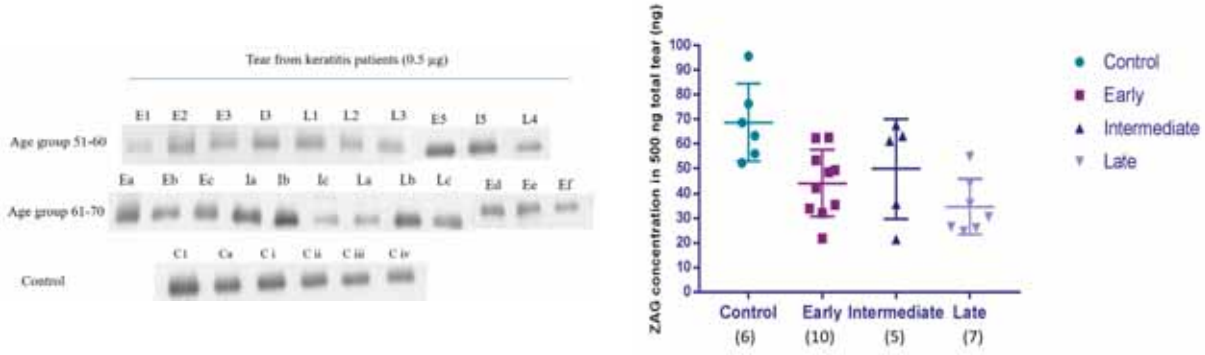

Fig1.1.4.3 Analysis of ZAG concentration in A. flavus infected keratitis patients total tear from individual subjects. Five hundred Nano gram of total tear from individual patient were subjected to 1D SDS PAGE. [C- Control, E- Early, I-Intermediate, L-Late (Stage of infection)] Western blot membrane was scanned to quantify the band volume and used for calculating the protein concentration. Graph represents ZAG concentration in 0.5 µg of total tear in individual. The solid line represents the median value of ZAG concentration in each group. The numbers below each group are the number of samples used for analysis.

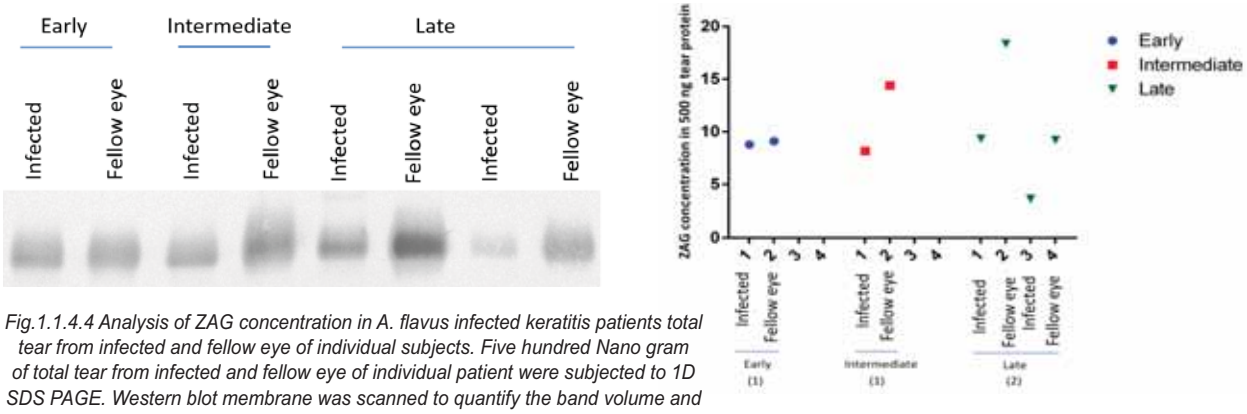

Fig.1.1.4.4 Analysis of ZAG concentration in A. flavus infected keratitis patients total tear from infected and fellow eye of individual subjects. Five hundred Nano gram of total tear from infected and fellow eye of individual patient were subjected to 1D SDS PAGE. Western blot membrane was scanned to quantify the band volume and used for calculating the protein concentration. Graph represents ZAG concentration in 0.5 µg of total tear in individual patient. The numbers below each group are the number of samples used for analysis, where each sample includes an infected and a fellow eye tear.

infection shows ZAG concentration as 36 ng. The result showed clearly that ZAG expression level decreases upon *A. flavus* infection at early stage and continue to decline as the disease progressed. Further analysis of ZAG expression level, in fellow eye tear from *A. flavus* infected keratitis patients, showed comparatively higher ZAG concentration than tear from infected eye (Fig. 1.1.4.4). Samples from all three stages of infection, results in declined ZAG concentration upon *A. flavus* infection. These results support the previous data with DIGE.

ZAG can be used as a potential biomarker for identifying early stage of fungal infection, which aids in faster clinical anti-fungal treatment to patients. It also demarcates the infection caused by *Fusarium* and *A. flavus* with different protein regulation patterns. Understanding the role of ZAG in defense mechanism against specific pathogen will lead to therapeutic purposes.

1.1.5 Work to be Undertaken

Result will be further validated for usefulness of ZAG level to differentiate *A. flavus* and *Fusarium* keratitis using patient tear. One hundred and twenty samples in total will be checked. Thirty tear samples in each category of patients control, early, intermediate and late stage will be used for this. ELISA and SRM assays will be used for this analysis.

1.2. Tear proteome profiling and quantitative proteomics using Mass Spectrometry

Investigators : Prof.K.Dharmalingam, Dr. J. Jeya Maheshwari
Clinician Scientists: Dr. N.Venkatesh Prajna, Dr. Lalitha Prajna
Team Members : Dr. K. Jeyalakshmi and Mr. Naveen Luke Demonte

1.2.1 Tear proteome profiling

Using mass spectrometry, 2897 proteins with high confidence and rank one peptide 1103 proteins with two peptides and high confidence were identified in control tear. Using a similar approach, 1966 proteins were identified in tear from keratitis patients of which 1028 were identifications with 2 or more peptides. Combining the proteins identified from control and patient tear in this study, a total of 4260 tear proteins identified reliably, the highest number of proteins reported in tear till date.

1.2.2 Comparative tear proteome analysis

Proteins identified in neat tear from keratitis patients were compared with that of control tear and a label-free quantitative analysis was done. This analysis revealed a subset of 177 proteins to differ significantly in abundance in tear during A. flavus infection. Of these, 150 proteins were found at high levels in keratitis patients tear whereas only 27 proteins were significantly lower in patient tear. In addition to these, 177 proteins that were quantified with high confidence, 1,235 proteins were present exclusively in tear from keratitis patients. This indicates the synthesis and secretion of new proteins in response to fungal infection.

1.2.3 Complement pathway proteins in control and patient tear

Examination of the protein identification data reveals that most of the complement proteins were not found in control tear. However, in the patient tear, proteins representing all the three complement pathways were found at high levels (Figure 1.2.3.1). This data show that the complement pathway proteins are found in tear from patients and probably reflects an antifungal mechanism elaborated by the host to deal with the infection.

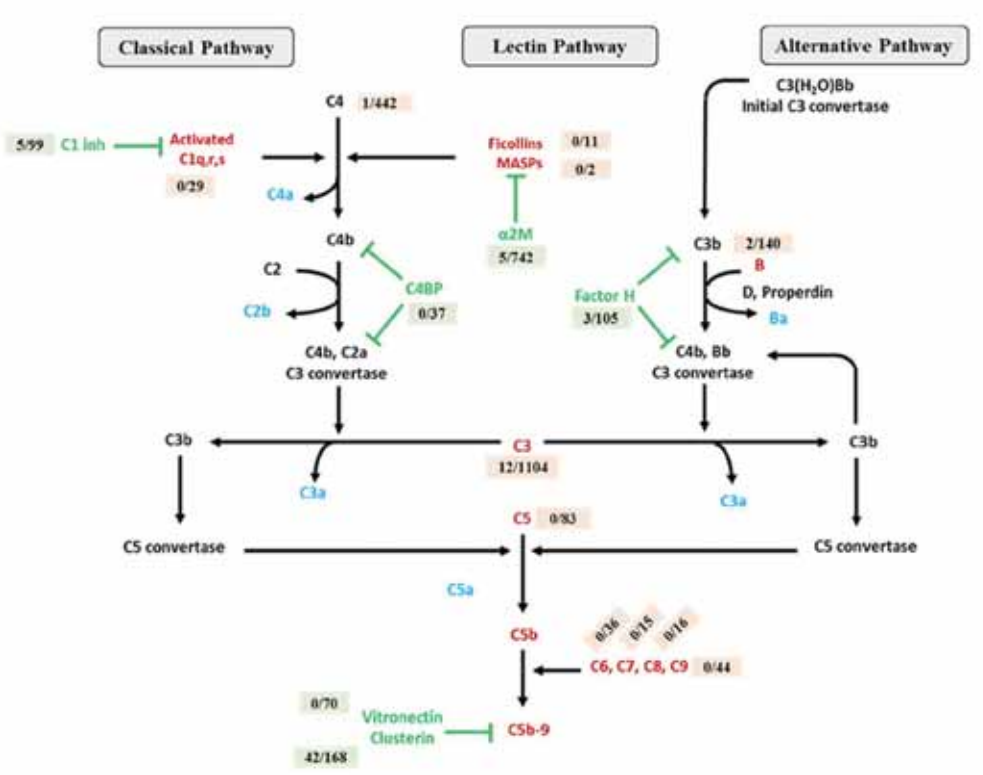

Figure 1.2.3.1 Mass spectrometry identification of Control and and patient tear

1.2.4 Neutrophil-mediated defense functions in tear proteins

Earlier studies have shown that neutrophils and their components provide active defense against fungal infection. Further, influx of neutrophils into nocturnal tear was also demonstrated. Several components of neutrophil-mediated defense proteins are found only in tear from patients. Most of the components associated with the formation of neutrophil extracellular traps are represented. Identification of proteins of the primary granules along with nuclear-localized histone proteins in the patient tear indicated that the neutrophils might employ NETosis for killing A. flavus hyphae. Twenty-four neutrophil proteins that have been reported to be associated with NETs associated were found in tear from keratitis patients. These results show that NETs may be a defense mechanism against *A. flavus* in the tear fluid of keratitis patients.

1.2.5 Proteins involved in coagulation cascade and wound healing

Proteins of coagulation cascade and the proteins involved in wound healing were identified in patient tear. The team also found increased amounts of thrombin as well as cleavage products of fibrinogen indicating the activation of coagulation cascade leading to fibrin clot formation. Surprisingly, plasminogen that is required for clearing fibrin clot is also up regulated suggesting a fine balance in clot formation and clearance. There was a significant up regulation of three heat shock proteins, HSP beta 1 (Hsp27), Hsp70 (1A variant), and Hsp90 alpha in tear from keratitis patients. These Hsp's have been implicated in wound healing. Identification of lumican in tear during infection indicates the recruitment of inflammatory cells into cornea for wound healing. The presence of vimentin, a pro-fibrotic protein, and MMP-9 in patient tear indicate that another set of factors required for wound healing process are also upregulated. Earlier studies have indicated that higher MMP-9/TIMP-1 ratios were found in the tear of fungal keratitis patients (and are an indicator of poor wound healing. Therefore, it is predicted that inhibitor of MMP-9 namely TIMP-1 will be up regulated in tear during infection to improve wound healing.

Interestingly, factor H and factor I along with other regulators of complement pathway were also found in the patient tear. Identification of the inhibitors acting on the soluble components of complement as well as membrane attack complex shows that a fine balance exists between activation and down-modulation of complement pathways. The role of pathogen-specific factors is significant to alter the balance.

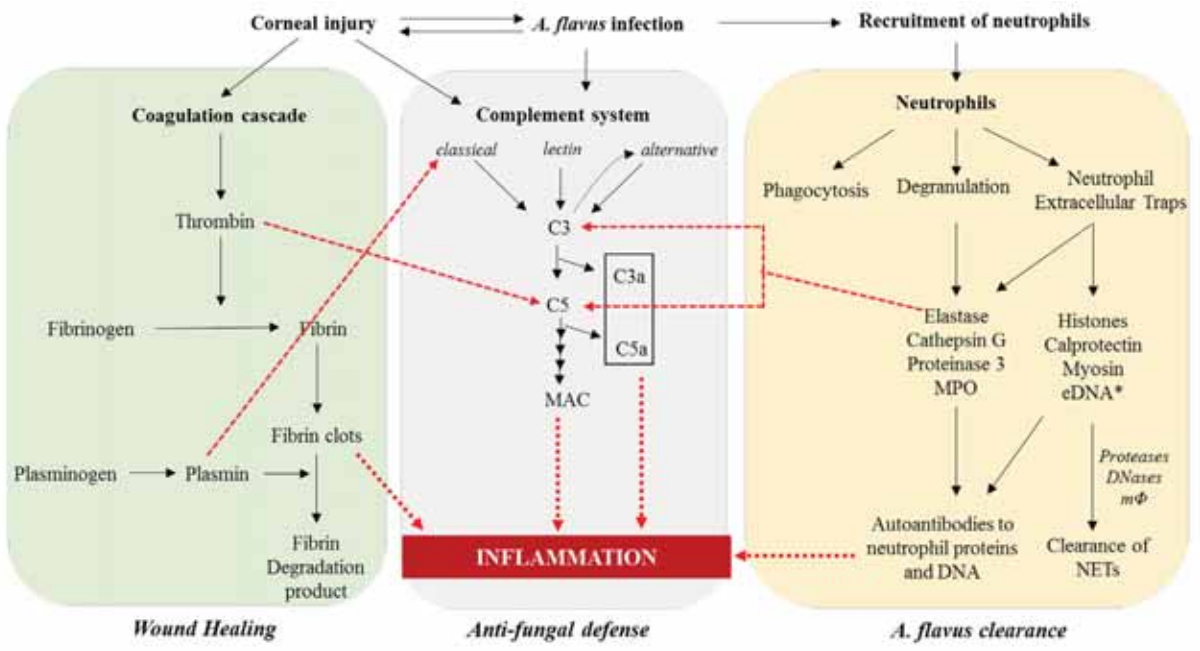

Fig. 1.2.5.1 Potential mediators of inflammation during A. flavus infection

Data from the experiments reported in this study clearly indicate that a fine balance exists between the destruction of pathogen and damage to the host tissue by the host immune activation. Human tear from mycotic patients reflects the ongoing defense as well as wound healing events (Figure 1.2.5.1). This is exemplified by the presence of all the components needed for complement activation, particularly the alternate pathway and neutrophil-mediated anti-fungal response. Proteins involved in coagulation and wound healing reflect the repair of the damages caused by the fungal invasion. However, the presence of proteins that down modulate these responses indicate an intricate equilibrium between the clearance of infection and overt host response.

1.2.6 Work to be undertaken

Among the pathways discovered during the previous year, complement pathway was examined in detail earlier. During this period the C3a, the inflammatory protein of the complement system will be quantified in patient tear.

Wound healing is another pathway that determines the outcome of infection. Irrespective of treatment some patients heal others do not. Therefore, examination of this pathway is essential to understand the outcome of the disease.

Demonstration of NETosis in vitro is another aspect which will be completed during this period.

1.3. Validation of complement factor H Levels in Mycotic Keratitis patients

Investigators : Prof. K. Dharmalingam, Dr. J. Jeya Maheshwari and Dr. A. Rabbind Singh
Clinician Scientists: Dr. N. Venkatesh Prajna, Dr. Lalitha Prajna
Team Members : Ms. K. Sandhya, Mr. S. Mohammed Razeeth and Mr. Naveen Luke Demonte

Comparative tear proteome analysis of mycotic keratitis patients showed that all the three complement pathways were activated in the patients as evidenced by their presence only in the patient tear. It is also clear from Figure 1.3.1.1 that the amplification of the central complement pathway occurs through the alternative pathway as the levels of factor B was very high. Upregulation of the complement factor H (CFH), a key regulator of alternative pathway further supports this observation. As complement plays a central role as a mediator of inflammation and thereby corneal damage, CFH is expected to be upregulated when there is an excessive activation of complement and thus, be used to determine the extent of activation as the infection progresses. Hence, we quantitated the levels of CFH in individual tear samples from *A.flavus* keratitis patients at different stages of infection with varying ulcer depth and size and the results were reported previously.

1.3.1 Work done during this period

The expression of CFH in *Fusarium* keratitis tear samples at different stages of infection were analysed as shown in Figure 1.3.1.1. Early stage tears were collected from patients whose duration of symptoms are less than 7 days, Intermediate stage from 7- 14 days of symptoms, more than 14 days were categorized under Late stage of infection.

Varied levels of CFH expression was observed in various stages of *Fusarium* keratitis tear samples.

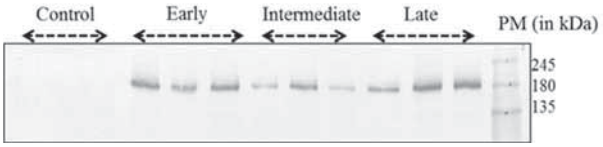

Fig .1.3.1.1: Western blot analysis of CFH for tear collected from various stage of Fusarium keratitis tear samples. 15 µg of total tear protein from Fusarium infected keratitis were resolved on 1D SDS-PAGE (8%), transferred onto nitrocellulose membrane and probed against anti-CFH antibody (SC 33156).

1.3.2 Differential expression of Factor H in *Fusarium* keratitis tear and in uninfected fellow eye of same patients

A total of 17 samples were taken for the analysis, for which both infected and fellow eye were examined for CFH expression. Out of the 17 samples, nine samples showed no expression of CFH in uninfected fellow eye (Fig 1.3.2.1A). 4 samples showed expression of Factor H in both infected as well as the fellow eye (Fig 1.3.2.1B). Four samples did not show any expression including the keratitis tear samples (Fig 1.3.2.1C).

1.3.3 Work to be undertaken

The level of CFH along with ulcer depth and ulcer location on the cornea appears to be three parameters that combined together has potential to predict treatment outcome. Further validation is in progress using this multi parameters scale for clinical use in deciding early surgery in this period.

Fig 1.3.2.1 A

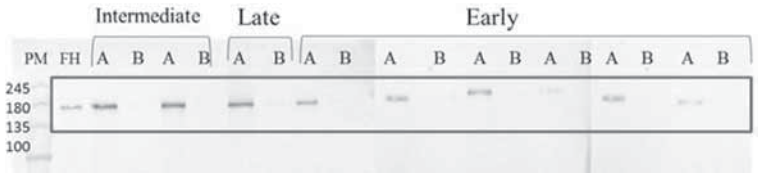

Fig 1.3.2.1 B

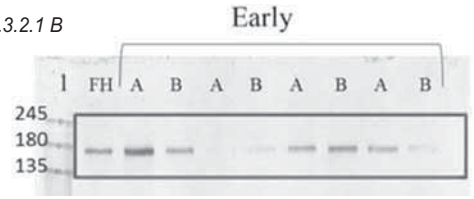

Fig 1.3.2.1 C

Figure 1.3.2.1 Western blot analysis of CFH for tear collected from the keratitis eye along with its fellow eye without infection. A indicates tears collected from Fusarium keratitis eye and B indicates tears collected from the fellow eye of the same patient.

1.4. Post-translational modifications of tear proteins from Keratitis patients

Investigators : Prof. K. Dharmalingam, Dr. J. Jeya Maheshwari
Clinician Scientists: Dr. N. Venkatesh Prajna, Dr. Lalitha Prajna
Team Members : Mrs. K. Jeyalakshmi

Glycoprotein enrichment using a plant lectin, Con A allows the selective enrichment of N -linked glycoproteins. In this study, enrichment of glycoprotein from total tear was carried out using conA columns. Samples were pooled to achieve a total protein concentration of 500 µg. Glycoproteins from the total tear were enriched using conA columns and the proteins in both the glycosylated and non-N-glycosylated fractions were identified using Orbitrap Velos Pro Mass Spectrometer. Previous report describes in detail the profile of glycoproteome of control and patient tear.

Interestingly, glycoproteome analysis indicated that glycosylation of tear proteins are altered during fungal infection. Comparative analysis of the N-glycosylated and non-N-glycosylated proteins identified in tear from keratitis patients and healthy individuals showed that there was a difference in the glycosylation profile of many of the proteins. Some proteins were differentially glycosylated in tears of fungal keratitis patients. Many proteins identified in control tear were not identified in ConA fraction (N-glycoproteins) of control tear. Intriguingly, the same set of proteins were identified in ConA bound fraction (N-glycoprotein) of tears from keratitis patients. Also, many proteins were identified in both the N-glycosylated and non-N-glycoprotein fractions

(conA flowthrough) suggesting that these proteins exist in both glycosylated and non-glycosylated forms. These observations state that the disease condition alters the post-translational modification of proteins in tears which resulted in glycosylation of some proteins during fungal infection.

1.4.1 Work to be undertaken

Analysis of the source of the glycosylation change in the tear will be examined.

1.5. Human corneal epithelial cell line as a model system to study fungal infection

Investigators : Prof. K. Dharmalingam,
Dr. J. Jeya Maheshwari,
Dr. O.G. Ramprasad
Clinician Scientists: Dr. N. Venkatesh Prajna,
Dr. Lalitha Prajna
Team Members : Ms. A. Divya

1.5.1 Introduction

Corneal Scarring due to trauma or infectious keratitis is the leading cause of vision impairment and monocular blindness. More than half of the corneal ulcers are reported to be fungal in origin. *Fusarium* and *Aspergillus* are the predominant cause of fungal keratitis in India and *A. flavus* accounts for more than 80% of the *Aspergillus* infections of the cornea and is more resistant to anti-fungal treatment. Cornea is an avascular tissue and it contains 5 layers in which corneal epithelium is the earliest cell type that encounters the invading pathogen and acts as a first line of defense to protect cornea. Fungi can colonize host corneal epithelium, penetrates deeper into the anterior stroma and causes severe infection. The innate immune response of corneal epithelium during fungal infection is still not clearly understood, since the experimental animal models are inadequate. Here SV40 immortalized Human Corneal Epithelial Cell line is used to study the immune response to *A.flavus*.

1.5.2. Phagocytosis and actin rearrangement assays:

HCE cells (1x105) were cultured in 18x18mm coverslip and infected with FITC labelled *A.flavus* conidia with m.o.i of 1:10 for indicated time period. Following infection cells were washed with 1X PBS, fixed with 4% PFA, permeabilized with 0.1% triton x-100 for 10 min and cells were incubated with TRITC-phalloidin (1:40 in 1X PBS) for 40min to stain cellular actin filaments. Coverslip was washed with PBS, mounted using vectashield mounting medium containing DAPI and viewed under Leica LAS AF confocal microscope.

HCE cells started to engulf *A.flavus* conidia within 15min and the engulfed conidia was completely encircled by F-actin rich filopodia (Figure 1.5.2.1).

1.5.3 Kinetics of actin rearrangement:

HCE cells(1x105) were cultured in 18x18mm coverslip and infected with FITC labelled *A. flavus* conidia (ATCC200026, CI1698 & CI1123) with m.o.i of 1:10 for various time point (15min, 30min & 60min). After infection cells were processed for actin staining as mentioned above and the images were examined under confocal microscope.

HCE cells infected with three different isolates of *A. flavus*, the engulfed conidia was found inside the vacuole coated with polymerized actin(Fig.1.5.3.1).

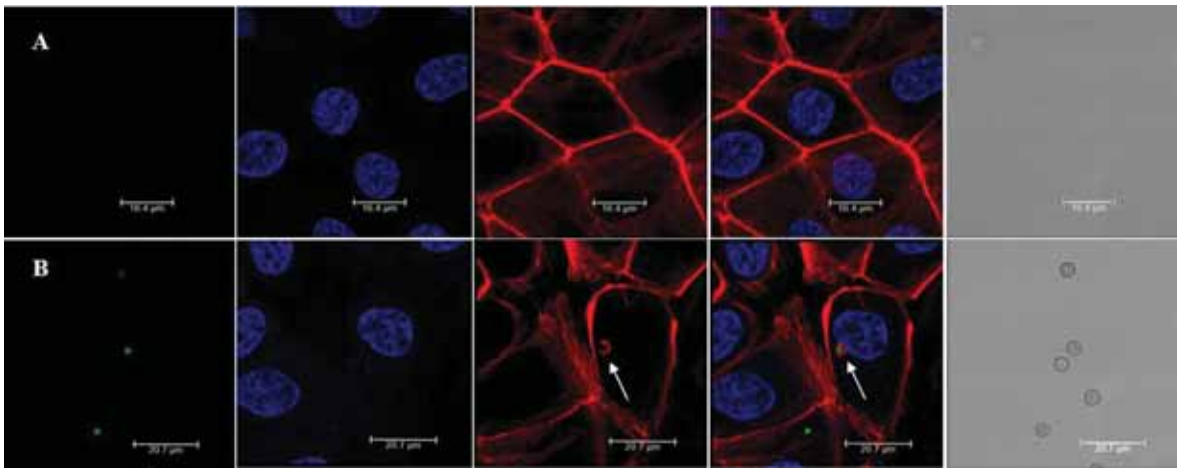

Figure 1.5.2.1: Confocal images of actin rearrangement after internalization of A.flavus conidia by HCE cells: A) Un infected HCE B) HCE infected with FITC-labelled A.flavus ATCC200026 conidia for 15min at 37ºC. The images correspond to middle section of the cells by z-stacking. From left to right, panels show fluorescence image of green channel (FITC labelled conidia), fluorescence image of blue channel (DAPI), fluorescence image of red channel (F actin staining with TRITC-phalloidin), merged overlay of all fluorescent channels, bright field. White arrow indicates actin ring surrounding the engulfed conidia.

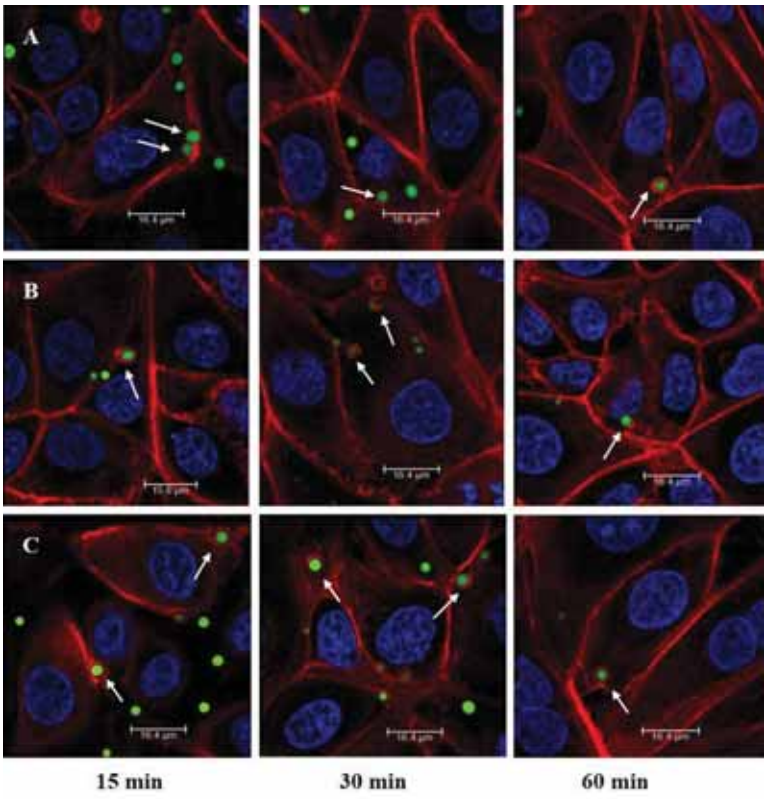

Figure 1.5.3.1: Colocalization of A.flavus conidia within actin filaments of HCE: HCE cells were infected for various time point with different isolates of A.flavus A) ATCC 200026, B) CI 1698 & C) CI 1123. Internalized conidia can be visualized by staining host actin (red). A.flavus conidia is labelled with FITC (green) and host nucleus is stained with DAPI (blue). White arrows indicate the actin ring surrounding the engulfed conidia.

The number of actin ring formation surrounding conidia was counted for 100 conidia that are associated to HCE cells in 5 randomly selected fields and the results were represented below (figure 1.5.3.2).

At various time period, the number of actin ring formation was found to be similar for all three isolates of *A. flavus*. There is no significant increase in the actin ring with increase of infection incubation time. Around 20% of the conidia associated to HCE cells were found to be capped with F-actin.

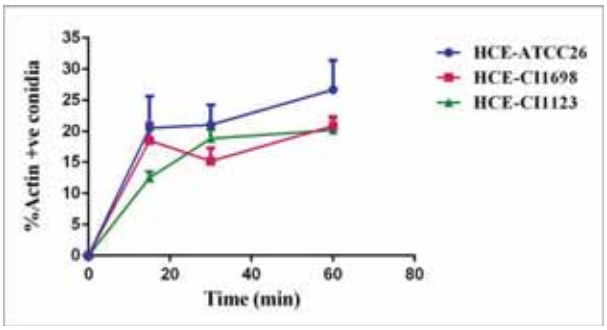

*Figure 1.5.3.2: Kinetics of actin rearrangement in conidia phagocytosis by HCE cells: The percentage of actin-positive conidia was calculated as follows: (the number of conidia surrounded by an actin ring or cup stained with TRITC-phalloidin/the total number of conidia associated to HCE cells) * 100. Data were averages from two independent experiments with triplicates, and standard deviations were indicated with error bars.*

1.5.4 Treatment with cytoskeleton inhibitors:

To evaluate the importance of host cell cytoskeletal rearrangements during the internalization of *A. flavus* by HCE cells, latrunculin B (1µM) were added to the medium 30min prior to infection. Following pre-treatment, the cells were infected with *A. flavus* in the presence of drug for 30min. Cells were processed for F-actin staining as indicated and analyzed by confocal microscopy.

In untreated HCE cells, the actin stress fibers were clearly seen (basal) and the cell periphery is uniformly stained with F-actin (Apical). Absence of stress fibers and intermittent staining of F-actin was observed in the latruculin B treated HCE cells. 1µM of latrunculin B was found to be efficiently inhibited the actin polymerization.

The drug treated HCE cells also able to engulf *A.flavus* and forms actin ring around the conidia(Fig.1.5.4.2). This indicate that the inhibitor was not completely block the actin polymerization and inhibit the engulfment. If the concentration of inhibitor is increased further, there might be absence of actin ring after infection.

In the presence of drug there is significant decrease (~2 fold) in the actin positive conidia for HCE cells infected with ATCC 200026 and CI1123.

This shows actin plays a crucial role in the initial engulfment of conidia by host cells. It is not clear for cells infected with CI1698 in which no difference in the conidial engulfment.

1.5.5 Endosomal Trafficking assays:

HCE cells($1x10^5$) were cultured in 18x18mm coverslip and infected with FITC labelled *A.flavus* conidia (ATCC200026) with m.o.i of 1:10 for 3hrs. After infection cells were processed for immunofluorescence analysis of early endosomal markers (CD71 & EEA1) and late endosomal markers (Rab7, LAMP1 & cathepsin D). Following infection, cells were washed with 1X PBS, fixed with 4% PFA, blocked and permeabilized with 0.1% triton x-100 in 5% BSA for 1hr and cells were incubated with respective monoclonal antibodies (1:50) for 1hr at RT. Finally, the cells were stained with goat anti-mouse IgG conjugated with dylight 550 (1:50) for 1hr at RT. Coverslips were washed with PBS, mounted using vectashield mounting medium containing DAPI and viewed under Leica LAS AF confocal microscope.

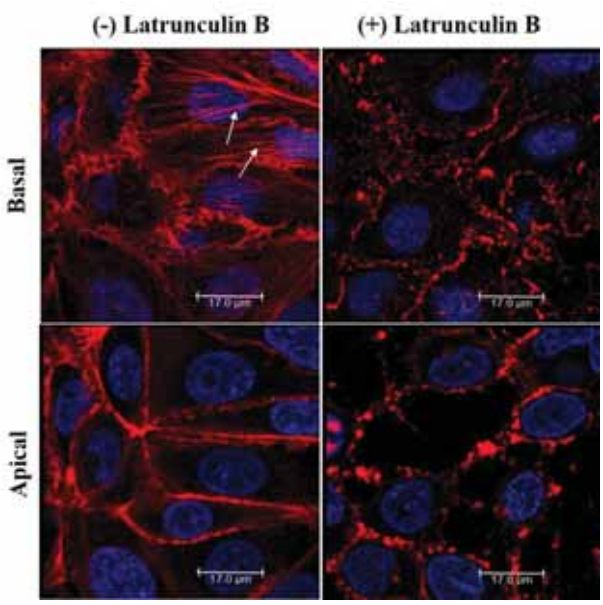

Figure 1.5.4.1: Blocking of actin polymerization in HCE cells by latrunculin B: HCE cells were treated with latrunculin B for 2hrs and actin filaments were stained with TRITC phalloidin (red) and nucleus was stained with DAPI (blue). White arrows indicate the actin stress fibers.

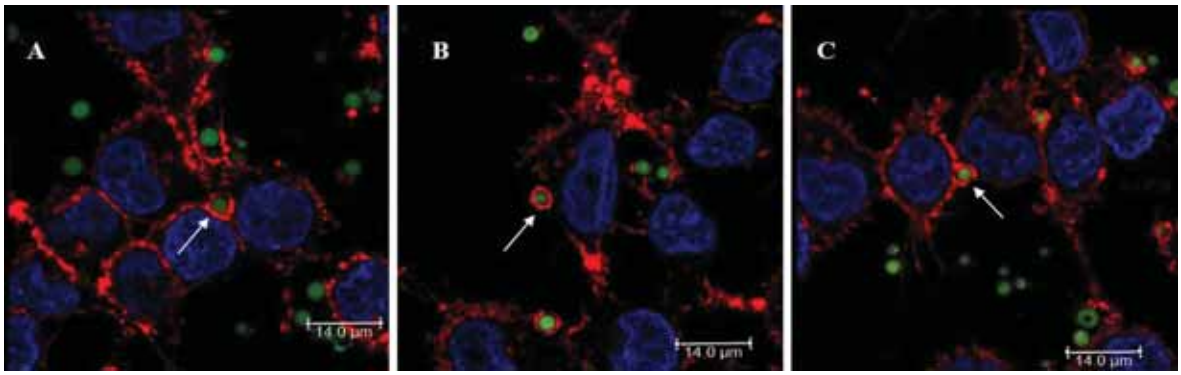

1.5.4.2: F-actin staining of HCE cells infected with A.flavus isolates in the presence of latrunculin B: Confocal images showing actin filaments (red), FITC-conidia (green) & host DNA (blue). Actin recruitment in the presence of latrunculin B was indicated as white arrows in HCE cells infected with A.flavus isolates A) ATCC 200026, B) CI 1698 & C) CI 1123.

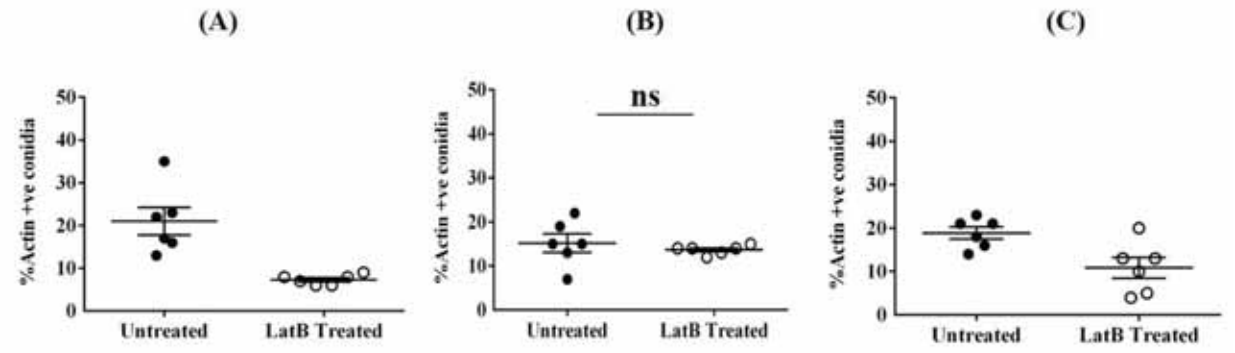

1.5.4.3: Effect of latrunculin B treatment on the engulfment of A.flavus by HCE cells: HCE cells were pre-treated with 1μM latrunculin B for 30min and infected with A.flavus isolates for 30min in the presence of drug. % Actin positive conidia was calculated from the confocal images. The scatter plot shows the % actin positive conidia of HCE cells infected with A.flavus isolates A) ATCC 200026, B) CI 1698 & C) CI 1123 in the presence and absence of drug.

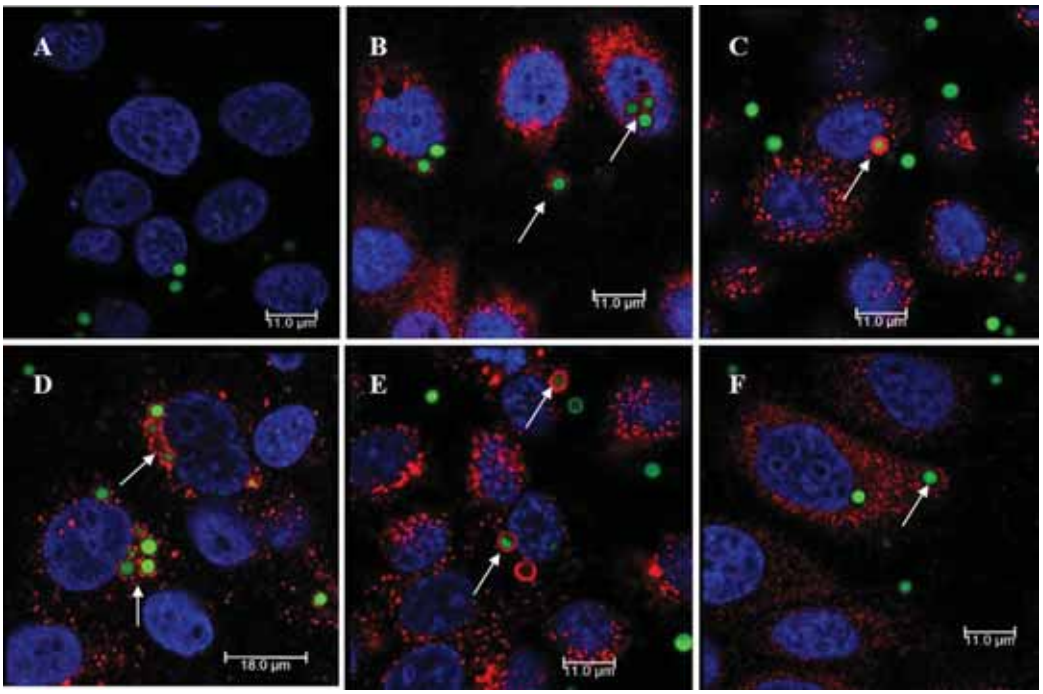

Figure 1.5.5.1: Maturation of A.flavus containing phagosomes in HCE: HCE cells were infected for 3hrs with A.flavus (ATCC 200026). Cells were stained for early and late endosomal markers (Red). A) Negative control B) CD71 C) EEA1 D) Rab7 E) LAMP1 F) Cathepsin D. A.flavus conidia is labelled with FITC (green) and host nucleus is stained with DAPI (blue). White arrows indicate the conidia within early and late phagosomes.

At 3hrs of infection the engulfed conidia were colocalized with proteins present in early (CD71 & EEA1) and late (Rab7, LAMP1 & Cathepsin D) endosomes.

1.5.6 Conclusion:

Human Corneal Epithelial cells engulfed the *A. flavus* and it was trafficked from early phagosomes to late phagosomes. Further the fate of pathogen and host after infection has to determined.

1.6 Identification of cross linked peptides of novel chemical cross linker treated cornea

Investigators : Prof. Rachel Williams[1], Dr. N. Venkatesh Prajna[2], Dr. O.G. Ramprasad[3], Dr. Atikah Haneef[1], Prof. K. Dharmalingam[3], Prof. Colin Willoughby[1], Dr. Naveen Radhakrishnan[2], Dr. Kishan Prajapati[2], Mrs. Karpagam[4] & Dr. Kannan[4]
1. Dept. Of Eye and Vision Science, Institute of Ageing and Chronic Disease, University of Liverpool, UK;
2. Aravind Eye Hospital, Madurai;
3. Aravind Medical Research Foundation, Madurai;
4. Aurolab,Madurai

Team Members : Ms. A. Divya, Mr. Naveen Luke Demonte, Ms. K. Priyadharshini, Ms. Jessica Judith Nunes, Ms. T.R. Divya

1.6.1 Introduction:

Keratoconus is a progressive, non-inflammatory eye disorder in which the normal round cornea thins and begins to bulge into a cone-like shape. This cone shape deflects light as it enters the eye on its way to the light-sensitive retina, causing distorted vision. Treatment options include the use of rigid contact lenses or penetrating keratoplasty in extreme cases. Recently keratoconus is treated with cross linking approach which improves the biomechanical stability of corneal stroma. This approach consists of irradiation with ultraviolet-A (UVA) in the presence of the photosensitizer, riboflavin (RF), as a chromophore, to stop progression of the keratoconus syndrome. The disadvantage of this method is the removal of epithelium which is not only painful but also presents a potential risk of corneal surface infection. As an alternative approach, a novel chemical cross linker NHS:EDCI:SA was used to treat keratoconus and the concentration of chemical cross linker was standardized at Liverpool. This

study focuses to identify the crosslinked peptides of novel chemical cross linker treated cornea by mass spectrometry.

1.6.2 Cross linking of model protein lysozyme:

30 µg of lysozyme was incubated with 15mM of NHS:EDCI:SA (1:1:1) for 15min at 37ºC. The crosslinked sample was analyzed in 1D SDS-PAGE.

Cross linked lysozyme dimer was observed around 30kDa. Cross linking was not 100% efficient since the monomer was observed in 1D SDS-PAGE (Fig 1.6.2.1).

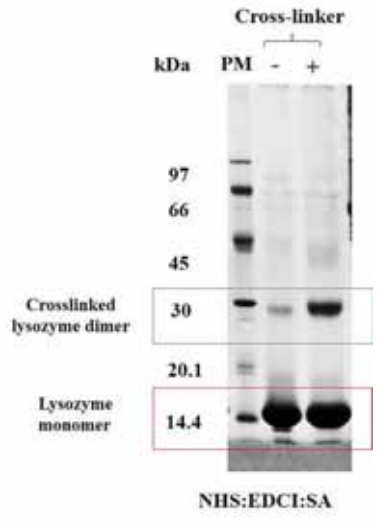

Figure 1.6.2.1: Lysozyme cross linked with NHS:EDCI:SA. 12.5% 1D SDS-PAGE of lysozyme treated with and without cross linker. Concentration of lysozyme used- 30µg. Gel was stained with colloidal Coomassie-G250. Length of gel-7cm. Red box- Monomer; Blue box: Dimer.

1.6.3 Cross linking of human Collagen I:

15 µg of collagen I was cross linked for 15min at 37ºC with different concentrations of cross linker (NHS:EDCI:SA). 1D SDS-PAGE was used to analyze the crosslinked samples (Fig 1.6.3.1).

In the presence of cross linker, the molecular shift in the collagen I chains (monomer & dimer) were observed and intensity of collagen I chains

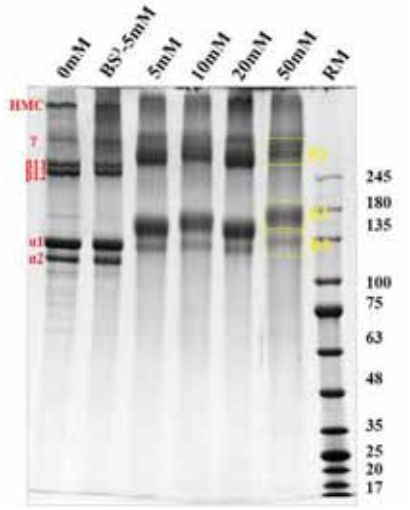

Figure 1.6.3.1: 1D profile of cross linked collagen I. 15µg of collagen I treated with different concentrations of cross linker was fractionated in 4-12% gradient 1D SDS-PAGE. Gel was stained with colloidal Coomassie-G250. Length of gel-7cm. Yellow box- Processed for mass spectrometry.

was decreased. At 50mM, molecular shift was observed very distinctly, which was taken for mass spectrometric identification of cross linked peptides. Gel pieces were destained, in gel digested, peptides were extracted and purified using C18 spin column for LC-MS/MS analysis.

EDC-NHS crosslinked peptides were higher when compared to that resulting from EDC-NHS-SA. The number of cross linked peptides were higher in the Band 1, which is the crosslinked form of collagen. Around 78% of cross linked peptides were identified and nearly 22% of peptides identified were non-crosslinked peptides at 50 mM conc. of the crosslinker.

1.6.4 Cross linking of Human Corneal Epithelial cell line:

Human corneal epithelial cells were treated with 183mM of cross linker (NHS:EDCI:SA) or 1X PBS for 15min at 37ºC. After treatment epithelial cells were

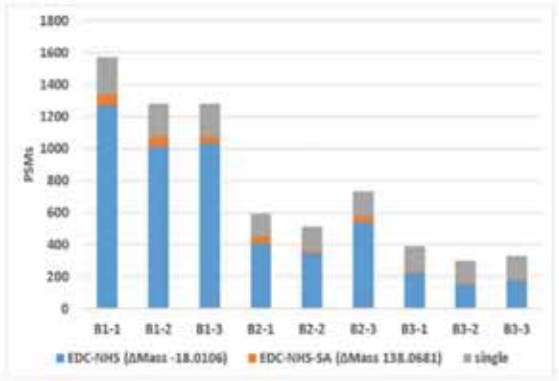

A

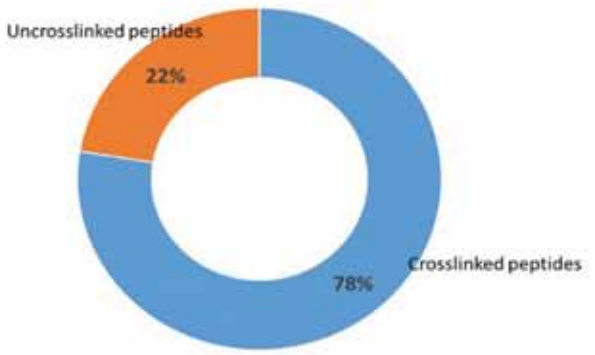

B

Figure 1.6.3.2: Kojak analysis results of 50mM cross linker treated Collagen I. A) Cross linked peptides resulting from both EDC-NHS and EDC-NHS-SA identified in all the three bands. B) % of crosslinked and non-crosslinked peptides

solubilized with 0.1% triton X-100 and soluble and insoluble fractions were separated by centrifugation. Protein content was estimated and the profile was checked in 1D SDS-PAGE.

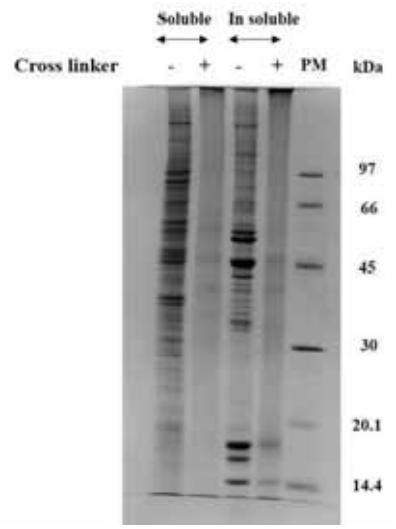

Figure 1.6.4.1: Cross linker treated epithelial cell line protein profile. 20µg of epithelial cell line proteins with and without cross linking treatment, fractionated in 12.5% 1D SDS-PAGE. Gel was stained with colloidal Coomassie-G250. Length of gel-13cm.

In the presence of cross linker, no protein bands were observed. Since the cell monolayer was immersed in the cross-linker solution, it penetrated in to the cells well and completely cross linked all the proteins. As, the molecular weight of cross linked protein was too high, it didn't enter into the gel.

1.6.5 Cross linker treatment in cadaver cornea:

Cadaver cornea was submerged in 183mM cross linker solution for 15min at 37ºC. After cross linker treatment, it was washed with 1X PBS and the epithelium, stroma and endothelium layers were separated. Proteins were extracted from all three layers of cornea and analyzed in 1D SDS-PAGE.

In the presence of cross linker, no protein bands were observed in all three layers of cornea (Fig 1.6.5.1) which is similar to the cross linked epithelial cell line profile (figure 1.6.4.1). As the cadaver cornea is completely submerged in the cross linker solution, the cross linker penetrated in all the three directions and cross linked everything.

1.6.6 Cross linker treatment in human eye globe:

Human eye globe was placed in 6well plate and 10mm trephine was placed over the cornea. Cross linker solution was added on the epithelial side of cornea and incubated for 15min at 37ºC. After cross linker treatment, it was washed with 1X PBS and the cornea was excised from eye globe. Further epithelium, stroma and endothelium layers were separated from cornea, proteins were extracted and analyzed in 1D SDS-PAGE (Fig 1.6.6.1).

When the cornea of eye globe is exposed to the cross-linker solution, no difference in the protein profile was observed with respect to control. The profile of epithelium, stroma and endothelium with and without cross linking was seemed to be similar (Fig 1.6.6.1). Further mass spectrometry has to be done to identify the crosslinked proteins and peptides.

1.6.7 Conclusion

Based on the analysis of crosslinked peptides from pure collagen, majority of the crosslinking of proteins are mediated by EDC-NHS instead of the desired crosslink by EDC-NHS-SA. Only 2% of the

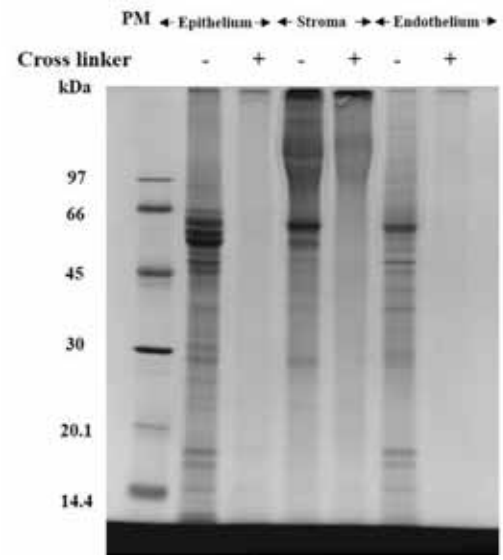

Figure 1.6.5.1: Comparison of corneal layer proteins with and without cross linker treatment of cadaver cornea. 10µg of epithelial, stromal and endothelium protein samples were loaded on 12.5% 1D SDS-PAGE and stained with colloidal Coomassie G250. Length of gel-7cm.

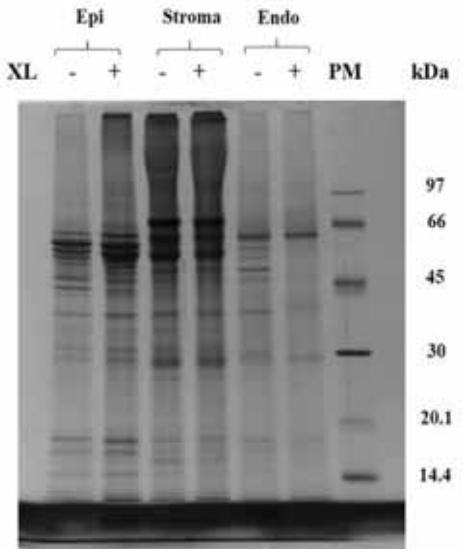

Figure 1.6.6.1: 1D SDS-PAGE profile of corneal layer proteins with and without cross linker treatment of eye globe. 10µg of corneal layer proteins fractionated in 12.5% 1D SDS-PAGE and stained with colloidal Coomassie G250. Length of gel-7cm.

total crosslinking has SA as a spacer. In 1D SDS-PAGE level, no difference in the profile of corneal layer proteins were observed when cross linker was exposed to the eye globe. Further mass spectrometry has to be done to check for cross linking.

1.7. Characterization of multiple proteoforms of alkaline protease secreted by *A. flavus*

Investigators : Prof. K. Dharmalingam, Dr. J. Jeya Maheshwari
Clinician Scientists: Dr. N. Venkatesh Prajna, Dr. Lalitha Prajna
Team Members : Mr. S. Mohammed Razeeth

1.7.1 Introduction

Alkaline protease is one of the most abundant exoproteins of *A. flavus*. Using a 2D approach, the existence of secreted alkaline protease (Alk) in 24 different proteoforms was observed (Selvam et al., 2015).

Alkaline protease was purified and its two proteoforms of 37kDa and 28kDa were examined. The organization of the isoforms was analysed using mass spectrometer bioinformatics analysis of the translated protein and the protein found in purified fraction.

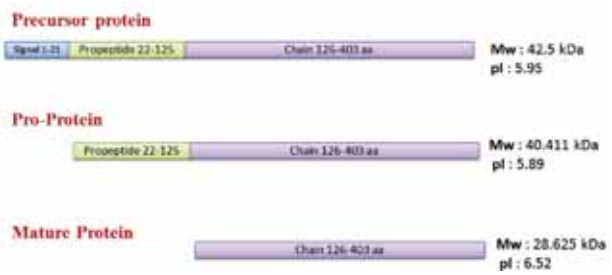

Fig 1.7.1.1: Different forms of alkaline protease

Alk has 403 amino acids of which 1-21 amino acids correspond to the signal peptide followed by propeptide (22-126 aa). The calculated molecular weight of the secreted form of Alk after removal of the signal peptide and propeptide is 28 kDa (277 aa) (Fig.1.7.1.1).

The 37kDa form was the predominant form. Analysis of the MS data of these two proteins showed that the 37kDa form of Alk is the protein with the pro-peptide (Fig 1.7.1.2).

It was demostrated previously that both proteoforms are functional and the proteoforms are several fold highly expressed in corneal isolates compared to saprophytes.

1.7.2 ATCC26 as the reference

Alk level is higher in all corneal isolates when compared to that in ATCC strain (a non-corneal

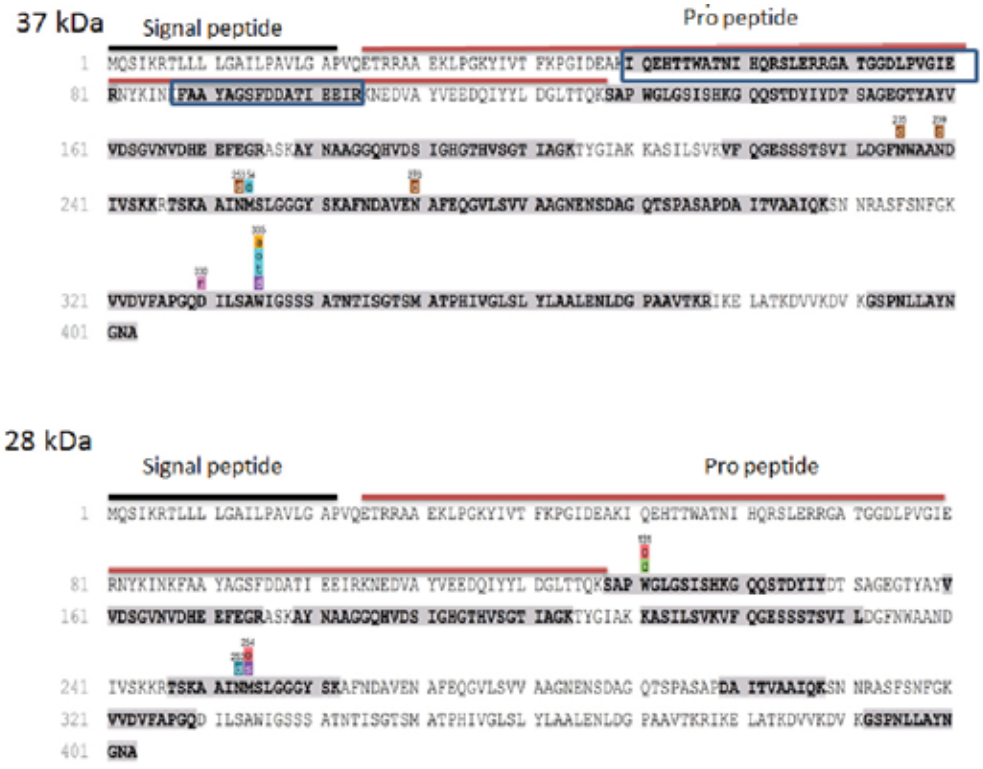

Fig 1.7.1.2. Comparison of peptide coverage for the 37 and 28 kDa forms of Alk

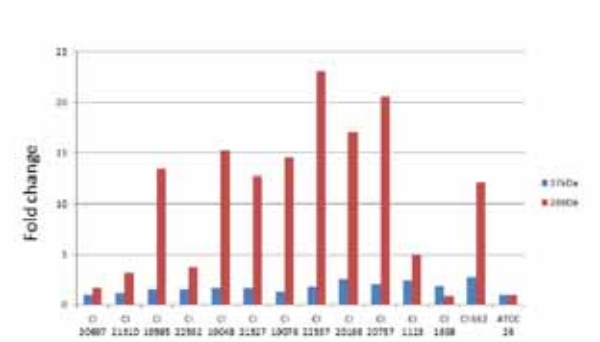

Fig. 1.7.1.3. Relative quantification of Alk 37 and 28 kDa forms across the corneal isolates with

A.flavus strains	Clinical significance
ATCC26	Saprophyte
CI1698	Healed (less virulent)
CI1123	Surgery (more virulent)
CI19565	Surgery (more virulent)
CI21310	Healed (less virulent)

Strain	ATCC26	CI1123	CI1698	CI19565	CI21310
Number of Reads (Million bp)	5	4.7	4.9	6.1	3.7
N50	57898	66721	54351	59529	51079
Maximum length	323045	275466	376828	252544	254220
Contigs	2427	3386	3321	3951	1641
Scaffolds	1107	1177	1009	1346	1614
Assembly Size(Mb)	36.58	36.56	36.57	37.55	36.69

isolate). Data in Figure 1.7.1.3 indicates that the 28 kDa proteoform shows higher fold variation in clinical isolates than the 37 kDa form. The significance of difference in the levels of the two forms of Alk is currently under study.

1.7.3 Work done during this period

In order to confirm the presence of multiple proteoforms, whole genome sequence analysis of the following clinical isolate was performed. The sequencing results are shown in the table. In one clinical isolate, presence of extra DNA shows genome expansion is common among filamentous fungi.

1.7.4 Work to be undertaken

Further the identification of other proteoforms in the fungal exoproteome and also their role in infection will be examined. In order to examine the virulence properties of various isolates whole genome sequencing of saprophytes and clinical isolates were completed. Genome annotation & Genome wide comparison for the five isolates is in progress.

Characterization of *A. fumigatus* and *A. flavus* exoproteomes during early stages of propagation

Investigators : Dr. Lalitha Prajna, Dr. J. Jeya Maheshwari, Prof. K. Dharmalingam Dr. Rabbind Singh

Team : Lakshmi Prabha, Project Fellow; Mohammed Razeeth, Project Fellow

Funding : Indo-French Centre for Promotion of Advanced Research

Rationale of the study

Aspergillus flavus and *Aspergillus fumigatus* are important human pathogens, the former responsible for corneal infections while the latter causes lung infection. During all stages of growth, fungus secretes a wide range of biological macromolecules including proteins. In pathogenic fungal species, secreted proteins play a crucial role in the establishment of infection. They are usually the main effectors that mediate interaction between the host and the fungus. The composition of the exoproteome is therefore a

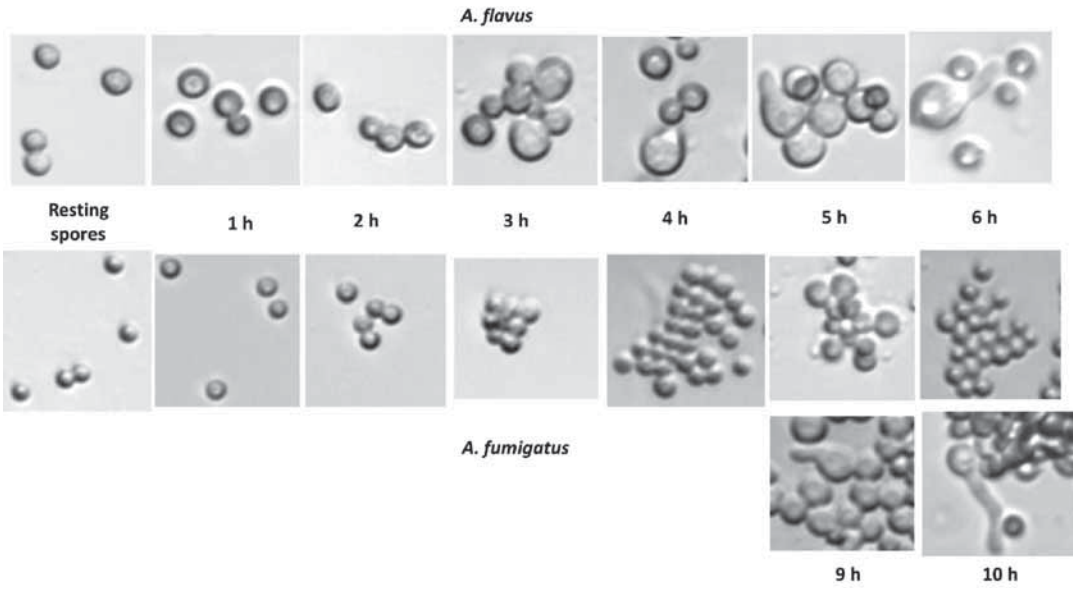

Figure 1.1. Time course analysis of growth of A. flavus and A. fumigatus. Equal number of spores (1X109) of each Aspergillus species were inoculated in 25 ml of Czapak-Dox broth and incubated at 30 °C with shaking at 200 rpm. At the indicated time points, the spores were observed under phase contrast microscope.

signature of each specific fungus and is dependent on the environment it encounters. Secreted proteins of the germinating conidia are probably the earliest fungal factors that help the pathogen to invade the host and could include potential virulence factors.

Objectives

- To identify the extracellular proteins of A. flavus and A. fumigatus conidia during germination
- Compare the exoproteins of A. flavus and A. fumigatus to understand the common and unique signatures of these two pathogenic species

Comparison of the germination of *Aspergillus* spores

Different stages of growth from resting spores to germination were compared in *A. flavus* and *A. fumigatus* through a time course analysis (Fig1.1).

A. flavus spores started swelling by the second hour and clumping was observed. The percentage of swollen spores increased in four hours, the germ tube emerged by the fifth hour and increased in length by the sixth hour. *A. fumigatus* spores were swollen and clumped by two hours but did not show any germ tubes until 8 hours. Spores had small emerging germ tubes by 8 that increased in length by 10th hour. In the minimal medium at a growth temperature of 30°C, A. flavus seems to grow faster than *A. fumigatus* based on the time required for the spores to form germ tubes. There was a heterogeneity in the rate at which the *Aspergillus* spores exited dormancy. Synchronized germination among all the spores were not observed. Only a smaller fraction (~15-20%) of the spores were found to germinate. When the growth of the spores was monitored for longer time duration, more than 95% of the spores had formed hyphae suggesting that the rate at which the spores break their dormancy is variable and lack of viability was observed in less than 5% of the spores.

Analysis of exoproteins of germinating conidia

The secreted proteins from the culture supernatant at 6 h and 10 h for *A. flavus* and *A. fumigatus*, respectively were prepared. The proteins were resolved on a 12.5% SDS-PAGE and compared as shown in Figure 1.2. The protein profiles were distinctly different between *A. flavus* and *A. fumigatus*. Each species has its own unique set of abundant protein as inferred from the SDS-PAGE profile.

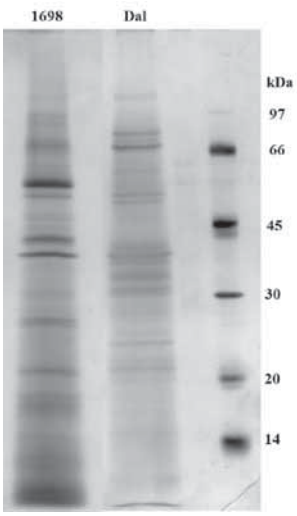

Figure 1.2. Comparison of the germinating conidial exoproteins of Aspergillus species. Spores (1X109) of A. flavus (1698) and A. fumigatus (Dal) were inoculated in 25 ml of Czapak-Dox broth and incubated at 30 °C for 6 h and 10 h, respectively. Exoproteins were prepared using optimized protocol from 14 ml of culture supernatant and resolved on a 12.5% SDS-PAGE. The proteins were visualized after silver staining.

Mass spectrometric identification of exoproteins of germinating conidia

Exoproteins of *A. flavus* (1698) and *A. fumigatus* (Dal) were identified using a shot-gun mass spectrometry analysis. A summary of proteins identified is given in Table 1.1.

The total number of proteins identified in Dal is lesser than that in 1698. This could be attributed to the difference in the amount of proteins secreted by the two species as every other condition such as the initial spore inoculum number, culture conditions, exoprotein preparation were identical.

Comparative analysis of the secreted proteins of *A. flavus* and *A. fumigatus*

The proteins identified in each species was subjected to orthology search using g:orth and the results of this analysis is given in Table 2.

By comparing the *A. flavus* proteins with the orthologs for *A. fumigatus* proteins (and vice-versa), it was found that 72 secreted proteins of the germinating conidia to be identical between the two species. The top abundant protein in both species was Bgt1, a 1,3-beta-glucanosyl transferase. Many of the common proteins were comparable in terms of

Table 1.1. Details of MS identification of exoproteins

	Identification based on one or more peptide identification	Identification based on two or more peptides identification
A. flavus (1698)	323	207
A. fumigatus (Dal)	209	132

Table 2. Details of the ortholog search for Aspergillus exoproteins

	Total number of proteins identified	Number of proteins with orthologs	Number of proteins for which no orthologs exist
A. flavus (1698)	323	231*	92
A. fumigatus (Dal)	209	184#	32

** 7 proteins of A. flavus mapped to two proteins each in A. fumigatus*

 # 5 proteins of A. fumigatus mapped to two proteins each in A. flavus and one protein mapped to three A. flavus proteins

abundance as evidenced by their PSMs. However, a subset of proteins was identified with high PSMs in one species but with relatively low PSMs in the other. These proteins were identified in both the secretome but an abundance in only one species suggest a specialized requirement for that protein in that *Aspergillus*.

Enrichment analysis of the exoproteins

Based on the GO term - biological processes, there was an enrichment of a proteins in the primary metabolic process, that included those involved in carbohydrate metabolism and proteolysis. When enriched based on the GO term – molecular function, majority of the query proteins were categorized as those with catalytic functions. Nearly 72% and 60% of proteins secreted by *A. flavus* and *A. fumigatus*, respectively during germination were enzymes.

Germinating conidial exoproteins are involved in carbohydrate metabolism

When a spore swells and germinates, a crucial event that occurs during this growth process is the softening of the cell wall. Softening of the cell wall involves the reorganization of the cell wall components to accommodate the emerging germ tube and subsequently, the hyphae. This process involves synthesis, breakage and reorganization of the existing cell wall polysaccharides. Hence, the team analysed the polysachharide metabolic enzymes that are secreted during germination.

β-glucan modifying enzymes

There are 46 β-1,3-glucan modifying enzymes in the *A. fumigatus* genome. Of these, 15 β-glucan modifying enzymes were identified in *A. fumigatus* (Dal), while 14 were identified in *A. flavus. A. flavus* and *A. fumigatus* share 12 common β-1,3-glucan modifying enzymes in the conidial exoproteome. Dal had three extra glucanases of which two did not have orthologs in *A. fumigatus* and, *A. flavus* had two extra glucanases and although both had orthologs in *A. fumigatus*, they were not identified in the *A. fumigatus* secretome.

The conidial exoproteins of *A. flavus* and *A. fumigatus* has a representation of all the five subtypes of β-1,3-glucan modifying enzymes. The identification of endo, exo β-1,3-glucanases along with the branching, elongation and cross-linking enzymes with high confidence as suggested by the number of PSMs indicate that these enzymes might be involved in the reorganization of the cell wall β-1,3-glucans during the germination of the conidia. The representation of each subtype of β-1,3-glucan

modifying enzymes by more than one enzyme indicate the redundancy in the enzymes for the different aspects of β-1,3-glucan modification. This redundancy also explains why single gene knockouts of many these enzymes always do not significantly affect the germination or growth of the mutants.

Chitinases

Fungal chitinases have an important role as that of glucanases during fungal morphogenesis by participating in the cell wall remodeling. Chitinases in *Saccharomyces cerevisiae* similar to that identified in *Aspergillus* have been reported to play a role chitin degradation during cell division and in Asci formation. Similar to *S. cerevisiae* proteins, *Aspergillus* chitinases might also be involved in chitin degradation during cell wall reorganization.

Alpha-mannosidases

Alpha-mannosidases have crucial role in protein glycosylation. Limited information is available on the α-1,2-mannosidases of *Aspergillus*. The involvement of O-mannosylation in cell wall integrity and polarized growth has been reported in filamentous fungi. But these studies have implicated the role of class I and II mannosidases that are localized to ER, Golgi, cytoplasm or lysosome. An additional category of mannosidases includes a group of secreted mannosidases.

In this study, multiple α-1,2-mannosidases were identified in the germinating conidial exoproteome of both A. fumigatus and *A. flavus*. Additionally, beta-mannosidase was identified only in *A. fumigatus* but not in *A. flavus* secretome. These α-1,2-mannosidases belong to GH38 family of glycosyl hydrolases that have been proposed to have a function in the scavenging of degraded glycoproteins.

Virulence factors

Proteases are important factors that allow the fungal species to adapt and survive in diverse environments. *A. flavus* exoproteome included 31 proteases as against 15 proteases in *A.fumigatus*. Four main families of proteases, namely aspartic, glutamine, metallo and serine proteases were found in both 1698 and Dal. Seven proteases (5 serine, 1 metallo and 1 aspartic proteases) were common between 1698 and Dal exoproteins. There was an overrepresentation of proteases in 1698 with 24 unique proteases when compared to Dal, which had only six unique proteases.

Yet another important virulence factor in *Aspergillus* species is the allergen. *A. fumigatus* is known to produce 22 allergens of which four were found in both *Aspergillus* species during germination. *A. fumigatus* secreted another six extra allergens than A. flavus, which had only three unique allergens in its exoproteome.

Work in progress

1. Identify proteins common and unique to *A. flavus* and *A. fumigatus*, with special reference to virulence.
2. Identification of exoproteins of germinating conidia of *Aspergillus* species at 37 °C
3. Comparison of proteins identified at 30 °C and 37 °C to understand the effect of temperature on the composition of the exoproteome

Predictive biomarkers for Diabetic Retinopathy among diabetic patients and stage-specific biomarkers for NPDR and PDR

Investigators	:	Dr. J. Jeya Maheshwari, Prof. K. Dharmalingam, Dr. Rajkumar, Nalam Hospital, Theni
Clinician Scientists:		Dr. Kim, Dr. Bhanu Pratap Pangtey
Team	:	Vignesh, Project Fellow, Dr. Piyush Kohli, Research Fellow
Funding	:	Mind Tree Grant

Rationale of the study

DR is a microvascular complication that develops in both type 1 and type 2 diabetics. Beyond 20 years of diabetes, nearly all type 1 and 50-80% of type 2 diabetic patients have some form of DR. The early stage of DR is non-proliferative (NPDR) can progress from mild to moderate to severe form. A subset of NPDR patients, develop neovascularization of retinal blood vessels leading to proliferative diabetic retinopathy (PDR). At any stage of DR, patients may also develop macular edema, which is exudation and accumulation of fluids in the macular region. Both DME and PDR are associated with poor visual outcomes. As early detection is important to manage DR patients, the aim of this project is to identify predictive and prognostic biomarkers for DR that can

1. predict the subgroup of diabetics who are at high risk of developing DR
2. monitor the progression among DR

Analysis of complement activation in DR

Previously, a discovery phase study was carried out using serum from DM and PDR patients and identified 57 differentially regulated proteins in PDR. A number of complement proteins were identified

to be up or down regulated. Complement system not only produces pro-inflammatory molecules such as C3a but is also involved in the active regulation of inflammatory response. As diabetes is a chronic inflammatory disease, the team examined the activation status of the complement system by measuring the levels of the precursor and the processed form of the central complement component, C3 protein.

Complement protein C3 is the converging point of all the three complement pathways. In our discovery phase experiments, we identified C3 to be both upregulated and downregulated. On careful analysis, it was found that the 110 kDa C3b form was 7-fold downregulated while the processed form at 41 kDa, C3dg was 1.6 fold upregulated in PDR when compared to DM patient serum. Differential levels of C3b (and C3dg) can be considered as an indicator of the activation of fluid-phase complement system. C3 is an abundant protein in serum that exists in the inactive precursor form. Upon activation, a 9 kDa peptide C3a is cleaved off from the C3-α chain to form the activated C3b-α'. If this activated form does not bind to microbial or host surface, it would be inactivated immediately to form iC3b-α'1 and is later degraded to C3dg. Using a monoclonal antibody raised against an epitope within the C3dg form, all the four forms, C3-α (120 kDa), C3-α' (110 kDa), iC3b-α'1 (68 kDa) and C3dg (42 kDa) can be detected by western blot analysis (Fig. 2.1.A). To examine the activation of complement system in patients representing different stages of disease progression, six different stages of the disease spectrum – non-diabetic, pre-diabetic, type II diabetic, NPDR-mod, and PDR- were included. Serum from 20 patients in each category were collected and the top-2 abundant proteins (albumin and IgG) were depleted. The albumin depleted serum was analysed by western blot using C3dg antibody. The levels of each of the four forms of C3 were quantified through a densitometric analysis. As C3dg is widely accepted as an indicator of complement activation, the distribution of the C3dg levels after normalization with the total C3 levels were compared across the different categories as shown in Fig. 2.1.B.

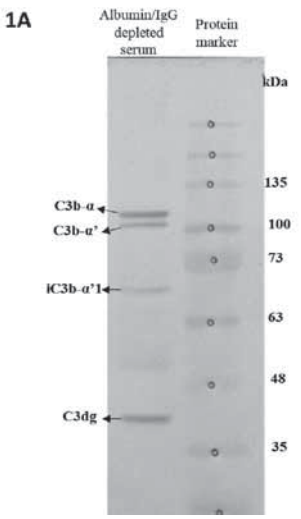

The median values of the C3dg

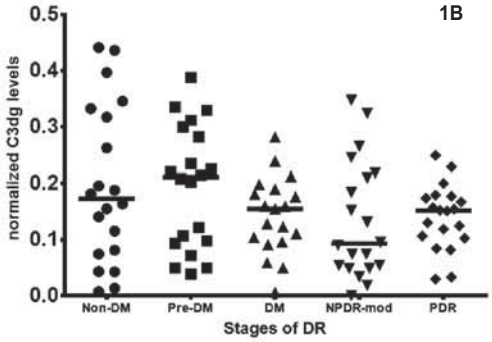

Figure 2.1. Analysis of C3dg levels across the DR disease spectrum. A. Representative blot showing the precursor C3 protein along with three processed form. Fifteen microgram of albumin and IgG depleted serum was analysed by immunoblot analysis using monoclonal antibody against an epitope in the C3dg region. B. Comparison of the normalized C3dg levels in the serum of patients from different stages of DM and DR. The median value is indicated in the scatter plot.

levels in non-DM and pre-DM does not vary much. However, the level shows a decreasing trend with DM and NPDR. Interestingly, the values in PDR patients were higher than that in the NPDR stage. Statistical analysis did not yield any significant relation between any of the two groups analyzed here. From the Figure 2.1.B, it can be observed that in all the sample category except PDR, there is a wide spread of values. However, the median value is capable of separating the samples in the non-DM, pre-DM and moderate NPDR into two clusters, while such a demarcation was not evident in DM or PDR. The correlation between the C3 processing and the progression of DR is currently being examined.

Functional analysis of circulating microRNAs and their regulatory role in Diabetic retinopathy

Investigators : Dr. O.G. Ramprasad, Prof. K. Dharmalingam, Dr. D. Bharanidharan, Dr. Kim Ramasamy

Project fellows : Ranjani Singaraj (till August 2017) and Evangeline Ann Daniel (from Nov. 2017 onwards)

Funding : SERB-Early career research grant and the Mindtree grant.

Introduction

MicroRNAs have been detected in various body fluids including serum. Levels of miRNAs in the serum of humans have been shown to be stable, reproducible, consistent amongst healthy individuals but show changes during pathophysiology, allowing them to be of potential value as clinical biomarkers of diseases

including cancers and metabolic disorders (Gilad et al., 2008).

The role of serum microRNAs in the progression of DM to NPDR and NPDR to PDR in humans is largely unexplored. Therefore, the rationale of this study is to identify the microRNAs and understand their regulatory function in the progression of microvascular complications among diabetic patients and also at the exploration of validating miRNAs as biomarkers. The major objectives of the study are:

- To reveal disease specific miRNAs from serum of PDR, NPDR and DM patients and compare it with serum samples of control healthy subjects.
- To identify potential molecular targets of differentially expressed miRNAs and their regulatory networks towards the understanding of disease pathogenesis.
- Validation of differentially expressed miRNAs for their functional implication using human retinal endothelial cell line grown under different glucose conditions and tissue biopsies from patients.

Results and Conclusion

The main approaches in the current study involved (i) analysis of select miRNAs in purified RNA samples using quantitative real-time PCR and (ii) whole miRNA profiling from serum samples of healthy control, DM, NPDR and PDR subjects using Next generation sequencing (NGS). The results from NGS experiment are described here. NGS allows us to identify the novel miRNAs differentially regulated in different stages of disease progression. Isolation of total small RNA including microRNAs from 200µl of the serum samples of DM, PDR patients, NPDR patients (mild, moderate, severe) and control healthy patients was done using Qiagen miRNA serum/ plasma kit. The miRNA yield in each sample was analyzed by Qubit miRNA fluorometric assay and has been reported in the previous annual report. Accordingly, micro RNA content was around 4-6 ng in control serum and 12-14 ng in DM, NPDR and PDR serum samples. miRNA profiles in the isolated small RNA population were analyzed using a Agilent Bioanalyzer (Fig.:1)

Small RNA library preparation and NGS

For library preparation, we used 10ng of the eluted small RNA using TruSeq Small RNA library prep kit from Illumina. The libraries were purified by loading the cDNA products into 6% TBE gels, cutting the bands corresponding to the microRNA population and purifying the cDNA construct using columns. The quality of the cDNA library was checked using a High-sensitivity DNA kit from Agilent. The quality was good with a single peak at the desired region (Fig.2). The library was normalized to 2nM. 12 pmoles of each of the four normalized samples were loaded into the flow-cell of V3 sequencing kit from Illumina. Single end sequencing was done (75 bp).

Condition	Number of MicroRNAs
Control	71
DM	146
NPDR (mild)	76
PDR	117

Table 1: Number of microRNAs identified in the serum samples of different conditions through Next generation Sequencing

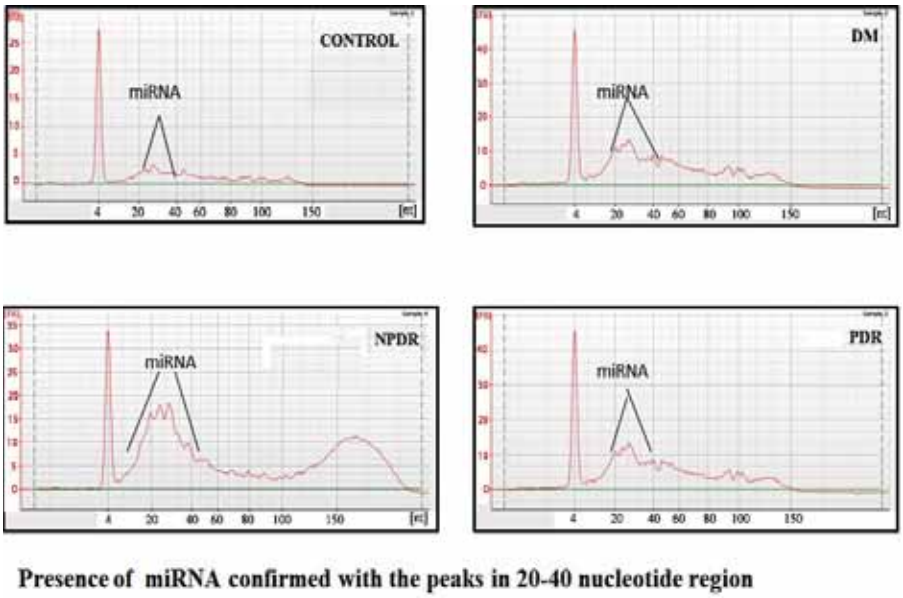

Figure 1: Electropherograms from Bioanalyzer for microRNA. miRNA were present in all the samples

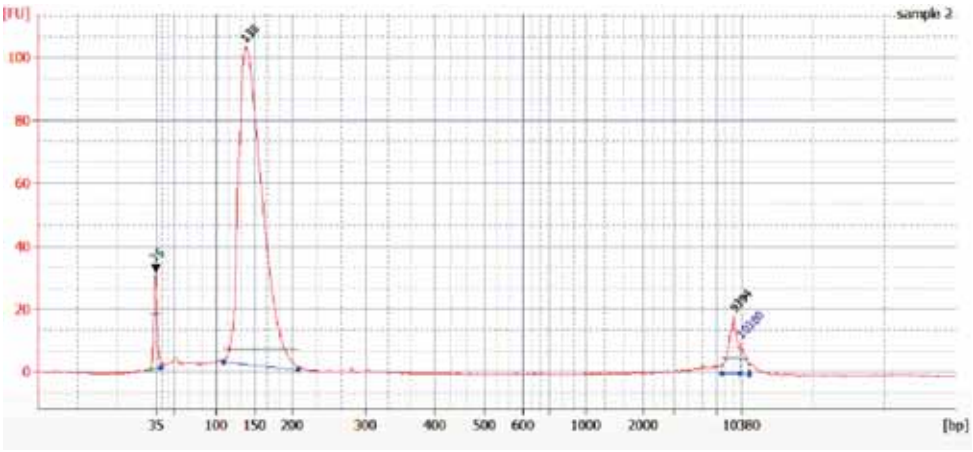

Figure 2: Representative electropherogram for cDNA after library preparation. A single peak at 150bp indicates the presence of the reverse transcribed microRNAs into cDNA along with the adapters.

The team identified hsa-miR-486-5p,hsa-miR-247,has-miR-92a-3p,hsa-miR-317,and hsa-miR-22-3p as the most abundantly expressed miRNAs in all the four conditions (Control, DM, NPDR and PDR).

Subsequent studies will analyse the differential expression of miRNAs in the four conditions, their target prediction and regulatory molecules affected using computational tools, their validation using real-time PCR and functional analysis using retinal endothelial cells.

Novel chemical cross-linking of the cornea for the treatment of keratoconus

Investigators : Prof. Rachel Williams[1], Dr. N. Venkatesh Prajna[2], Dr. O.G. Ramprasad[3], Dr. Atikah Haneef[1], Prof. K. Dharmalingam[3], Prof. Colin Willoughby[1], Dr. Naveen Radhakrishnan[2], Mrs. Karpagam[4] and Mr. Kannan[4]

Project fellows : Ms. T.R. Divya, Ms. A. Divya and Ms. Priyadharshini

1.Dept. of Eye and Vision Science, Institute of Ageing and Chronic Disease, University of Liverpool, UK

2.Aravind Eye Hospital, Madurai.

3.Aravind Medical Research Foundation, Madurai

4.Aurolab, Madurai

Funding : Engineering and Physical Sciences Research Council, UK and Aurolab, India

Introduction

Keratoconus is one of the major bilateral corneal dystrophies affecting the working or the young population in the age-group of 25-35 years. It is characterized by the thinning of the cornea followed by the formation of cone shaped cornea leading to defective vision in the form of severe astigmatism. In the keratoconic corneal epithelium, the basal layer normally degenerates leading to the dissolution of Bowman's layer. Scarring, thinning and bulging of the cornea occurs in the diseased eye. Decrease in the mechanical strength of the collagen fibrils in the cornea, significant loss of ECM, defective collagen cross-linking activity lead to keratoconus (Rabinowitz, 1998; Kenney et al., 2012). Conventional corneal crosslinking treatments serve to slow and, in some cases, halt the progression of the disease by increasing collagen fibril linkages within the cornea, thereby preventing extreme curvature. The conventional crosslinking protocol involves removal of the central corneal epithelium, application of riboflavin and the illumination of the affected eye with UV-A light (370 nm, 3 mW/cm2) for 30 minutes. But, the removal of the epithelium is painful and the risk of infection is increased.

Purpose of the study

This study aimed to develop a novel chemical cross-linker using EDCI/NHS [1-Ethyl-3-(3-dimethylaminopropyl)carbodiimide/N-hydroxysuccinimide] mediated chemistry and a suberic acid spacer to cause corneal cross-linking without removing the corneal epithelium, or the use of UV-A irradiation, therefore avoiding the pain associated with the conventional crosslinking treatment of keratoconus and the risk of infection.

Results

The cross-linker was prepared as a solution containing all the three components and the optimum concentration of 1:1:1 molar ratio of EDCI:NHS:Suberic acid formulation was standardized at Liverpool. A treatment time of 15 minutes with

the 1:1:1 molar ratios of the cross-linker was also optimised at Liverpool for treating porcine corneas as well as the cell layers harvested from the corneas. The same treatment conditions were employed for treating the human corneas and the harvested corneal cells at AMRF.

The team's earlier report (2016-17), had reported the cytotoxicity of the cross-linker on cell monolayers derived from the corneal layers of the cadaver cornea and keratoconic cornea with the full concentration of the cross-linker. In experiments involving the measurement of changes of stiffness of the cornea, the corneal buttons were immersed in the cross-linker solution at various concentrations. There was an increase of 74% in the tensile strength and 2.3 fold increase in the stiffness of the keratoconic corneas treated with the full or 1/8th diluted version of the cross-linker. In this report, the results following a pseudo-clinical treatment protocol for the application of the cross-linker to the corneas are discussed. The cross-linker is applied only to the corneal epithelial surface of the cadaver corneas using a trephine (Fig.:1)

The novel chemical cross-linker at the full or 1/8th concentration did not induce apoptosis in the corneal layers as analyzed by TUNEL assay. Cells from the explant cultures of the limboscleral region of the cross-linker treated cadaver globes were nicely proliferating and adherent to the cell culture vessels. The cells from central corneal epithelial layer, stromal layer and the endothelial layer of the cross-linker treated cadaver globes maintained their phenotype intact. The cross-linker at either concentration also did not induce any gross morphological changes in the corneal layers of the cadaver cornea as seen by H&E staining of the corneal sections (Fig.: 2). The epithelium, bowman's layer, stroma and the endothelium were intact after the application of the cross-linker. Morphometrical measurements indicated that the cross-linker didn't induce changes in the thickness of the cornea.

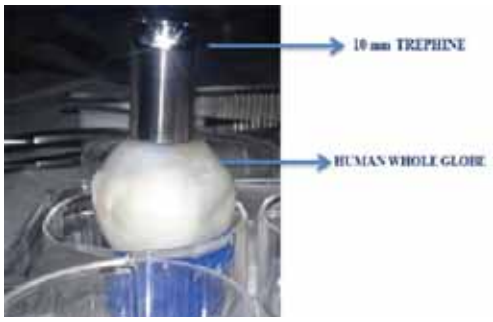

Figure 1.: Pseudo-clinical treatment protocol for the application of the cross-linker. Full concentration or 1/8th concentration cross-linker solution or PBS control was applied to the corneal epithelial surface of a human cadaver eye using a trephine for 15 min at 37˚C in a CO_2 incubator.

Cross-linker penetration assays were done using fluorescently conjugated cross-linker named NHS-FITC. The full concentration cross-linker penetrated upto 700 μm into the corneal stroma whereas the 1/8th diluted cross-linker penetrated upto 200 μm into the stroma to induce stiffening of the cornea.

Tensile test analysis of the cornea at Aurolab from the cross-linker treated cadaver globes indicated that the full concentration cross-linker treatment induced a 1.72 fold change in the stiffness of the cornea compared to the untreated PBS control. The 1/8th cross-linker treatment even induced a better 2.12 fold increase in stiffness compared to the PBS control (Fig.3).

Whole keratoconic corneas were treated with different concentrations of the cross-linker or PBS only at the epithelial surface. Live dead-assay performed on whole keratoconic cornea using fluorescent Calcein AM (live cells in green) and Ethidium homodimer (dead cells in red) indicated that live cells were significantly higher in number in 1/8th concentration cross-linker treated than in the full concentration treated keratoconic cornea (Fig.4). Hence novel cross-linker at 1/8th concentration is good to use for making a formulation for further trials.

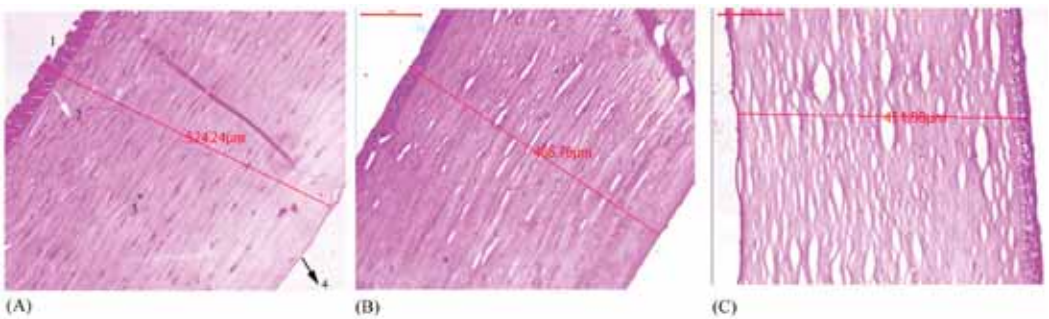

1. Epithelium 2. Bowman's Layer 3. Stroma 4. Endothelium

Figure 2: H&E staining of cadaver corneal sections from cadaver globes treated with PBS control (A) or 1/8th cross-linker (B) or full concentration of the cross-linker (C). The measurements indicate the representative thickness of the cornea in each treatment condition. Scale bar, 100 μm.

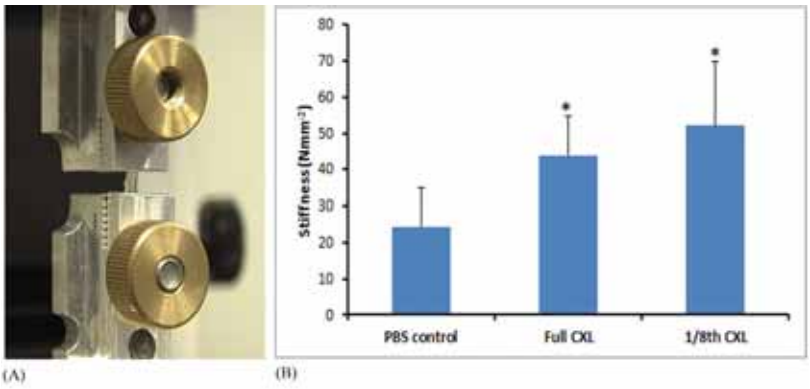

*Figure 3: (A) Adapters holding the dog bone punch shaped corneal tissue in the tensile testing machine where a force of 50N is applied from the attached load cell. (B) Changes in stiffness of the corneal tissues from PBS control treated or full concentration cross-linker (CXL) treated or 1/8th concentration cross-linker treated cadaver globes. * indicates p<0.05 in comparison to the PBS control.*

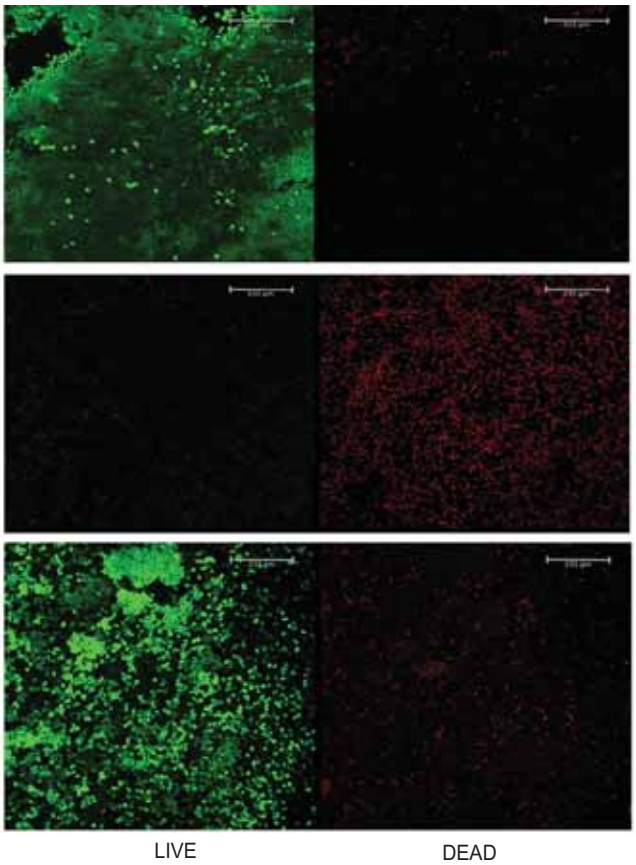

Figure 4: Whole keratoconic corneal buttons were exposed to either PBS or full concentration cross-linker or 1/8th concentrated cross-linker only to the corneal epithelial surface and live-dead assay was performed. Cells in green correspond to live corneal epithelial cells and cells in red indicate dead corneal epithelial cells.

Conclusion

The novel chemical cross-linker at 1/8th concentration increased the tensile strength and stiffness of the human keratoconic cornea as well as cadaver cornea without causing any significant cytotoxicity, change in phenotype of the constituent cells of the corneal layers or change in the gross morphology of the corneal layers and without causing apoptosis to the constituent cells of the corneal layers. The extent and the type of molecules involved in the cross-linking in the corneal layers is being analyzed by proteomic analysis. Thus, the novel chemical cross-linker is an alternative therapeutic approach to conventional corneal cross-linking for keratoconus and is ideally suitable for further clinical trials.

OCULAR PHARMACOLOGY

The main research focus of the Department of Ocular Pharmacology is to understand the molecular mechanism(s) involved in the pathogenesis and to develop appropriate inhibitors for the management of the major form of glaucoma, i.e. primary open angle glaucoma (POAG) and glucocorticoid (GC) induced ocular hypertension(OHT)/glaucoma.

In POAG, the role of RhoA/ROCK signaling in the pathogenesis of glaucoma is being investigated and the development of Rho kinase inhibitors (RKI) as a new class of IOP lowering drugs for its management. Through Wellcome-DBT funding and collaboration with University of Liverpool, the research team is engaged to address whether microRNA is playing a regulatory role in mediating steroid responsiveness or not in GC-induced glaucoma.

Studying the role of Rho-A ROCK signalling in conventional outflow pathway using Human Organ culture anterior segment (HOCAS), an implication in Glaucoma therapy

Investigators	:	Dr. S. SenthilKumari, Dr. Gowripriya, Dr. SR. Krishnadas,
Junior Research Fellow	:	S. Ashwin Balaji
Funding Source	:	Science and Engineering Research Board (SERB) (May, 2015-March, 2018)

Introduction

Aqueous humour secretion is not static, a series of physiologically dynamic processes responsible for aqueous humour circulation and the generation of intraocular pressure. In addition to diurnal variations, blood pulsations with each heartbeat transmit waves that create transient changes in IOP of 1-4 mmHg in magnitude (Ocular pulse). In in-vivo condition, this kind of biomechanical stress plays an important role in tissue remodelling, affecting cell and tissue behaviour. However, the exact mechanism by which the trabecular meshwork tissues sense and respond to different types of mechanical stimuli such as elevated intraocular pressure (IOP), circadian rhythm, ocular pulse and shear flow is not well understood.

Previously it was reported that, cyclic mechanical stress as a result of pulsatile blood flow decrease trabecular outflow facility by 30% in perfused human and porcine anterior segments and Rho kinase inhibitors have a potential role in decreasing such resistance in TM in culture. In a previous study by the team, dynamic mechanical stress (cyclic IOP) caused a 20% reduction in percentage change in aqueous outflow facility in human eyes as compared to control eyes (unpublished data). Therefore, in the present study, the effect of SB772077B (SB77), ROCK inhibitor in overcoming the aqueous outflow resistance mediated by cyclic mechanical stress in human organ cultured anterior segment (HOCAS) was investigated.

Rho kinase is a small GTPase involved in the regulation of many cellular processes. In trabecular meshwork, Rho kinase is involved in the synthesis of

extracellular matrix components and permeability of Schlemm's canal endothelial cells. HOCAS system has been exploited to understand how the RhoA/ROCK signaling is involved in sensing mechanical stress in trabecular meshwork and to evaluate the efficacy of Rho kinase inhibitor in reducing aqueous outflow resistance was investigated.

HOCAS with biomechanical stress model was established using post-mortem human eyes as described previously (Ramos and Stammer, 2008). In this study, paired eyes were used and both eyes received IOP oscillations (cyclic pulse) after baseline stabilization. The effect of SB77 (50µM) on aqueous outflow facility, activation /inactivation of Rho A-ROCK signaling and ECM protein expression was investigated. The results of the present study revealed that, treatment with SB77 significantly reduced the outflow resistance medicated by cyclic mechanical stress and the increase in outflow facility is substantiated with inactivation of RhoA/ROCK signaling and decreased expression of ECM markers.

Results

Paired eyes from donors (N=5) of a mean ± SD age of 78.6± 7.2 years were used for this study. The mean elapsed time between death and culture was 30 ± 9.2 hours and the elapsed time between death and enucleation was within 6 hours (4.4 ± 1.2 hours). A representative graph showing IOP profile in anterior segments in response to cyclic pulse in presence or absence of SB77 is shown below.

The details of human donor eyes used for the present study including cause of death, time of death, enucleation time and outflow facility in response to IOP pulsations in presence or absence of SB77 is given in the table below.

An overall decrease in outflow facility of -16 ± 7.0% was observed in anterior segments those received IOP pulsations. Treatment with 50µM SB77 caused significant enhancement in outflow facility by 15%.

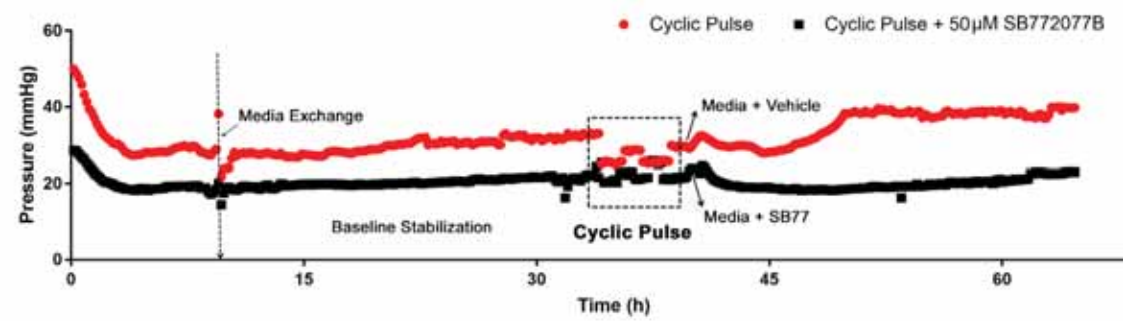

Representative graph showing IOP profile in anterior segments receiving cyclic pulse in presence/absence of SB77

Donor Code	Age (Yr) / Sex	COD	TOD-TOE (h)	TOD-TOC (h)	Δ Outflow Facility from Baseline		% Facility Change	
					Cyclic pulse	Cyclic Pulse + SB77 (50µM)	Cyclic Pulse	Cyclic Pulse + SB77
1	72 / M	Cardiac Arrest	5	27	0.85	1.27	-15.35	27.01
2	85/ M	Cerebral Injury	3.5	24	0.89	1.17	-10.53	16.67
3	70/ M	Cardiac Arrest	4.5	28	0.91	1.11	-8.65	11.20
4	85 / F	Respira-tory Arrest	3	25	0.80	1.03	-19.95	2.82
5	81/ M	Cardiac Arrest	6	46	0.74	1.19	-25.90	19.44
Mean ± SD	78.6± 7.2		4.4 ± 1.2	30 ± 9.2			-16.1 ± 7.0	15.4 ± 9.06

COD - Cause of Death; TOD- Time of Death; TOE – Time of enucleation; TOC - Time of Culture

It has been earlier documented that, the cyclic IOP (mechanical stress) not only increase the outflow resistance but also activates Rho A/ ROCK signaling. Therefore, in the present study, the status of activation of Rho A/ROCK signaling after IOP pulsations in presence or absence of SB77 was investigated by western blot analysis. The mechanism by which SB77 enhances outflow facility in anterior segments under mechanical stress was also investigated. Anterior segments showed increased activation of Rho A in response to cyclic IOP and the presence of SB77 inactivate such response. This further indicates that, the increase in outflow resistance in response to cyclic IOP is mediated through the activation of RhoA/ROCK signaling and such activation was inhibited by SB77 treatment.

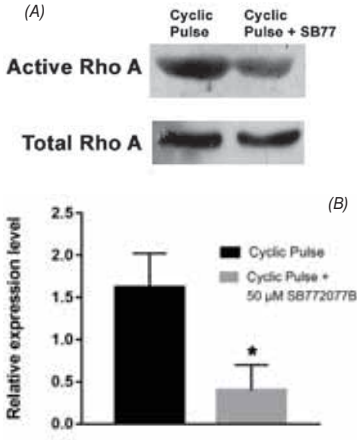

Figure showing the westernblot analysis of active Rho A and total Rho A (A) in response to IOP pulsations with or without SB77 treatment. (B) Densitometry analysis showing the fold change in the expression of Rho A. Significant decrease in Rho A protein was observed in anterior segments received IOP oscillations in presence of SB77 as compared to its untreated eyes.

Fibronectin (FN) is an ECM protein and increased accumulation in TM has been associated with increased aqueous outflow resistance in glaucoma. Therefore, in this study the levels of secreted FN in the conditioned media collected at baseline, during pulse, after pulse was investigated using Sandwich ELISA and the levels of FN in each time point is given below.

The mean levels of FN at baseline in anterior segments received cyclic pulse was found to be 235.1±9.7 ng/ml and showed significant increase during and after IOP pulsations ($p<0.5$) (during pulse: 298.6± 25.4 and after pulse: 308.4 ± 12.27 ng/ml). A significant decrease in FN level was observed in SB77 treated anterior segments which indicates that the increase in outflow facility is by reducing the secretion of FN upon SB77 treatment.

Conclusion

The findings of the present study reveal that, TM responded to biomechanical stress (Cyclic pulse/ oscillations) and showed decreased outflow facility (increased IOP). The decreased outflow facility is

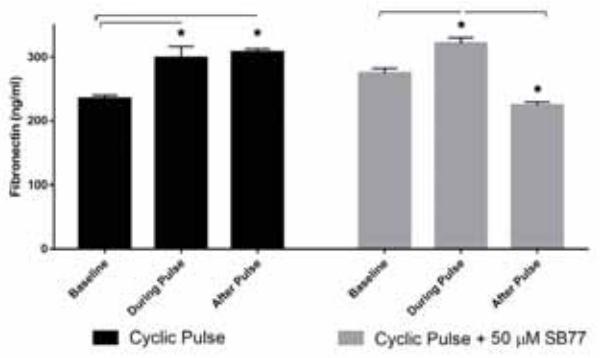

ELISA analysis showing the levels of FN in conditioned media from HOCAS with cyclic pulse in presence/absence of SB77

mediated through the activation of Rho A/ROCK pathway and increased fibronectin secretion. The presence of SB77, Rho kinase inhibitor blocked the cyclic stress mediated effects.

Role of miRNA in the regulation of Glucocorticoid Receptor (GR) signalling and development of new therapeutics for steroid-induced glaucoma

Investigators	:	Dr. S. Senthilkumari, Dr. C. Gowripriya , Dr. Bharanidharan, and Dr. R. Sharmila
International Collaborator	:	Prof. Colin Willoughby, Faculty of Life & Health Sciences, University of Ulster, Northern Ireland, UK
Research Associate	:	R. Haribalaganesh
Junior Research Fellow	:	K. Kathirvel
Research Assistant	:	T. Madhu Mithra (AMRF supported)
Funding Source	:	Wellcome-DBT/India Alliance Intermediate Fellowship (2017- 2022)

Introduction

Glucocorticoid (GC) - induced glaucoma (as a side-effect) associated with steroid use is an important clinical condition. The responsiveness of steroid varies from individuals to individuals. The susceptible individuals are at risk of developing optic neuropathy leading to blindness. Patients with primary open angle glaucoma (POAG) are 90% responders which eventually enhance the susceptibility of losing vision. However, the molecular basis for such responsiveness towards steroids is not clearly understood. We hypothesize that the microRNAs (small non-coding RNA) have a regulatory role in

mediating glucocorticoid receptor signaling and the development of miRNA mimics / inhibitors would be beneficial for GC-induced glaucoma. Therefore, the key goal of the present study is to understand the role of miRNAs in the regulation of glucocorticoid receptor (GR) signaling in the TM and to develop new miRNA therapeutics for the treatment of steroid – induced OHT/ glaucoma. In order to achieve the above research goals, the first and foremost objective of the present study is to establish steroid-induced ocular hypertension (SI-OHT) model using HOCAS.

Result

HOCAS was established with paired or single eyes. One eye received dexamethasone (DEX) (500nM) treatment and the contralateral eye received 0.1% ethanol as vehicle control after baseline stabilization. IOP was calculated every hour and average IOP of 3-5h before drug infusion was taken as baseline IOP for calculation. Mean IOP was calculated for every day after treatment. Then Δ IOP was calculated using the formula: (Actual IOP averaged over 24 h - Basal IOP of individual eyes on certain day).

The mean (± SD) donor age was 62.5± 20.8 years. The characteristics of human donor eyes used to establish steroid-induced OHT model is summarized in the table below. The elapsed time between enucleation and culture is 37.4 ± 20 h. Out of 18 eyes (8 paired eyes; 2 single eyes) studied, 6 eyes were discarded due to fungal contamination after drug treatment.

DEX-induced OHT in HOCAS

Human eyes were perfusion cultured with either 500nM DEX or 0.1% ETOH as vehicle control for upto 7 days as described previously (Mao et al.2011). A representative IOP profile after DEX (500nM) treatment is shown in the figure below.

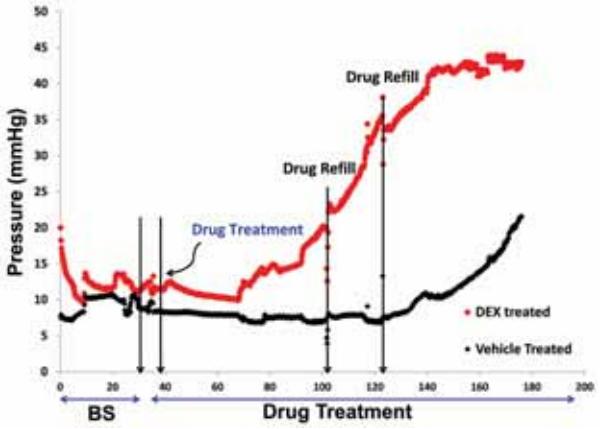

Representative intraocular pressures (IOP) graph showing the anterior segment receiving 500nM DEX or 0.1% ETOH (Vehicle) treatment. The DEX treated eye showed increase in IOP over the period of treatment as compared to vehicle treated eye.

Out of 12 eyes, 7 eyes received DEX treatment and 5 received 0.1%ETOH. The data of 2 eyes those received vehicle (17-03-OD& 17-04-OS) were excluded for the analysis. DEX treatment showed significant IOP elevation in 5/7 eyes (more than mean Δ 5mmHg). A representative data from a pair of DEX-responder is shown in the figure below.

The morphology of human trabecular meshwork in fresh and perfused anterior segment without any treatment for 7 days was assessed by light microscopy (Fig.A and B). The morphology of the TM in both eyes was similar suggesting the suitability of the system for perfusion organ culture of human anterior segment. The DEX treated anterior segment showed high deposition of pigments (ECM) (Fig.D) as compared to vehicle treated eyes (Fig C).

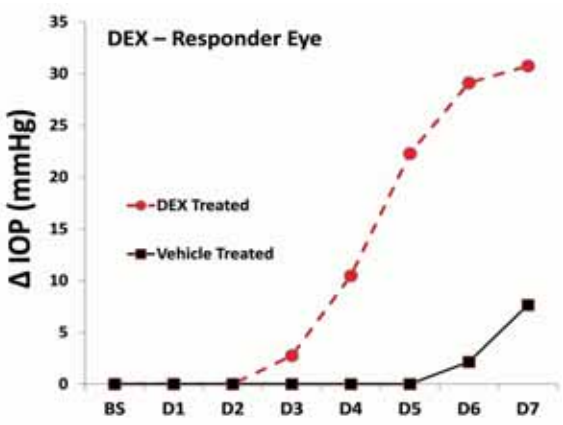

Representative data from a pair of DEX-Responder eye is shown. The mean Δ IOP in vehicle and DEX treated was calculated to be 1.40 and 13.6 mmHg respectively. Human anterior segments from paired human eyes were subjected for perfusion culture. When IOP was stable, one eye was treated with 0.1% ETOH as control (Black dots) and the fellow eye was treated with 500nM DEX (Red dots). The basal IOP on day 0 (before drug treatment) was set at 0 mmHg, and the ΔIOP was plotted over time.

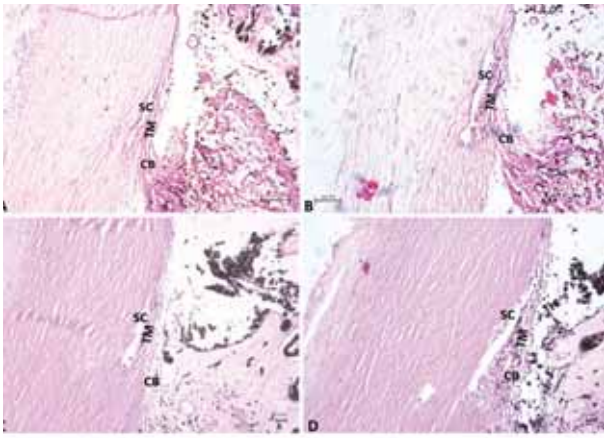

Morphology of the TM from human anterior segment without perfusion (A), after perfusion for 7 days (B), anterior segment received 0.1% ETOH as vehicle(C) and DEX treatment (D). TM-Trabecular meshwork; SC- Schlemm's canal and CB- Ciliary body.

Code	Age/ Sex	COD	Time B/W Death & Enucleation (h)	Time B/W Enucleation & Culture (h)	Experiment group	Treatment	Remarks
17-03	73/M	CVA	1.5	46	OD	0.1% ETOH	Single eye Data included
					OS	DEX	
17-04	75/M	CVA	3	48	OD	DEX	Single eye Data included
					OS	0.1% ETOH	
17-05	74/M	Respiratory arrest	4	32	OD	0.1% ETOH	Data included
					OS	DEX	
17-06*	60/F	Cardiac arrest	3	48	OD	-	Data included
					OS	DEX	
17-07	22/M	Head injury	2.5	20	OD	DEX	Data included
					OS	0.1% ETOH	
17-08	55/F	Cardiac arrest	6	46	OD	DEX	Discarded- Fungal contamination
					OS	-	
17-09	55/M	Respiratory arrest	7.15	48	OD	DEX	Discarded- Fungal contamination
					OS	0.1% ETOH	
17-11	75/F	Respiratory arrest	4	35	OD	0.1% ETOH	Discarded- Fungal contamination
					OS	DEX	
17-13*	83/F	Respiratory arrest	4	63	OD	DEX	Data included
18-03	51/F	Respiratory arrest	1.30	5	OD	DEX	Data included
					OS	0.1% ETOH	
					OS	0.1% ETOH	

** Single eyes (N=2). COD: Cause of death*

DEX-induced MYOC Expression in HOCAS

The differential protein expression levels of MYOC and FN upon DEX treatment by ELISA was investigated in cell soup collected during perfusion at different time intervals. MYOC is a secreted glycoprotein and its physiological function is unknown in TM and other ocular tissues (Stone et al., 1997; Ngyune et al., 1998). MYOC expression can be inducible in TM cells with DEX treatment and it is one of the markers for TM cell identification (Clark et al., 2000). FN is an ECM protein and increased

Expt No	ETH	DEX
17-03	1.3	1.6
17-04	1.0	0.8
17-05	0.8	2.9
17-06	-	1.1
17-07	1.3	5.5
17-13	-	3.5
18-03	4	1.54

DEX-induced MYOC protein levels by ELISA

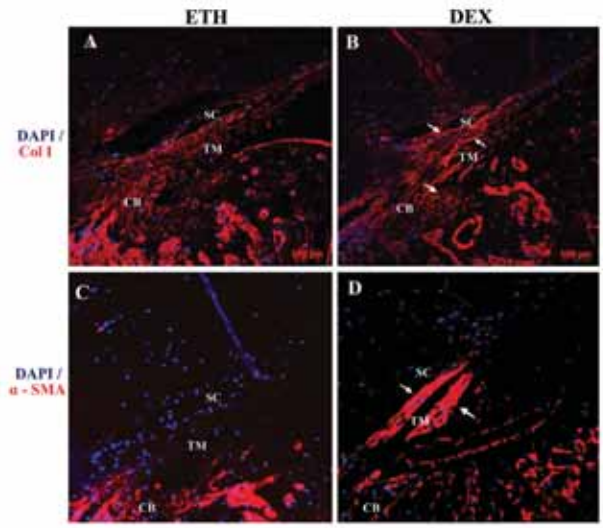

DEX increases both COL1A (ECM) and α-SMA in TM (B, D) as compared to their vehicle treated eyes (ETH) (A,C) respectively. SC-Schlemm's Cananl; TM – Trabecular meshwork; CB – Ciliary Body. Arrow indicates high positivity.

accumulation by DEX is reported previously Therefore, in the present study, the levels of secreted MYOC & FN upon DEX treatment were investigated. Out of 7 eyes received DEX treatment, 3 eyes (2 paired eyes; 1 single eye) showed more than 2 fold change (Mean (± SD) fold change: 3.9 ± 1.3 and it is summarized in the table below. Conditioned medium was collected from paired/single human anterior segments at different time intervals (Before treatment (D0), D1, D3, D5 and D7). After estimating the total protein, the samples were assayed for MYOC by Sandwich ELISA. The estimation of FN levels in cell soup is in progress.

Effect of DEX on Actin and COL IA in TM

The effect of DEX on smooth muscle actin (α-SMA) and ECM is shown below.

DEX treatment not only elevates IOP but also increases actin staining and ECM in TM region (B), as compared to vehicle treated (A). Actin staining was very prominent in JCT region of TM and outer wall of SC whereas strong positivity was observed more in TM region (D) as compared to vehicle treated anterior segment (C). The increase in COL1A correlates with increased deposition of pigments as seen in H&E staining.

Conclusion:

The findings of the present study are summarized in the table below: Out of 7 eyes received DEX treatment, 5 were graded as steroid responder eyes based on IOP profile. The non-responder eyes (based on mean Δ IOP) in question need to be reconfirmed with other parameters such as FN levels and Immunohistochemistry (αSMA & COL1A).

Expt No	Mean Δ IOP (mmHg)		MYOC (Fold Change)		Responder (R) / Non-Responder (NR)
	Vehicle	DEX	Vehicle	DEX	
17-03	Excluded	12.2	1.3	1.63	R
17-04	Excluded	18.0	1.0	0.83	R
17-05	0.67	3.2	0.8	2.94	??? NR
17-06	NA	10.5	NA	1.12	R
17-07	1.40	13.6	1.3	5.55	R
17-13	NA	4.4	NA	3.50	??? NR
18-03	1.3	9.6	4	1.54	R

Benchmarking tools for miRNA and mRNA sequence data analysis

Investigators : Dr. S. Senthilkumari and Dr.Bharanidharan

International Collaborator : Prof. Colin Willoughby, Faculty of Life & Health Sciences, University of Ulster, Northern Ireland, UK

Project Fellow : K. Kathirvel

Funding Source : Wellcome-DBT/India Alliance Intermediate Fellowship (2017-2022)

Introduction

MicroRNAs (miRNAs), about 19-22 nucleotide long, which regulates gene expression by binding with 3' untranslated region (UTR) of their target mRNAs, finally leads to mRNA degradation or translation repression. Expression levels of certain miRNAs are altered in many diseases, including Glaucoma, i.e miR-184 in ocular diseases.

Likewise, differential gene expression profiling became very easy, after the hit of RNA-sequencing, into the field of transcriptomic research. RNA-seq has been widely used technology for various aspects such

as quantification of genes/ isoforms and detection ncRNA, splice junctions, etc. miRNA and mRNA profiling through Next-generation sequencing (NGS) helps us to study their expression profiles in the pathology of steroid-induced glaucoma. Challenges of NGS are shifted from generating sequence to the analysis of large datasets computationally. Employing different tools for each steps in analysis, helps us to develop a separate pipeline to obtain the miRNA and mRNA expression profiles in steroid-induced glaucoma. There are several aligners and quantifiers, but no single pipeline for both miRNA and mRNA seq data analysis can be used in all cases. Developing miRNA and mRNA-seq data analysis pipeline for steroid-induced glaucoma will help us to better understand the pathology of the disease.

Totally, 21 miRNA-seq datasets from three different normal human ocular tissues, includes Cornea (n= 7), Ciliary body (n= 7) and Trabecular meshwork (n=7) were retrieved from SRA database which was deposited by Michelle Drewry et al., (2016). Unpublished RNA-seq data from control cornea was taken as input for mRNA-seq data analysis pipeline development. Human reference genome assembly GRCh38 was downloaded from Ensembl along with corresponding GTF (gene transfer format) annotation file for reference mapping. Known human mature miRNA dataset which contains 2588 miRNA sequences and their genomic locations were retrieved from miRBase (version 21, released on Jun 2014) for miRNA quantification. The FastQC toolkit was used to check the quality of raw reads. In miRNA pipeline, Low-quality reads were filtered with a quality cut of Phred score 20 and Illumina three prime adapter sequences (TGGAATTCTCGGGTGCCAAGG) were also removed by using cutadapt 1.9.1. Reads which are below 16 and above 30 nucleotides long were removed before the alignment by using reformat.sh shell script from bbmap short read aligner. In mRNA-

	BOWTIE	BOWTIE2	BWA	STAR
TM1	48.14	44.08	49.08	48.06
TM2	86.54	81.51	87.97	87.17
TM3	68.98	63.71	71.33	69.39
TM4	87.34	83.67	88.58	87.64
TM5	87.17	85.25	87.72	86.88
TM6	87.01	85.51	87.49	86.53
TM7	85.62	83.65	86.26	85.57
CB1	96.79	91.66	98.99	98.18
CB2	98.93	95.07	99.86	99.42
CB3	99.44	98.29	99.93	99.21
CB4	98.56	97.62	99.78	98.04
CB5	97.52	96.12	98.81	97.64
CB6	98.88	96.84	99.54	98.88
CB7	99.37	97.74	99.83	99.21
CORNEA1	93.04	87.89	98.30	92.84
CORNEA2	97.06	90.57	99.32	98.03
CORNEA3	81.66	79.04	82.56	81.34
CORNEA4	87.10	85.06	87.81	87.12
CORNEA5	89.14	84.77	90.13	89.51
CORNEA6	84.60	81.74	85.47	84.84
CORNEA7	85.62	87.20	89.09	88.11

Alignment rate of each aligners for three different ocular tissues. CB - Ciliary body; TM -Trabecular meshwork.

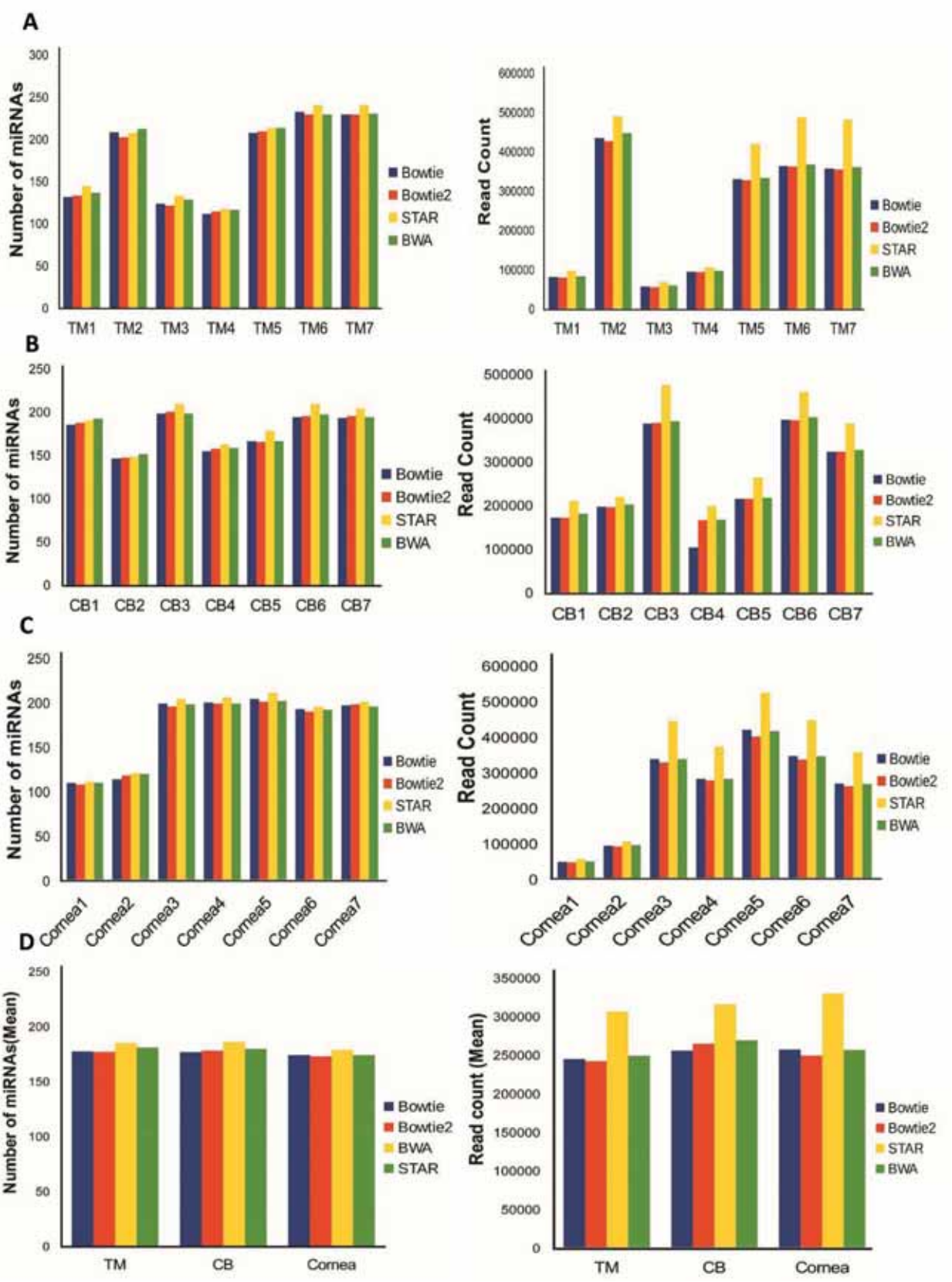

Number of miRNAs and read count of (A) TM, (B)CB and (C) Cornea obtained from various aligners. (D) Mean values of number of miRNAs and read counts from all tissues.

seq pipeline, Adapters were removed by using bbduk.sh shell script from bbmap short read aligner. Each miRNA genome was mapped with GRCh38 by four different aligners such as Bowtie, Bowtie2, BWA, and STAR. Simultaneously, two different aligners were used, TopHat and STAR to map the draft RNA-seq data with GRCh38. Latest versions of these aligners were installed in Ubuntu 16.04 operating system and ran with slight parameter changes in server equipped with 2 CPUs, 32 core and 420 GB of RAM. Featurecounts, was utilized for miRNA quantification and Cufflinks, HTSeq & Featurecounts were employed for gene/isoforms quantifications.

Results

In miRNA-seq data analysis, the average sequence reads of TM, CB, and Cornea were 447289, 540202 and 531607 respectively. On average, fifty to hundred thousand sequence reads were removed after Low-quality and nucleotide length based filter. All aligners were run continuously with different parameters until getting a better alignment rate. The comparison of alignment rate of aligners based on tissue type is shown.

Aligned reads in a BAM/SAM file format was used as input for Featurecounts miRNA quantification. After miRNA quantification from Bowtie alignment, we found 258, 303 & 235 miRNAs are collectively expressed from TM, CB, and Cornea respectively. Likewise, a total number of miRNAs and their read count from three different tissue samples (n=21) which were aligned with four different aligners were obtained and demonstrated. miRNAs, which read count is more than ten was taken for further analysis. We further, compared the number of miRNAs and read counts within and across different aligners and tissue types, and finally, STAR aligner+ Feature counts was found to be the best pipeline.

Similarly in mRNA-seq data analysis, the total reads of RNA-seq data was more than 61million after filtering. Quality-filtered reads were mapped with GRCh38 reference genome assembly by TopHat and STAR. Both aligners were run continuously with different parameters until getting a good alignment rate. The alignment rate of TopHat and STAR was 57.2% and 85.15%, respectively. Aligned BAM files were undergone for gene/isoform quantification. A total number of mRNA transcripts from three different quantifiers were obtained and shown below. TopHat+HTSeq have shown to perform better than other tools based on total number of transcripts.

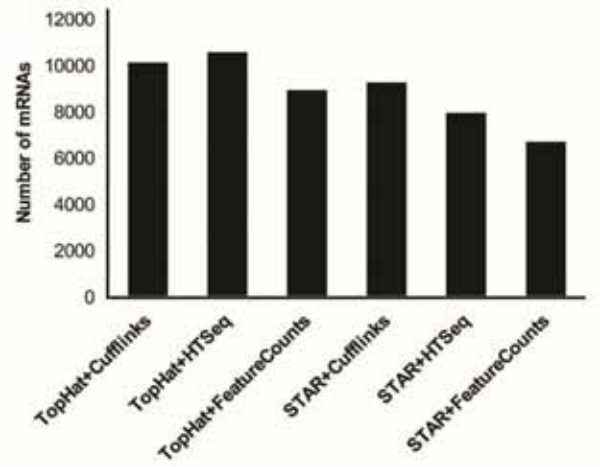

Graph showing total number of mRNAs from different combinations of pipelines

BIOINFORMATICS

The department seeks an agile and predictive understanding of the complexity of biological process and disease mechanism in eye research with the help of huge omics data from genome projects and high-throughput technology (next generation sequencing and microarray). The department write algorithms and pipelines to get critical answers faster from NGS data. It also focuses on non-coding RNA expression and their regulatory role in eye diseases by integrating data from NGS and public, in close collaboration with wet lab scientists. It has reliable infrastructure and framework comprising LINUX and Windows based servers and desktop workstations, which allow to integrate omics data and study them at systems level. It further provides to customize data analysis tailored to the needs of individual research projects across all the research groups.

Clinical exome analysis pipeline for eye disease next-generation sequencing panel

Investigator : Dr. D. Bharanidharan
Research Scholar : K. Manojkumar
Funding : DST-SERB

Introduction

Next-generation massively parallel sequencing technology enables the comprehensive genetic sequencing of all or part of the human genome, and its improvements in chemistries and workflows have paved the way into the clinical diagnostic arena. Its efficiency enables the availability of high speed and low-cost genomic sequencing of multiple samples. The whole genome sequencing (WGS), i.e. sequencing the entire genome, and whole exome sequencing (WES), i.e. sequencing the protein coding regions alone advance the discovery of novel variant/gene that is about 85 % of mutations among all the genetic variations and therapeutic interventions. WGS is now technically feasible and cost-effective, however, it is still expensive as the cost of data analysis and storage has been much higher than initially expected. Yet, WES has been the successful cost-effective tool for the discovery of casual variants for many eye diseases starting from single gene disorders and moving on to more complex genetic eye disorders, including complex traits and cancer. WES has become available as a diagnostic test performed in Clinical Laboratory Improvement Amendments - certified and College of American Pathologists - accredited clinical laboratories. Yet, it produces the large quantity of data (raw reads) that requires a significant amount of bioinformatic analysis to produce biologically meaningful information. Indeed, the output must be accurate and consistent in identification of variants that account for the impact on phenotype, shifted the current bottleneck towards to data management and analysis. The constant updates in sequencing chemistries, bioinformatics tools and reference genome, and many different tools and data formats posing a great challenge in data analysis process to obtain meaningful clinical variants. Here, the team provide an automated comprehensive analysis pipeline for clinical exome data, which would provide more accurate variant call list.

Results and Conclusions

In order to develop updated comprehensive pipeline for SNVs and InDels separately for eye diseases, the team collected all the new and updated versions of the alignment tools and variant callers as shown in the overall workflow (Fig. 1). Here, we report the updated results of benchmarking that was carried out on the exome data set, HapMap/1000 CEU female, NA12878 as a reference data since it has highly accurate and well characterized set of genome-wide reference material, including BED and VCF file of high-quality sequence regions and variant calls respectively, developed through the Genome in a Bottle Consortium (GIAB), the National Institute of Standards and Technology (NIST). In comparison, a simulated data has been generated using both hg19 and hg38 human genome for benchmarking. We performed all the evaluation work for SNVs and InDels separately for both human genome builds; analysis using hg38 human reference genome has been updated in this report.

The comparison of SNVs and InDels of NA12878 whole exome data against NIST reference call set showed different performance between aligners and callers as previously described. By combining both precision and sensitivity (F-Score), we found that six pipelines, BWA_DeepVariant, Novoalign_DeepVariant, BWA_GATK, Novoalign_

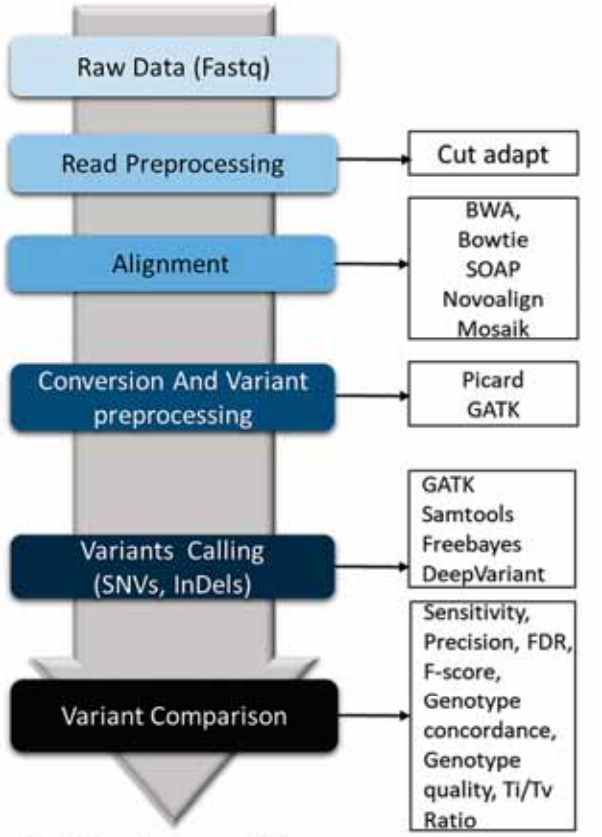

Fig.1 Analysis workflow

Figure 2. Receiver operating characteristic (ROC) curve for SNV (a, c) and InDel (b,d) performed by top 6 pipeline using NA12878 genome data. F-score was used as the function of depth (a,b) and Genotype quality (c,d)

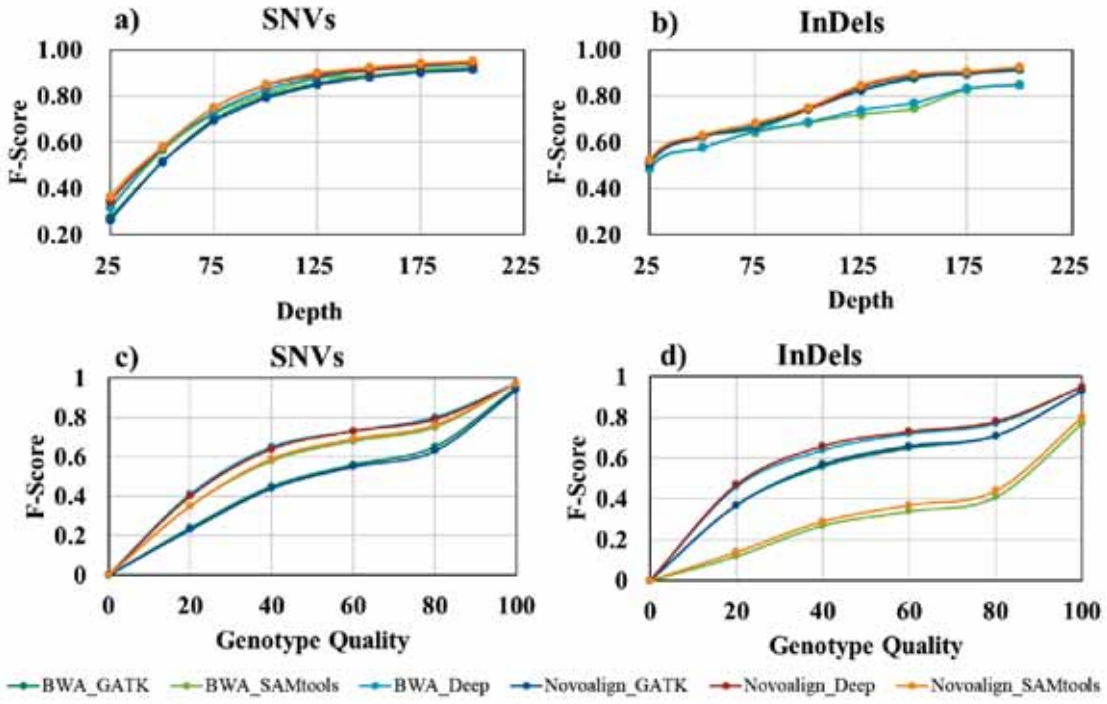

Fig.3 InDel Detection performance test using NA12878 genome data for different aligners and callers. Negative value of x-axis indicates the deletion and positive values for insertion of InDels at different length. Y-axis indicates the F-score value

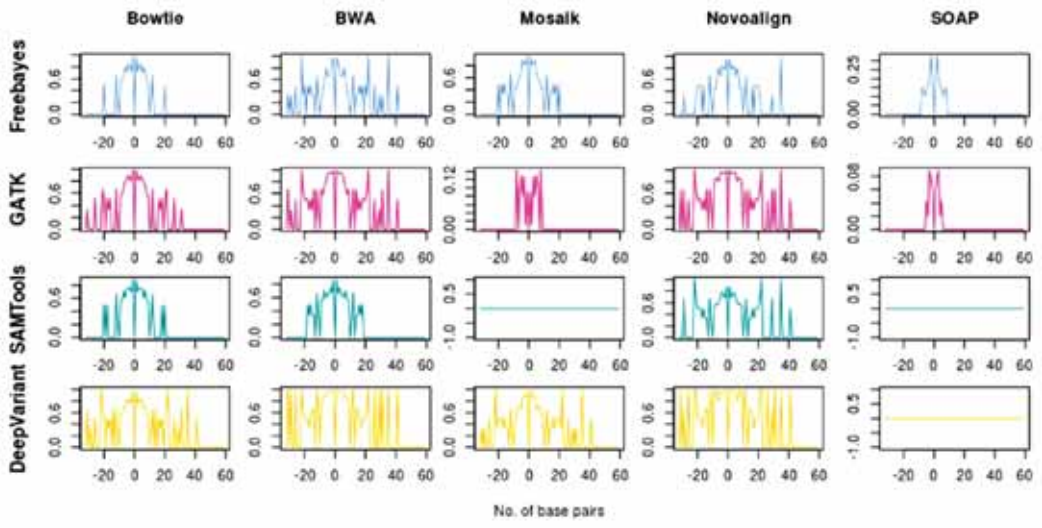

GATK, BWA_Samtools and Novoalign_Samtools outperformed well. However, there are subtle differences performance when they dealt with SNVs and InDels separately. To explore further, how depth and genotype quality affects the performance of top pipelines, the receiver operating characteristic (ROC) curves were plotted (Fig.2). About 150x most of the variants were detected, which indicates that this depth is sufficient for the analysis. All the 6 pipelines perform at roughly the same level. On the other hand, InDel detection rate was calculated based on F-score at the different base pair lengths for pipelines as shown in the Fig.3. In depth analysis of InDel detection rate at higher base pair length, showed that BWA_DeepVariant and Novoalign_DeepVariant performed well followed by BWA_GATK and Novoalign_GATK. Notably, the former 2 pipelines had accurately determined 8 deletions and 10 insertions with F-score of 1. In agreement with other previous comparison, similar results were obtained using simulated data set for both hg19 and hg38.

In order to improve the accuracy in variant detection, the concordance among top 4 pipelines BWA_SAMtools, Novoalign_SAMtools, BWA_DeepVariant and Novoalign_DeepVariant for SNVs and BWA_GATK, Novoalign_GATK, BWA_DeepVariant and Novoalign_DeepVariant for InDels along with GiaB true variants dataset were compared for SNVs and InDels separately (See Figure 4). All the top 4 pipelines had identified around 95-99% of true positive SNVs and around 89-97% of InDels using 4 different input sequences. Of these, Novoalign_DeepVariant and BWA_ DeepVariant shared the higher number of SNVs with GiaB. Whereas, BWA_ DeepVariant and Novoalign_ DeepVariant shared the most of the InDels with GiaB.

Fig. 4. Concordance of variants detected by top performing pipelines with GiaB list for SNVs (i) and InDels (ii). i&iiA. GiaB Variant call list iB. BWA-Samtools. iiB BWA-GATK. i&iiC. BWA-DeepVariant. i&iiD. Novoalign-DeepVariant. iE. Novoalign-Samtools. iiE.Novoalign-GATK

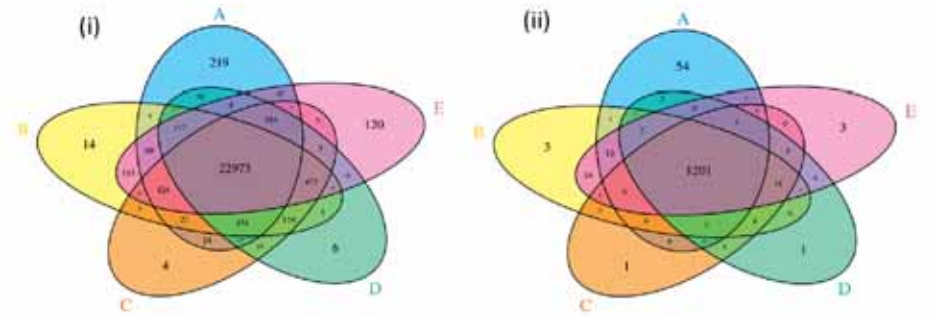

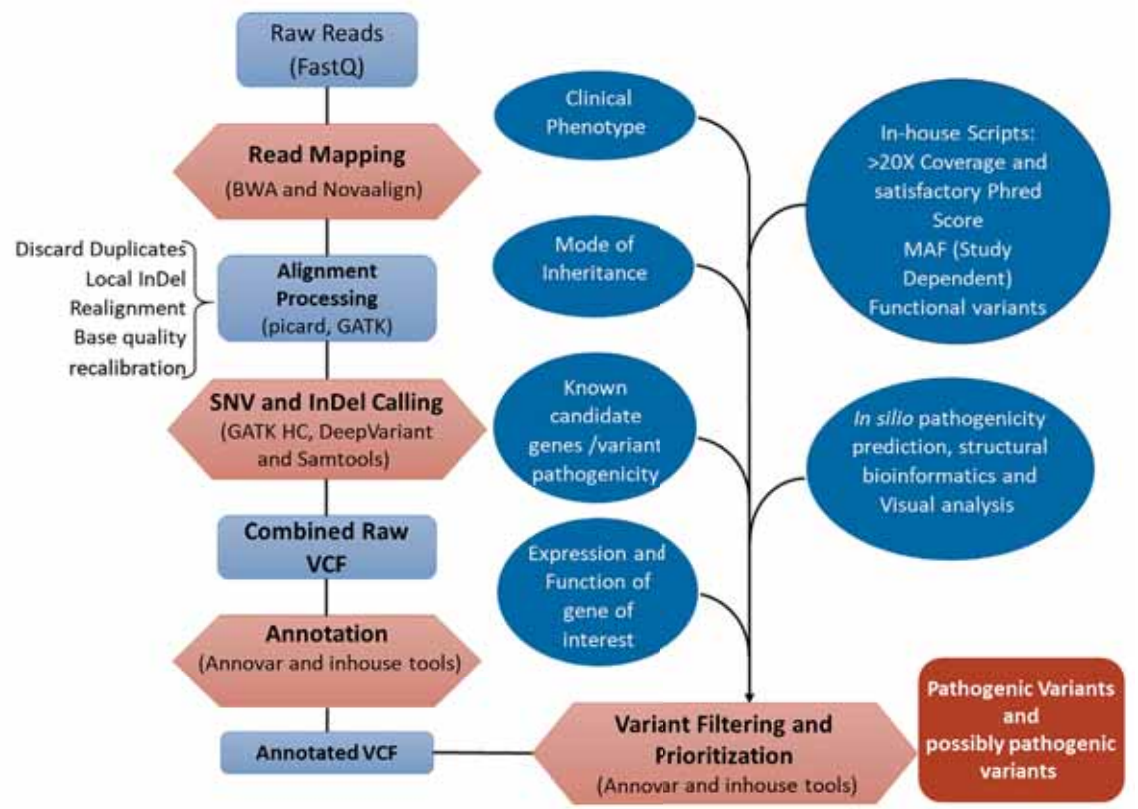

Fig.5. Clinical Exome Analysis workflow

Conclusion

Different aligners and variant callers should be used for SNVs and InDels separately for any exome data, even for the patient with eye diseases. The benchmarking results show that two aligners BWA and Novoalign can be used for both SNVs and InDels; while, amongst four variant callers, DeepVariant can be used for both, and samtools for SNVs and GATK for InDel. The team suggests the combination of top performing pipelines would yield accurate variant calling for clinical exome data. However, care must be taken for false positives in detecting causal variants. The clinical exome pipeline we use is shown in the Figure 5, where in a stringent protocol is used to prioritize pathogenic variants.

An *in silico* approach for identification of aberrant metabolic pathways in retinal angiogenesis towards early diagnosis and development of personalized medicine

Investigator : Dr. D. Bharanidharan
Postdoctoral Fellow : Dr. S. Umadevi
Funding : SERB - NPDF

Introduction

Retinal angiogenesis is found to be the leading cause of blindness in numerous clinical conditions such as diabetic retinopathy, retinal vein occlusion, age related macular dystrophy, macular edema and retinopathy of prematurity. The neovascularization in angiogenesis develops in individuals with unique metabolic switch. The analysis of altered metabolic pathways in patient may help to understand the disease status and could be attractive customized therapeutic targets. The simplest way to identify pathway aberrance is to compare normal and disease sample data from the same individual. But it is often unavailable in clinical situation, especially at the time of treatment resistance in advanced stage of disease. To achieve this, the present work uses the concept of quantifying aberrance pathway of the disease samples by comparing with accumulated normal samples from other experiments. This study majorly focuses to analyze the gene expression data obtained from microarray and RNA-Seq on series of steps, include data processing, gene-level statistics and individualized pathway aberrance score (iPAS). As the preliminary of this meta-analysis of retinal angiogenesis diseases pathways, microarray gene expression data of diabetic retinopathy samples were analyzed, and iPAS was calculated.

Results and Conclusion

Microarray data sets of human diabetic retinopathy samples along with control (GSE53257, GSE60436 and GSE70754) were downloaded from the public repository NCBI-GEO database. Among them the former was found as the outlier in the principal component analysis and excluded from the study. The rest of the datasets contain 22 disease and 11 control samples. In the data processing step, genes with multiple probes were summarized by maximum value aggregation of probe-level expression. All the samples including control in 2 different datasets were merged and quantile normalized using R scripts. This step adjusted the distribution of each experimental data so that they are comparable. Further, the gene-level statistics was analyzed by calculating Z scores, which indicates the standardized expression level by the mean and standard deviation of all the diabetic retinopathy samples. The genes with top 2.5% and bottom 2.5% of Z score were indicated as the upregulated and downregulated genes respectively (Fig. 1).

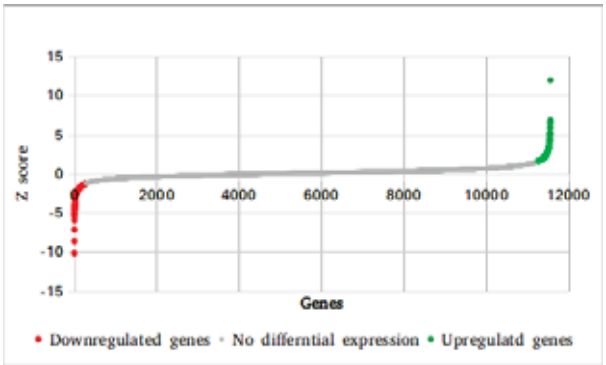

Fig 1. Z score of genes in the diabetic retinopathy samples

In the pathway level statistics, five methods were used as the candidates for iPAS including average of Z -score, Fisher's exact test, gene set enrichment analysis (GSEA) and two non-parametric tests, Euclidean distance and Mahalanobis distance. Initially, pathways associated with the differentially expressed genes was analyzed in DAVID Bioinformatics Resource 6.8. Based on the pathway information, the gene set enrichment analysis was carried out (Fig. 2). Of these, cytokine receptor interaction and PI3K-Akt signaling pathway are identified as most involved pathways, which have been shown to regulate angiognesis/cancer. The iPAS analysis reveals that, though the Euclidean distance between the diabetic retinopathy and control sample is comparatively less, that impacts the significant pathway aberration (GESA score of Fig. 3).

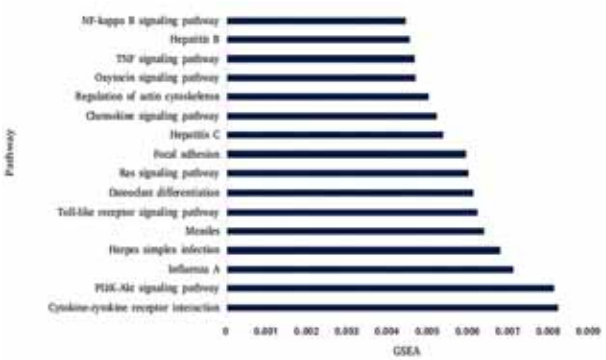

Fig 2. Gene set enrichment analysis of differentially expressed genes

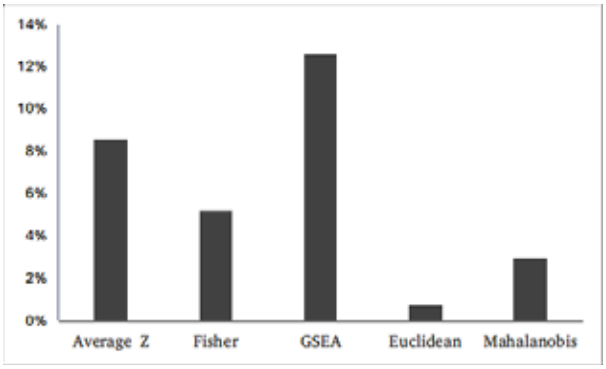

Fig 3. iPAS values of differentially expressed genes

Conclusion

This study predicts the common pathway mechanisms that regulate the angiogenesis in diabetic retinopathy using common transcriptional profiles characterized by Z-score. Further, combining all transcriptomic data of other eye diseases would detect more sensitive unique molecular aberrances of retinal angiogenesis. This would let to understand the individual's disease mechanism and helps for future application of custom therapeutic decision.

Comparative genomics of *Pseudomonas aeruginosa* ocular isolates from keratitis patients with different clinical outcomes

IInvestigators : Dr. D. Bharanidharan,
Dr. M. Vidyarani,
Dr. Lalitha Prajna
Research Scholar : K. Kathirvel, T. Kannan
Funding : Aravind Eye Hospital

Introduction

Pseudomonas aeruginosa is a destructive opportunistic pathogen responsible for bacterial keratitis characterized by ocular pain, infiltration of inflammatory cells, stromal destruction, corneal

perforation and leading to vision loss if untreated. *P. aeruginosa* contributes to a significant proportion of bacterial keratitis, responsible for 6% to 39% of cases in the United States and 8% to 21% in South India (Sy et al., 2012). It has been suggested that the most severe keratitis is caused by *P. aeruginosa* and corneal damage can occur in as little as 24 hrs (Eby and Hazlett, 2016). Pseudomonas aeruginosa can cause a wide range of infections, carrying a wide array of virulence factors that contribute pathogenesis. Keratitis pathogenesis is a complex process, where in several virulence factors has been implicated including Cell-associated structures such as type IV pili and flagella, slime polysaccharide, proteases such as elastase B (LasB), alkaline protease (AprA), protease IV (PrpL) and *P. aeruginosa* small protease (Pasp) and exotoxins. However, several studies revealed that exotoxins ExoU and ExoS that belong to the type III secretion system (T3SS) is an important contributor to keratitis pathogenesis (Lomholt et al., 2001). ExoU strains has been reported to cause more severe infection. Moreover, clinical isolates from keratitis are preferentially carries exoU gene rather than exoS in their accessory genome (Lomholt et al., 2001), while the core genome, approximately 90% of the complete genome, consisting of most of the virulence genes (Wolfgang et al., 2003). Besides, the clinical isolates, carrying multiple antimicrobial drug resistance in the accessory genome, are associated with poor clinical outcome in patients with keratitis (Murugan et al., 2016). In a SCUT study, exoU strains with elevated fluoroquinolone resistance suggest worse clinical outcome in *P. aeruginosa* keratitis patients. Increased gentamicin resistance involving exoU strains has also been reported (Sy et al., 2012) and suggest that multi-drug resistance strains carrying exoU gene and other virulence factors may lead to treatment failure (Murugan et al., 2016). Furthermore, it has been reported that subpopulation of UK-keratitis associated *P. aeruginosa* isolates may be adapted with specific features to cause eye infections (Stewart et al., 2011). However, link between specific genotypes and clinical outcome or risk factors remains unclear.

To better understand the infection, genome-wide identification of genetic features responsible for multiple virulence and multidrug-resistant mechanisms in keratitis P.aeruginosa isolates that impact on the patient outcomes is important. this study report the analysis of five P.aeruginosa isolates from keratitis patients with different clinical outcome, wherein, the patients were grouped based on the corneal healing and who underwent surgery. All five isolates in the patient groups were differed in their antimicrobial susceptible profiles and the presence of T3SS virulence factors. The objective was to determine if the clinical isolates showed a relationship between antimicrobial susceptibility and virulence factors and patient outcomes

Results

Five *P. aeruginosa* ocular isolates (BK2-6) with different antimicrobial susceptibility and clinical outcomes were selected for sequencing. Two isolates (BK2 and BK6) were initially recovered from the corneal scrapings of patients who subsequently responded to treatment and presented with a healed ulcer during follow-up. The other three isolates (BK3, BK4 and BK5) were grown from corneal buttons obtained during surgery from patients who did not respond to treatment. The whole genome sequencing was performed by Illumina Nextseq platform with paired-end method at Genotypic, Bangalore. The data were preprocessed and assembled using CLC Genomics workbench version 8. Annotation was carried out using RASTtk and PROKKA (Table 1).

Comparison of TypeIII secretion systems (Table 2), showed that MDR strains BK3 and BK6 carries the exoU system. Although exoU gene presence was identified in BK5, it might not be active due to nonsense mutation. Thus, all non-MDR strains carry exoS system for their virulence.

Isolates	BK2	BK3	BK4	BK5	BK6
Genome size (mb)	6.3	7.1	6.5	6.3	7.1
G+C	66 %	65 %	64 %	66 %	66 %
Number of scaffolds	45	113	69	68	129
Maximum length (bp)	703333	594831	700326	877303	602407
Minimum length (bp)	506	504	509	509	510
N50	370564	191913	347365	350169	232253
CDs	6037	7009	6141	6055	6722
Hypothetical proteins	1042	1460	1079	1078	1327
#tRNA	61	65	60	61	60

Table 1. General Genomic features of ocular Pseudomonas aeruginosa strains.

TypeIII secretion System	BK2	BK3	BK4	BK5	BK6	Function
ExoY	P	-	-	-	-	adenylate cyclase, disrupts actin cytoskeleton and cause cell rounding
ExoU	-	P	-	P*	P	phospholipase, induces cytotoxic effects leading to rapid necrotic cell death
ExoS	P	-	P	P	-	GTPase-activating (GAP) and ADPribosyltransferase, inhibit bacterial internalization and epithelial cell migration
ExoT	P	P	P	P	P	GTPase-activating (GAP) and ADPribosyltransferase, inhibit bacterial internalization and epithelial cell migration

*Table 2. Presence (P) of genes of Type III secretions systems in all five isolates. * Insertion of one base, causing early termination.*

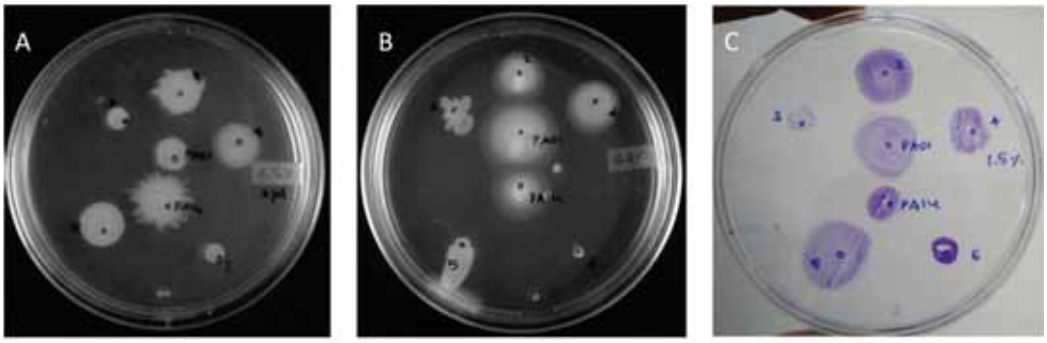

Fig. 1. Swarming, Swimming and twitching motility in *P. aeruginosa* isolates.

In addition, several virulence factors were identified in all the isolates. They share many of the virulence factors and some of them unique (Data not shown). For example, the gene Flic was identified in BK4 and BK5 (non-responder group), which has been reported to induce inflammasome and impairs the bacterial clearance. Moreover, Flid, Flic, FliS, Flgl,FleP, FleI/FleG genes responsible for flagellar system are present only in BK4 and BK5. The motility assay was carried out for all five isolates and PA01 (Fig. 1), confirming the presence of swimming, twitching and swarming motility in BK4 and BK5.

In order to find the intrinsic and acquired resistance against antimicrobial drugs, first the detection of mutations in amino acid levels were performed against PA01 as reference. Multiple point mutations in ampC gene were identified, which reported to have ampC over-expression and have significant mechanism of beta – lactamase resistance. Also, several mutations were identified in gyrA and parC, where in the changes T83I and S87L in gyrA and parC genes in BK6 isolate reported have fluoroquinolones resistance. 10 amino acid residues and two deletions 372MSDNNVGYKNYG383 → VDSSSSYAGL_ _ in OprD gene that are resistant to carbapenem drug was detected in four isolates (BK2, BK4-6). On the other hand, various antibiotic resistance genes were identified in all the isolates that are resistance to Aminoglycoside, β-lactamase, Fosfomycin, Phenicol, Tetracycline, Trimethoprim, Sulphonamide drugs, especially strains BK6 and BK3 showed additional resistance genes: tet(G), dfrB5, sul1 that are responsible for Tetracycline, Trimethoprim, Sulphonamide drugs resistance.

In addition, mutational analysis was carried out in genes of MexAB-OprM multidrug efflux systems, which exhibit intrinsic antibiotic resistance of *Pseudomonas aeruginosa*. Mutations in regulatory genes (MexR, NalC, NalD) have been associated with overproducing MexAB-OprM and exhibiting an elevated multidrug-resistant (MDR) phenotype. A point mutation in mexR gene, three mutations in NalC and 4 in NalD were detected by comparing PA01 (Table 3). The effect of mutations compared to wild type was shown in the figure 2. V126E amino acid change in MexR gene, detected only in BK1, BK3 and BK6, showed no effect on the protein structure. G71E and S209R in NalC, commonly present in all the strains, highly destabilizing the protein stability and affecting the DNA binding respectively. Interestingly, one novel point mutation D79E in NalC was identified only on BK3, shows no effects on protein stability.

Isolate	Mutations in MexAB-OprM		
	MexR	NalC	NalD
BK1	V126E	G71E, S209R	R38K
BK2	-	G71E, S209R	G206S
BK3	V126E	G71E, D79E, S209R	-
BK4	-	G71E	N130S
BK5	-	G71E, S209R	-
BK6	V126E	G71E, S209R	L85P

Table 3. Mutations detected in MexAB-OprM efflux pump regulatory genes.

L85P and G206S, detected in NalD of BK6 and BK2 respectively, affected the protein stability and altered the interactions with neighboring residues. V126E amino acid change in mexR gene, detected only in MDR strains, showed no effect on the protein structure. G71E and S209R in NalC, commonly present in all the strains, highly destabilizing the protein stability and affecting the DNA binding respectively (Data not shown). Of mutations R38K (BK1), G206S (BK2), L85P (BK3) and N130S (BK5) detected in NalD, L85P and G206S affects the protein stability. Mutations that destabilize protein stability and DNA binding in the secondary repressor NalC along with primary repressor mexR mutation, might play important role for overproducing mexAB-OprM efflux pump and multidrug resistance. Further, novel mutations in NalD, another transcriptional regulator of mexAB-OprM pump, affecting protein stability may have role to play and suggesting further studies. These data show that ocular isolates can widen their drug resistance profiles by affecting the repressors to overproduce efflux pumps.

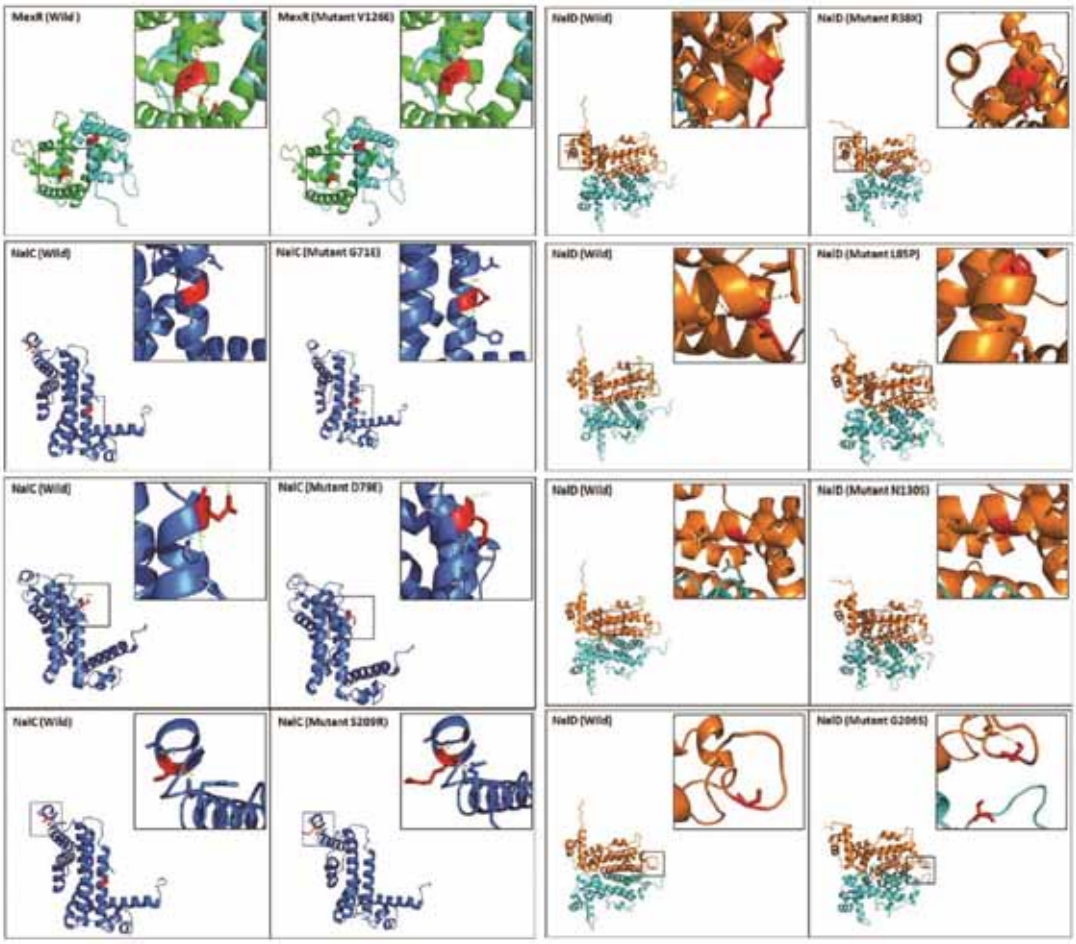

Fig.2. Wild (Left) and mutant (Right) protein structures of MexAB-OprM efflux pump regulatory genes. Mutations (shown as sticks) and their interactions with neighboring residues are shown in the box.

Conclusion

This study combined clinical data and whole genome analysis of ocular isolates of *P. aeruginosa* to link genetic basis of bacteria with different outcome of the patients. Isolates prefers either ExoU or ExoS for the infection, not both the phenotype. The strains isolated from poor outcome patients carries fliC gene or having multiple drug resistance mechanisms. Further, identification of virulence associated genes and deeper understanding of drug resistance would help us to find the reasons for treatment failure and suggest better disease management.

References

- Eby, A.M., Hazlett, L.D., 2016. Micro. Biochem. Tech. 8, 9-13.
- Lomholt, J.A., Poulsen, K., Kilian, M., 2001. Infect.Immun. 69, 6284–6295.
- Murugan, N., Malathi, J., Umashankar, V., Madhavan, H.N., 2016. Gene. 578, 105-111.
- Stewart, R.M., Wiehlmann, L., Ashelford, K.E., Preston, S.J., et al., 2001. J.Clin.Microbiol. 49, 9931003.
- Sy, A., Srinivasan, M., Mascarenhas, J., Lalitha, P., et al., 2012. IOVS. 53, 267–272.
- Wolfgang, M.C., Kulasekara, B.R., Liang, X., Boyd, D., et al., 2003. PNAS. 100, 8484-8489.

OCULAR MICROBIOLOGY

The department focuses on cellular and molecular basis of ocular infectious and inflammatory diseases that pose a major challenge to the community with a high morbidity rate. The thrust area of research is the elucidation of bacterial virulence and drug tolerance mechanisms, host-pathogen interactions and the genetic dissection of drug resistance in ocular pathogens. Experimental approaches to study host pathogen interactions involve *invitro* cell culture models and *exvivo* analysis of ocular tissue samples. Since inflammation is a leading cause of ocular morbidity and blindness worldwide, studies investigating the functional and molecular aspects of ocular inflammation could find applications in clinical management.

Analysis of bacterial persistence mechanisms in recalcitrant ocular *Pseudomonas aeruginosa* infections

Principal Investigator : Dr. Vidyarani Mohankumar
Funding Agency : SERB
Project Fellow : R. Sangeetha

Background

Pseudomonas aeruginosa, a leading cause of Gram negative bacterial keratitis, causes corneal scarring and severe visual disability. In some patients, even the drug susceptible bacteria are not cleared completely by antibiotics, leading to persistent infection. Bacterial persistence is the ability of bacteria to tolerate exposure to lethal concentrations of bactericidal antibiotics. Such drug tolerance in sensitive isolates is mediated by a persister subpopulation that survives high antibiotic concentration and grows back to original population once antibiotic stress is removed. This study aims to identify the bacterial persistence mechanisms by comparing the drug tolerance mechanisms of *P. aeruginosa* isolates obtained from keratitis patients who did not respond to standard antibiotic treatment.

Results

Analysis of antibiotic killing dynamics

In ocular infections that were incurable by antibiotic treatment, Most of the isolates were sensitive to the antibiotics tested invitro. In these cases, treatment failure could possibly be due to the selection of high persister cells that survive exposure to a given antibiotic and revive under highly specific conditions.

To determine the killing kinetics of moxifloxacin and tobramycin, overnight cultures of *P. aeruginosa* isolates were diluted 1:100 and incubated at 37°C for 4h to ensure logarithmic growth. After 4h of incubation, antibiotics were added at the concentration of 100µg/ml. Then, samples were taken at different time points (1h, 4h, 8h, 24h and 48h) and plated on LB agar plates to determine colony forming units. Surviving colonies were tested for resistance by plating them in the presence of the respective drug to which they were tolerant.

In all the isolates, maximum cell death was observed between 1-4h time points. The fraction of surviving persister cells decreased with increasing

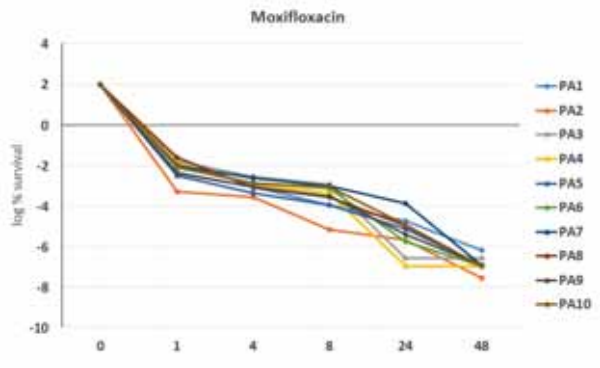

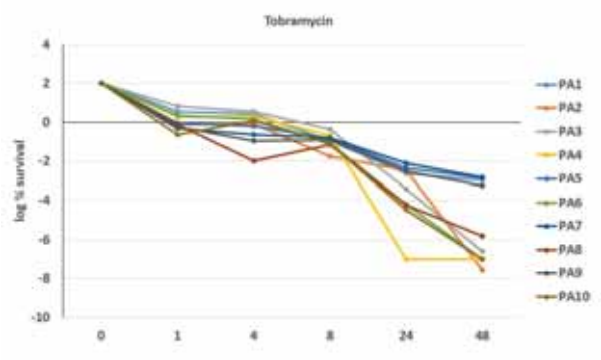

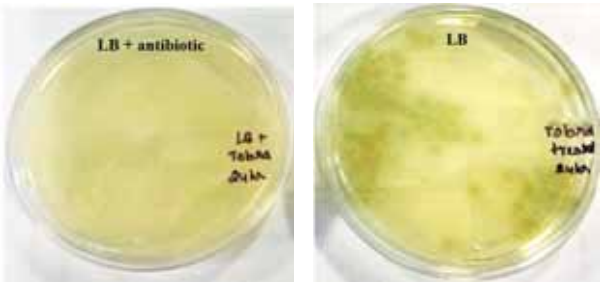

Figure 1. A. Killing dynamics of moxifloxacin and tobramycin at a concentration of 100µg/ml at 37°C. Different colors represent ten different P. aeruginosa isolates. B. Persisters were examined for resistant mutants in the presence of antibiotics (100µg/ml)

antibiotic exposure time. None of the tested isolates survived moxifloxacin treatment after 48h, and complete bacterial killing occurred between 24-48h. However, with tobramycin treatment, four out of ten isolates survived even after 48h. None of the surviving colonies had turned resistant to the respective antibiotic with which they were treated.

Functional analysis of drug tolerance mechanisms

Enhanced efflux activity has been shown to facilitate drug tolerance in dormant *E. coli* cells. To investigate this possibility in *P. aeruginosa* persisters, a semi-automated fluorimetric assay using the common efflux pump substrate EtBr was used to study the accumulation and efflux capabilities of the bacterial isolates under defined conditions. Ethidium bromide emits weak fluorescence when outside the cell in aqueous medium, whereas within the cell it fluoresces strongly. Hence the kinetics of EtBr transport will reflect the overall efflux capacities of the bacterial isolates, allowing bulk measurements in a single experiment.

To achieve maximum accumulation, conditions that promote accumulation and prevent efflux of EtBr (with efflux pump inhibitor CCCP at 25°C) inside the bacterial cells were employed for 60 min. The fluorescence was measured in an automated plate reader (wavelength excitation at 518nm and emission of 605nm) at every five minutes for 1hr. Then, the tubes were centrifuged and the medium was discarded and replaced by 1× PBS containing glucose (without CCCP) and again fluorescence was measured to study the efflux kinetics. Each experiment was conducted in triplicates.

Maximum accumulation was seen in tobramycin treated bacterial cells, whereas in moxifloxacin treated cells, the accumulation was lesser than that of untreated total cells. Previous exposure to tobramycin

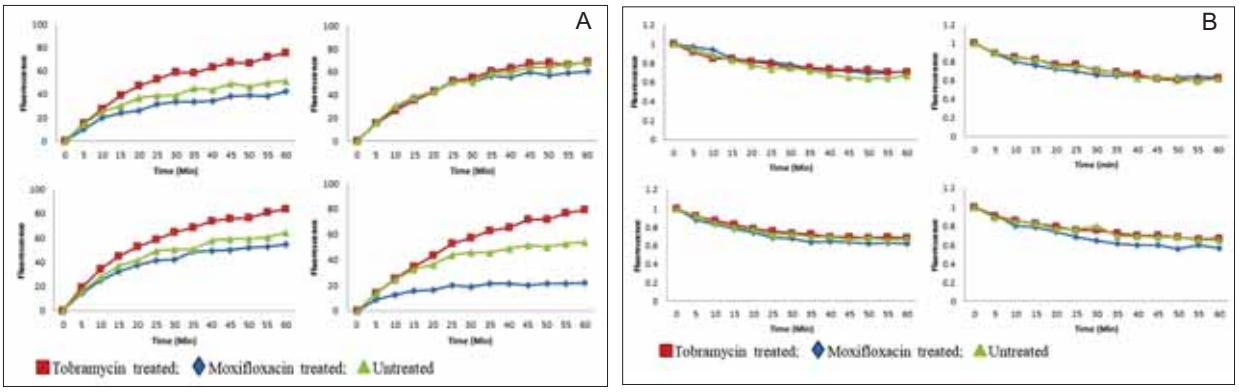

Fig.2.A. Representative images showing accumulation of EtBr (2µg/ml) in persister and total cells in the presence of CCCP (15µg/ml) at 25°C. B. Representative images showing EtBr efflux from persister and total cells in the presence of glucose at 37°

could have increased the membrane permeability, thereby causing increased accumulation in these cells. The efflux kinetics was almost similar in all the three bacterial populations and the results were comparable among all the isolates.

Analysis of transcriptional regulation in persister cells

The relative expression levels of efflux pump genes (mexA, mexX) and virulence genes (proIV and exoA) were analyzed in persister and total bacterial population. Total RNA was isolated from antibiotic (moxifloxacin and tobramycin) treated persister cells and untreated total cells and the transcript levels were determined by real time qPCR with rplu as housekeeping gene. Moxifloxacin treated cells had lower expression of efflux genes in all the isolates whereas in tobramycin treated cells, two isolates had increased expression of mexA and mexX. Expression of protease IV was either unaltered or downregulated in moxifloxacin treated cells whereas two tobramycin treated isolates had increased expression of protease IV.

Conclusion

Persister cells form a fraction of drug sensitive isolates and remain in a quiescent state by downregulating their gene expression. The findings indicate that while efflux activity remains unaffected in persisters, increased accumulation in tobramycin treated cells may promote tolerance to the drug due to increased antibiotic stress. Similar to the accumulation ability, transcriptional regulation was also different among the persisters isolated from the two different classes of antibiotics.

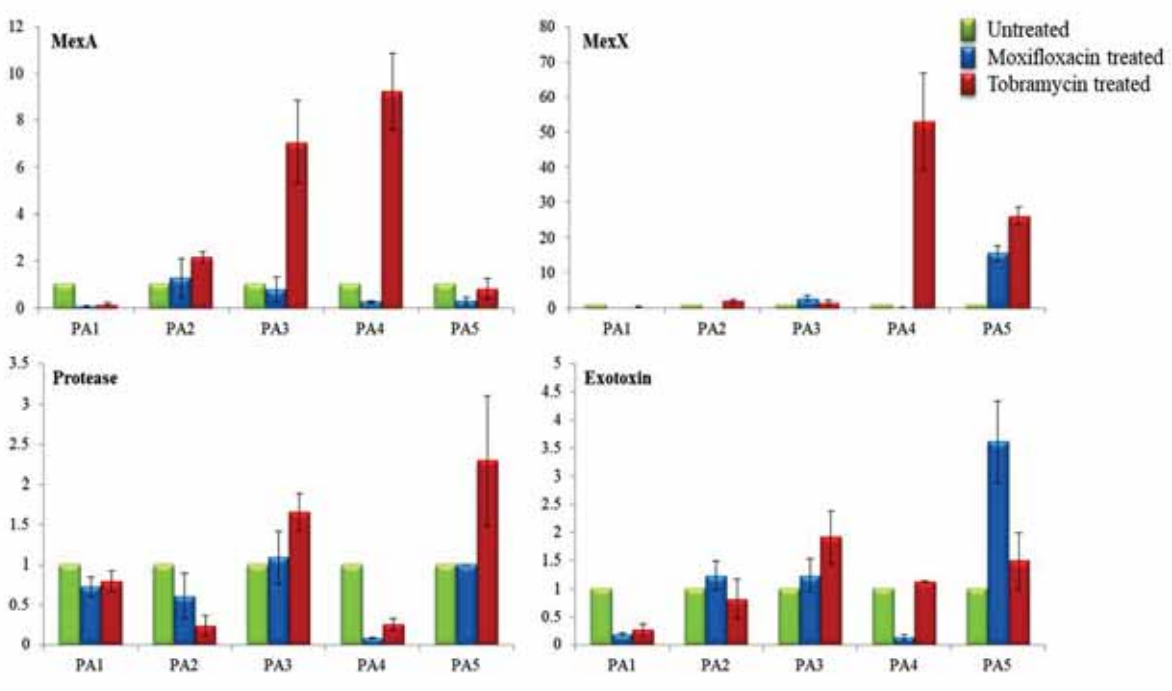

Fig 3. Relative expression levels of efflux and virulence genes in untreated and antibiotic treated P. aeruginosa isolates.

Functional characterization of drug resistance mechanisms in corneal isolates of *Pseudomonas aeruginosa*

Investigators : Dr. Vidyarani Mohankumar, Dr. Bharanidharan Devarajan, Dr. Lalitha Prajna
Funding Agency : AMRF
Project Fellow : T. Kannan

Background

Bacterial keratitis caused by *P. aeruginosa* progresses rapidly and may result in corneal perforation or vision loss if left untreated. The bacteria can easily develop resistance to a variety of antibiotics, which poses a big therapeutic challenge. Various mechanisms of antimicrobial resistance include mutational alteration of target protein, enzymatic drug inactivation, decreased influx or increased efflux of drugs, biofilm formation

and acquisition of resistance genes from other species. Multidrug resistant (MDR) clinical isolates of *P. aeruginosa* often exhibit more than one of the aforementioned resistance mechanisms. This study was carried out to analyze the possible drug resistance mechanisms in ocular *P. aeruginosa* isolates obtained from keratitis patients. After an initial analysis with five *P. aeruginosa* isolates, the results were validated with six MDR (BK7-12), six drug sensitive (BK14, BK16-20) and two single drug resistant isolates (BK13 and 15), selected based on the clinical outcomes and antimicrobial susceptibility pattern.

Results

Drug efflux

Constitutive or inducible expression of the efflux systems may confer resistance to a broad range of antimicrobials. The overall efflux activity of the isolates was tested with Etbr based real time fluorimetric assay and the efflux pump inhibitor (EPI) based MIC reversal assay. Expression levels of MexAB and MexXY-oprM efflux system genes were assessed by real time PCR.

Real time accumulation and efflux determination

A semi-automated fluorimetric assay using the common efflux pump substrate EtBr was used to study the accumulation and efflux capabilities of the bacterial isolates under defined conditions. The Etbr fluorescence was measured at an excitation wavelength of 518nm and emission of 605nm respectively in a Spectramax Multimode reader.

Conditions that result in maximum accumulation of Etbr (25°C in the presence of EPI) inside the bacteria were employed. EtBr and CCCP were added to the bacteria resuspended in PBS and the fluorescence was measured at 5 min time intervals for one hour. Then, the cells are washed with PBS to remove the EtBr present outside the cells and the fluorescence was measured under maximum efflux (with glucose and without CCCP) conditions at 37°C.

In most of the isolates, the fluorescence quickly shot up at 5min and then gradually increased to reach a plateau at 1h. The isolates that showed maximum EtBr accumulation were BK10, BK7 (resistant), BK20 and BK17 (sensitive) (Fig. 1). Following accumulation, EtBr efflux was monitored at different time intervals and overall the results were comparable between sensitive and resistant isolates. Highest efflux activity was seen with BK15, BK16 and BK18. The efflux activity was similar among resistant isolates, whereas in sensitive isolates low to moderate efflux activities were noted (Fig. 2).

Relative expression of efflux pump genes

Among the various efflux systems present in *P. aeruginosa*, the clinically relevant Resistance-nodulation-division (RND) efflux system has broad substrate specificity and mediates active efflux of various antibiotics and chemotherapeutic agents. The RND efflux pump, mexAB-OprM actively transports β-lactams, chloramphenicol, trimethoprim, fluoroquinolones and tetracyclines. MexXY contributes resistance to aminoglycosides, chloramphenicol, tetracycline etc. The expression levels of mexAB and mexXY-oprM genes were compared among resistant and sensitive isolates using sybr green based real time quantitative PCR with rplu as a housekeeping gene and PAO1 as control.

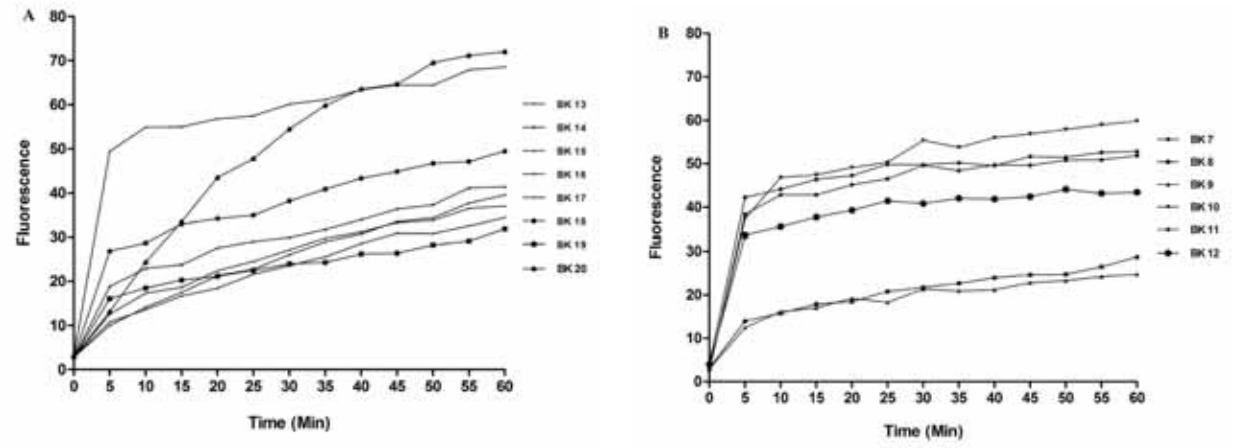

Figure 1. Real time accumulation of Ethidium bromide in drug sensitive (A) and MDR isolates (B). Fluorescence produced by the accumulation of Etbr (2µg/ml) was measured in the presence of CCCP (15µg/ml) at 25°C for 60 min. Fluorescence produced by the negative control was deduced as background fluorescence.

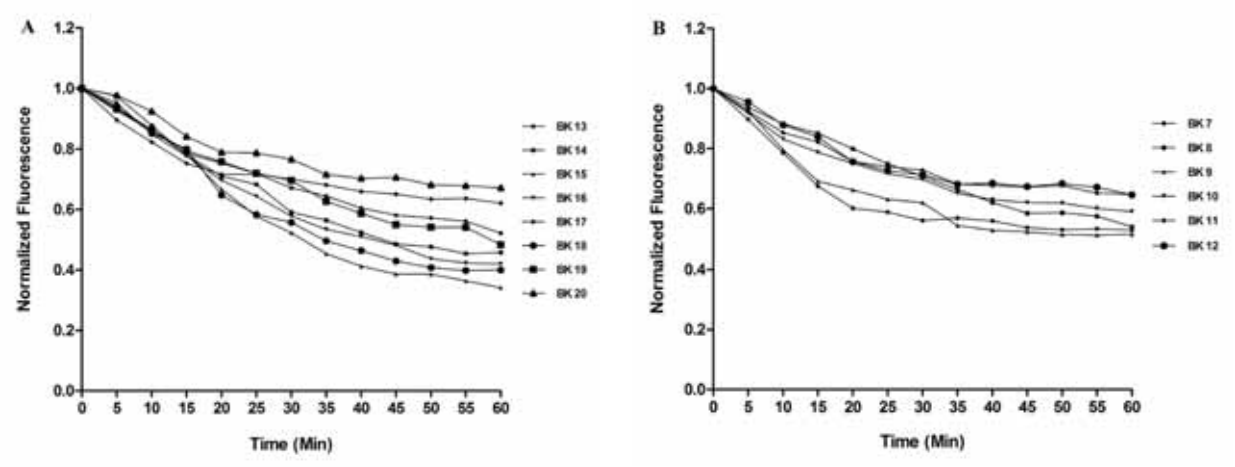

Figure 2. Real time Efflux assay. Efflux of Ethidium bromide in drug sensitive (A) and MDR isolates (B) was measured in the presence of glucose (0.4% V/V) at 37°C for a time period of 60 min.

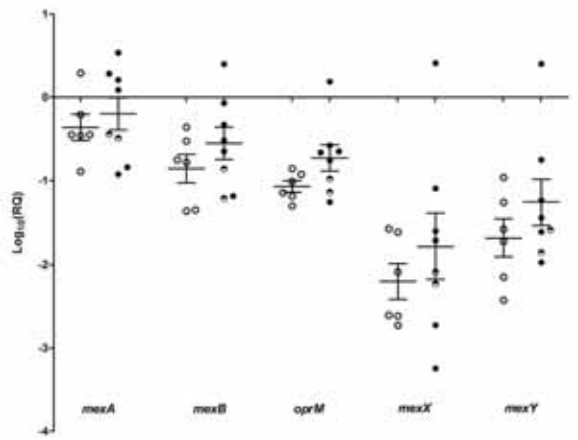

Figure 3. Expression levels of efflux pump genes in P. aeruginosa isolates relative to the reference strain PAO1. Open circles represent sensitive isolates, closed circles represent resistant isolates and half filled circles represent single drug resistant isolates.

Compared to PAOI, the expression of mexAB and mexXY-oprM genes were highly variable in all the isolates. The MDR strain BK10 had increased transcript levels of all the five efflux genes. Expression of mexA was very high in isolate BK9, and slightly higher in three MDR strains including BK10 and one drug sensitive isolate. Expression levels of all five efflux genes were relatively higher in resistant isolates (Fig.3).

Efflux Pump Inhibitor based MIC reversal assay

To functionally assess the over expression of efflux pumps, an EPI based MIC reversal assay was performed with the eight resistant isolates. The MIC reversal assay can determine if inhibiting active efflux could resensitise the bacteria. The MIC of moxifloxacin and tobramycin, the most commonly

MIC (µg/ml)								
Moxifloxacin					Tobramycin			
CCCP	-	+	-	-	-	+	-	-
EDTA	-	-	+ (0.2 mM)	+ (0.1 mM)	-	-	+ (0.2 mM)	+ (0.1 mM)
Isolates								
BK 7	1024	128	32	128	1024	512	128	256
BK 8	512	64	256	256	256	256	32	128
BK 9	1024	1024	64	256	512	256	128	512
BK 10	128	128	4	16	256	64	32	128
BK 11	256	256	64	256	256	128	256	256
BK 12	>1024	1024	512	1024	1024	256	512	1024
BK 13	16	1	1	2	(S)	ND	ND	ND
BK 15	(S)	ND	ND	ND	16	2	2	2

Table.1 MIC was determined using broth dilution method, in the presence and absence of CCCP (25µg/ml) and EDTA (0.1mM and 0.2 mM). The MIC of CCCP was 100µg/ml.

used antibiotics for *P. aeruginosa* keratitis were tested in the presence and absence of an efflux pump inhibitor CCCP. Isolate BK 13, which was initially resistant to moxifloxacin, regained its sensitivity to the drug in the presence of CCCP. The MIC of moxifloxacin against BK7 and BK8 reduced four and eight fold respectively in the presence of CCCP. The remaining isolates did not show any changes in moxifloxacin MIC, indicating that active efflux does not play a role in mediating drug resistance in these cases. Similarly for tobramycin, BK15 which initially showed resistance only to this drug was resensitized in the presence of CCCP. Except BK8, the MIC of tobramycin against all other MDR isolates reduced by two to four fold upon treatment with the efflux pump inhibitor (Table 1).

Bacterial Membrane Permeability

The permeability of bacterial membranes was tested by the addition of a membrane permeabilizer (EDTA) followed by MIC reversal assay for moxifloxacin and tobramycin (Table 1). In the presence of EDTA, isolate BK13 regained its sensitivity to moxifloxacin and BK15 regained its sensitivity to tobramycin. Three MDR isolates showed 16-32 fold reduction in moxifloxacin MIC at 0.2mM EDTA concentration. These findings suggest that poor membrane permeability could possibly contribute to drug resistance in these isolates.

Isolates	Biofilm density
BK 7	Weak
BK 8	Strong
BK 9	Strong
BK 10	Weak
BK 11	Moderate
BK 12	Weak
BK 13	Strong
BK 14	Moderate
BK 15	Strong
BK 16	Moderate
BK 17	Moderate
BK 18	Weak
BK 19	Moderate
BK 20	Strong
ATCC	Strong
PAO1	Strong
PA14	Strong

Table.2 Biofilm forming capacity of ocular isolates

Biofilm Formation

Bacteria in a biofilm are usually 100-1000 fold less susceptible to the antibiotics than the planktonic bacteria and thus the resistance to a particular drug depends on the extent of biofilm formation. In this study, four resistant isolates and one sensitive isolate formed strong biofilms. All other isolates formed moderate to weak biofilms (Table 2). The stronger biofilms in resistant strains may create a physical barrier to antimicrobials and thereby confer broader drug resistance.

Mutational alteration of target genes

Mutations that cause amino acid alterations in the quinolone resistance determining regions (QRDRs) of gyrA and parC were determined by big dye terminator sequencing. The gyrA and parC genes in resistant isolates were amplified and then sequenced in a 3130 Genetic Analyzer. Two single amino acid substitutions of Ile for Thr-83 in gyrA and Leu for Ser-87 in parC were found in all the MDR isolates. Apart from this, one more substitution of Thr for Pro-752 in parC was also present in four MDR isolates (Table 3). The mutations were not present in the two single drug resistant isolates, BK 13 and BK15.

Conclusion

Emergence of multi drug resistant bacterial strains poses a great challenge for treatment. In this study, the possible drug resistance mechanisms were characterized in corneal *P. aeruginosa* isolates and the mutational alteration in QRDR was found as the most common and predominant mechanism of resistance. Alterations in membrane permeability and increased drug efflux were found to confer resistance in single drug resistant isolates. Deeper understanding of the resistance mechanisms could provide a solution to tackle antibiotic resistance or to suggest appropriate combination therapies.

Isolates	Amino acid replacement positions		
	GyrA	ParC	
	83	87	752
PAO1	Thr	Ser	Pro
BK 7	Ile	Leu	Thr
BK 8	Ile	Leu	-
BK 9	Ile	Leu	Thr
BK 10	Ile	Leu	-
BK 11	Ile	Leu	Thr
BK 12	Ile	Leu	Thr

Table.3. Amino acid alterations in GyrA and ParC

KAP studies on risk factors of ocular Leptospirosis in south India and using KAP as a parameter of impact evaluation of the disease

Investigator : Dr. SR. Rathinam, Head of Uveitis Service, Aravind Eye Hospital, Madurai
Funding by Indian Council of Medical Research
Project Technicians: Mr. Ulaganathan, Ms. Sulochana

Introduction

To explore Knowledge, Attitude and Practices of the community (farmers, rural as well as urban population), Postgraduate medical students and practitioners on Leptospirosis in South India.

Results

The community was divided into smaller subcategories which included Medical Community and the General Community. General Community included farmers, corporation workers involved in cleaning, general rural as well as urban population. The team conducted focus group discussion and private, one on one interviews to assess the base line knowledge. After the above step, specific questionnaire was developed for medical and non-medical group. Sampling frame for community was completed

The questionnaire was standardized based on pilot study and focus group discussion.Question preparation was followed by question application and validation of questions. After validation, the core study was started. Onsite and outreach training were given to the field worker. Data collection, data entry and data management are under progress.

CONFERENCES ATTENDED

Annual meeting of Association for Research in Vision and Ophthalmology (ARVO) 2017

Baltimore, Maryland, USA, May 7-11

Mr. Mohd Hussain Shah, Department of Molecular Genetics attended the meeting. This helped him gain more knowledge in the field of Molecular genetics as well as ophthalmic science in general.

He also presented his research work as a poster entitled“ Identification and characterization of variants and a novel 4bp deletion in the regulatory region of SIX6, a risk factor for Primary Open Angle Glaucoma”. Mr. Shah received the travel grant from Indian Council of Medical Research (ICMR), Council of Scientific and Industrial Research (CSIR) and Department of Biotechnology (DBT), Government of India to attend this conference. He also visited the research facility at National Eye Institute (NEI), Bethesda and presented his work.

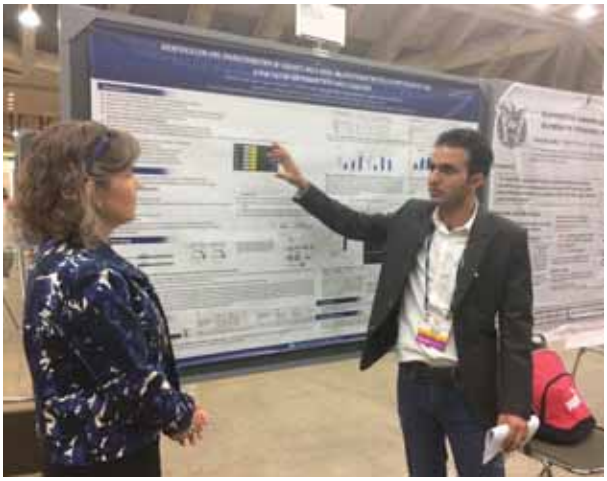

Mr. Mohd Hussain Shah presenting poster at ARVO

Annual Meeting of International Society for Stem Cell Research (ISSCR) - 2017

Boston, USA, June 14-17

Ms. K. Lavanya and Ms. S. Yogapriya from the Department of Immunology and Stem Cell Biology attended the meeting and presented their research work as posters.

Ms. K. Lavanya presented her work titled “MicroRNA profiling of enriched human corneal epithelial stem cells”. She received travel grant from Indian Council of Medical Research. She visited the research facility at Schepens Eye Research Institute, Boston and Rockefeller University, Newyork.

Ms. S. Yogapriya presented her work titled “Identification and Quantification of Human Trabecular Meshwork Stem Cells”. She was supported by ISSCR organizers for her travel and registration. During her trip, she interacted with Dr. Cynthia Grosskreutz, Glaucoma specialist at Novartis. She visited Dr. Ula Jurkunas lab at Schepens Eye Research Institute and Dr. Janey Wigg's lab at Massachusetts Eye and Ear Hospital, Boston.

Glaukopedia 2017

Jaipur, September 15-17

Dr. P. Sundaresan, Senior Scientist attended Glaucoma Society of India (GSI) meeting and delivered an invited talk on” Current trends in POAG and PACG genetics”.

Ms. Yogapriya and Ms. Lavanya at the ISSCR meeting

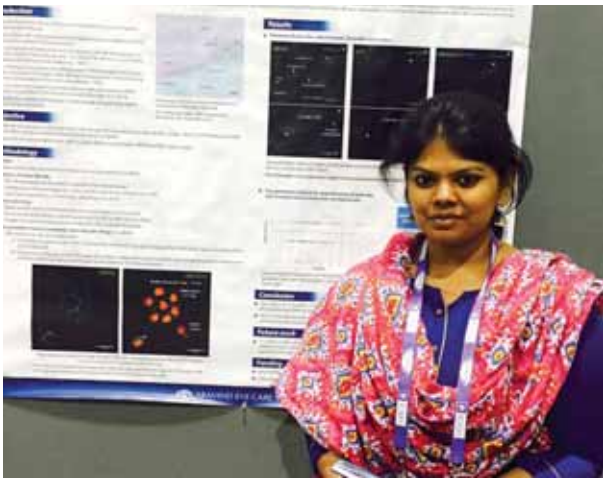

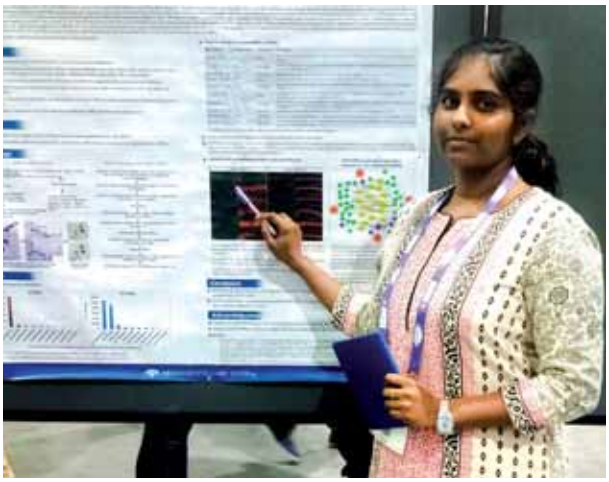

Dr. P. Sundaresan at Glaukopedia 2017 Meeting

Dr. P. Sundaresan at 2nd International Conference of Founder Populations at Kochi

2nd International Conference on Founder Populations - The Landscape of Genetic variants in Asian Founder Populations-from Near to Far East.

November 9-12,2017 Kochi, Kerala

Dr. P. Sundaresan delivered an invited talk on “Gene discoveries for some of the inherited eye diseases”.

33rd Asia Pacific Academy of Ophthalmology (APAO) Congress meeting

Hong Kong, Feb 8-11, 2018

Dr. P. Sundaresan attended the Congress and delivered an invited talk titled “Molecular genetics of POAG- Especially SIX6 gene involvement in the pathogenesis”. During the congress, he attended Asian Eye Epidemiology Consortium (AEEC) meeting and Asian Eye Genetics Consortium (AEGC). In addition, Dr. P. Sundaresan interacted with AECS collaborators especially Dr. Rachel Williams from University of Liverpool, UK, Dr. Tin Aung from SERI, Singapore and Dr. Calvin Pang from Chinese university of Hong Kong as well as discussed with other research scientists and colleagues .

Awards

Tamil Nadu Scientist award

Tamil Nadu State Council for Science and Technology presented Tamilnadu Scientist award for the year 2013 to Dr. P.Sundaresan under the discipline of Biological Sciences. Minister for Higher Education, Govt. of Tamil Nadu presented the award at Anna University, Chennai on September 25, 2017.

Indian Eye Research Group Meeting Awards

Madurai, July 29-30, 2017

Mr. Mohd Hussain Shah, Senior Research Fellow received Best Poster Award for the presentation on “Identification and characterization of variants and a novel 4bp deletion in the regulatory region of SIX6, a risk factor for Primary Open Angle Glaucoma” during the Indian Eye Research Group meeting.

Dr. P. Sundaresan receiving the Tamil Nadu Scientist Award

Mr. Mohd Hussain Shah receiving the Best Poster Award at the IERG meeting

Mr. Ashwin Balaji receiving the Best Oral Presentation Award at the IERG meeting

Prof. K. Dharmalingam presenting the Dr.VR. Muthukkaruppan Endowment Award to Mr. Kathirvel

Mr. Ashwin Balaji, Junior Research Fellow, Department of Ocular Pharmacology received the Best Oral Presentation award for the presentation on "Effect of cyclic IOP on outflow facility and activation of Rho A / ROCK signal cascade in human eyes".

Best Poster Award

Innovations and Challenges in Biomedical Sciences Research

Holy Cross College, Tiruchirappalli, December 12-14, 2017

M.Durga, Senior Research Fellow, Department of Molecular Genetics participated in the conference and won first prize for the poster tittled "Mutation analysis of carbohydrate sulfotransferase 6 gene (CHST6) for Macular Corneal Dystrophy (MCD) in Indian population".

Junior Research Fellowship

Lady Tata Memorial Trust, Mumbai

Ms.S. Yogapriya, Junior Research Fellow,Department of Immunology and Stem Cell Biology received Fellowship from Lady Tata Memorial Trust, Mumbai.

Prof.VR.Muthukkaruppan Endowment Award

Students and colleagues of Prof.VR.Muthukkaruppan, Advisor, Aravind Medical Research Foundation created an Endowment in his name in 2014 out of which an award will be given to the best researcher at the Institute every year. The award is given based on the scientific merit of abstracts and presentation by the research scholars. The award carries a certificate and cash prize of Rs.25,000/-.

Prof. VR.Muthukkaruppan Endowment Award 2017 was given to Mr. K. Kathirvel, Department of Bioinformatics for his outstanding research work on "Comparative genomics of Pseudomonas aeruginosa ocular isolates from keratitis patients".

CONFERENCES / WORKSHOPS CONDUCTED

15th Research Advisory Committee (RAC) Meeting

March 17, 2017

During the meeting faculty members of AMRF presented their work and received feedback. Oral presentations by the research scholars were evaluated by a panel of three RAC members: Dr. D. Karunagaran, Professor and Head, Department of Biotechnology, IIT, Chennai; Dr. Kumaravel Somasundaram, Professor, IISc, Bangalore and Dr. Anuranjan Anand, Faculty, JNCASR, Bangalore. The best presentation was selected for Prof. VR. Muthukkaruppan Endowment award.

15th Research Advisory Committee Meeting

Indian Eye Research Group (IERG) Meeting

Madurai, July 29-30, 2017

Aravind Medical Research Foundation hosted the 24th annual meeting of IERG at Madurai. A total of 146 participants attended the meeting including 30 invited faculty. The meeting had 103 presentations; two orations, 15 invited talks, 17 free papers and 69 posters.

A special breakout session on Recent Advances in Microbiology and Immunology, Genomics and Proteomics, Cell and Molecular Biology, Biochemistry and Pharmacology and Clinician Researcher Interface was conducted to discuss the current status in India and recommendations on how to take it further for the betterment of our population.

The meeting concluded with the note that all centres should work together to take translational research further in India, with specific reference to stem cells and gene therapy.

The meeting was supported financially by the Department of Biotechnology, Science and Engineering Research Board, Indian Council of Medical Research, Council of Scientific and Industrial Research as well as by the sponsorship from Spinco Biotech Pvt. Ltd., Agilent Technologies, Fortune Bioservices Pvt. Ltd., GE Healthcare, Genotypic Technology Pvt. Ltd. and Ponmani Chem-Glass Agencies.

Participants of Indian Eye Research Group (IERG) meeting

Highlights of the IERG Meeting

Dr. Debasish Sinha, Associate Professor of Ophthalmology, Wilmer Eye Institute, Johns Hopkins University School of Medicine, Baltimore receiving the 18th Bireswar Chakrabarti Oration Award

Prof. G Kumaramanickavel, Research Director - Narayana Nethralaya,Bangalore and Aditya Jyot Eye Hospital, Mumbai receiving the 6th D. Balasubramanian Oration Award

Dr. Calvin C. P. Pang, Professor of Ophthalmology and Visual Sciences, The Chinese University of Hong Kong, China delivering the invited talk

Prof. D. Balasubramanian discussing the current status of Ophthalmic research in India during the breakout session

Poster session

One-day Workshop on "Novel chemical cross-linking for the Treatment of Keratoconus

November 18, 2017

The workshop was organised by Prof. Rachel Williams, University of Liverpool, UK and Dr. Venkatesh Prajna, Director - Academics, Aravind Eye Care System. The main objective of this workshop was to bring together clinicians and researchers on a single platform to discuss the importance of the novel chemical cross-linker being developed to treat Keratoconus and its advantages over the conventional UV-crosslinking. The novel cross-linker is being tested through a collaborative project involving University of Liverpool, Aravind Eye Hospital, Aravind Medical Research Foundation and Aurolab.

Clinicians from various centres of Aravind Eye Hospital, researchers from AMRF, University of Liverpool, Narayana Nethralaya and representatives of Aurolab attended this meeting. Dr. Ashish Kumar, AEH Madurai and Dr. J.K.Reddy, Sankara Hospital, Coimbatore talked about the conventional UV-cross-linking practised in the clinic for the treatment of keratoconus. Dr. Atikah Haneef, Liverpool talked about the effects of novel chemical cross-linker on porcine tissue while its effects on human cadaver and keratoconic cornea were described by Dr. Ramprasad, AMRF. Prof. K. Dharmalingam, Director - AMRF spoke about the proteomics of cross-linking in the cornea and Dr. Arkasubhra Ghosh, Narayana Nethralaya described the role of pro-inflammatory molecules in keratoconus condition. The participants had a good discussion at the end and suggestions were put forth to further refine the experimental methodologies with the cross-linker and ways to increase the efficiency of the novel chemical cross-linker to treat keratoconus.

Brainstorming Session on Proteomics in Health Care

4th January 2018

The main objective of this session was to emphasize the growing importance of proteomics in health care. There were 34 participants who were mostly research scholars from different universities and from AMRF. The programme started with an introduction on this yearly event, which is conducted as a part of the programme support for research on human mycotic keratitis. This programme allows the dissemination of the knowledge particularly in the field of clinical proteomics to the young scientist. The brainstorming session included invited talks from experts in the field of proteomics namely Prof. Kumaravel Somasundaram, Indian Institute of Science; Prof. S. Karuthapandian, Alagappa University; Prof. Balamurugan, Alagappa University and Dr. Kathiresan, Kalasalingam University. The speakers provided a detailed description of their research findings and how proteomics was used as the technology platform in their research. The last part of the session included presentation from three research scholars who are supported by the DBT grant and their work on fungal keratitis. The workshop concluded with a discussion with the participants on their feedback as well as their expectations on future events.

Participants of the Workshop on Novel Chemical Cross-linking for the treatment of Keratoconus

Participants of the Brainstorming session on Proteomics in Healthcare

GUEST LECTURES DELIVERED BY VISITING SCIENTISTS

Dr.Kalal Iravathy Goud, Consultant/ HOD, Molecular Biology and Cytogenetics lab, Apollo Hospitals, Hyderabad
Topic: Importance of molecular diagnosis in a tertiary care hospital, March 11, 2017

Dr. Krishna Kannan, Director, R&D, Biomolecular Integrations, Little Rock, Arkansas
Topic: Immunology of Age-related macular degeneration, April13, 2017.

Prof. Geeta K Vemuganti,
Dean, School of Medical Sciences, University of Hyderabad, Gachibowli, Hyderabad Topic: Stem Cell Research: Beyond limbal epithelial cells, July 31, 2017.

Prof. Colin Willoughby, Professor of Molecular Ophthalmology, Institute of Ageing and Chronic Disease, University of Liverpool, Honorary Consultant Ophthalmic Surgeon, St. Paul's Eye Unit, Royal Liverpool University Hospital, Liverpool
Topic: Evolution of the EYE, September 18, 2017.

PUBLICATIONS 2017-18

Yelchuri, Madhavi Latha; Madhavi, Bhagyashree; Gohil, Nilam ; Sajeev, Hitha Sara Venkatesh Prajna, N, Senthilkumari S

- *In Vitro Evaluation of the Drug Reservoir Function of Human Amniotic Membrane Using Moxifloxacin as a Model Drug*

Journal of Cornea 2017;0:1-6

Prakadeeswari G, Haripriya A, Sundaresan P.

- *MTHFR and MTHFD1 gene polymorphisms are not associated with pseudoexfoliation syndrome in South Indian population"*

Int Ophthalmol. 2017 Mar 15. [Epub ahead of print]

Mohd Hussain Shah, Noemi Tabanera, Subbaiah Ramasamy Krishnadas, Manju R. Pillai, Paola Bovolenta, Periasamy Sundaresan

- *Identification and characterization of variants and a novel 4 bp deletion in the regulatory region of SIX6, a risk factor for primary open-angle glaucoma*

Molecular Genetics & Genomic Medicine 2017; 5(4) : 323 - 335

Roopam Duvesh, Venkatesh R, Kavitha S, Pradeep Y. Ramulu, Krishnadas, SR, and Sundaresan P

- *Genetic Complexity of Primary Angle-Closure Glaucoma in Asians"*

Advances in Vision Research, Volume I Part of the series Essentials in Ophthalmology p 291-313. (Book Chapter)

Renugadevi K, Asim Kumar Sil, Vijayalakshmi P, and Sundaresan P

- *Molecular Genetic Analysis and Diagnosis of Albinism Patients in India*

JSM Genet Genomics 2017 4(1): 1024

Tin Aung1, Mineo Ozaki, Mei Chin Lee et al

- *Genetic association study of exfoliation syndrome identifies a protective rare variant at LOXL1 and five new susceptibility loci*

Nature Genetics 2017

Boomiraj Hemadevi, Prajna NV, Srinivasan M, Sundaresan P

- *Genetic Perspective of Corneal Endothelial Dystrophies*

Journals of JSM Genet Genomics 2017

Bhagya S, Lalitha P, Lalan Kumar Arya, Rathinam S.

- *Polymerase Chain Reaction and its Correlation with Clinical Features and Treatment Response in Tubercular Uveitis*

Journal of Ocul Immunol Inflamm. 2017 Jun 30:1-8.

Gowthaman G, Saumi Mathews, Karthik Srinivasan, Kim Ramasamy, Sundaresan P

- *Establishment of human retinal mitoscriptome gene expression signature for diabetic retinopathy using cadaver eyes*

Journal of Mitochondrion E pub 2017 July

Roopam Duvesh, George Puthuran, Kavitha Srinivasan, Venkatesh Rengaraj, SR Krishnadas, Sharmila Rajendrababu, Vijayakumar Balakrishnan, Pradeep Ramulu & Periasamy Sundaresan

- *Multiplex Cytokine Analysis of Aqueous Humor from the Patients with Chronic Primary Angle Closure Glaucoma*

Current Eye Research (Published online on 22.09.2017)

Durga M, Prajna NV, Lumbini Devi, Sundaresan P

- *Genetic Analysis of CHST6 Gene in Indian Families with Macular Corneal Dystrophy*

Int J Gen Sci 4(1): 1-10.

Anand Rajendran; Pankaja Dhoble; Sundaresan P; Saravanan V; Praveen Vashist; Dorothea Nitsch; Liam Smeeth; Usha Chakravarthy; Ravilla D Ravindran; Astrid E Fletcher.

- *Genetic risk factors for late age-related macular degeneration in India*

British Journal of ophthalmology Nov 19 . E pub.

Kotnala A., Senthilkumari S., Halder N., Kumar A. Velpandian T.

- *Microwave assisted synthesis for A2E and development of LC-ESI–MS method for quantification of ocular bisretinoids in human retina*

Journal of Chromatography B 1073 (2018) 10–18

Nongpiur ME, Cheng CY, Duvesh R, Vijayan S, Baskaran M, Khor CC, Allen J, Kavitha S, Venkatesh R, Goh D, Husain R, Boey PY, Quek D, Ho CL, Wong TT, Perera S, Wong TY, Krishnadas SR, Sundaresan P, Aung T, Vithana EN.

- *Evaluation of Primary Angle-Closure Glaucoma Susceptibility Loci in Patients with Early Stages of Angle-Closure Disease.*

Journal of Ophthalmology. 2018 Jan 5. [Epub ahead of print]

ONGOING RESEARCH PROJECTS

No	Projects	Funded by	Investigators	Research Scholar
MICROBIOLOGY				
1.	Analysis of bacterial persistence mechanisms in recalcitrant ocular pseudomonas aeruginosa infections	SERB	Dr.M.Vidyarani	R.Sangeetha
2.	Functional characterization of drug resistance mechanisms in corneal isolates of Pseudomonas aeruginosa	AMRF	Dr. M. Vidyarani	T. Kannan
3.	KAP studies on risk factors of ocular leptospirosis in south and using KAP as a parameter of impact evaluation of the diseases	ICMR	Dr. SR. Rathinam	Ulaganathan Sulochana
PROTEOMICS				
4.	Programme support for research on Human Mycotic Keratitis	DBT	Dr. N. Venkatesh Prajna Dr. K. Dharmalingam Dr. Lalitha Prajna Dr. Chitra Thangavel Dr. J. Jeya Maheshwari Dr. O.G. Ramprasad Dr. Rabbind Singh	A.Dhivya Sandhya Nithyalakshmi Priyadharshini Naveen Luke Demonte S. Mohammed Razeeth Dr.C. Sathya Priya K.R.P. Niranjana Nithya B. Muthukumar R.V. Angela Asir O. Ruthra Dr. Jeyalakshmi Dr. Partho Chattoraj
5.	Predictive biomarkers for diabetic retinopathy among diabetics and stage specific biomarkers for NPDR and PDR.	Bagchi grant	Dr. K. Dharmalingam Dr. R. Kim Dr. J. Jeya Maheshwari Dr. O.G. Ramprasad	Roopesh R.Pai Naveen Luke Demonte Vignesh Ranjani Anjhu Nair R. Sharmila
6.	Pathogenic Aspergillus: Interaction with innate immune cells (Indo-French Collaborative project)	CEFIPRA	Dr. Lalitha Prajna Dr. J. Jeya Maheshwari Dr. K. Dharmalingam Dr. Rabbind Singh	Lakshmi Prabha Kanmani Razeeth P.M.Vaishali

7.	Prospective multicentre discovery and validation of diagnostic circulating and urinary biomarkers and development of sensor(s) to detect sight threatening diabetic retinopathy - Biomarker and biosensor study in UK and India (Indo-UK collaborative project)	Research Councils UK	Dr. K. Dharmalingam Dr. Kim Dr. J. Jeya Maheshwari	Nivetha Seetha
8.	Functional analysis of circulating microRNAs and their regulatory role in Diabetic Retinopathy	SERB	Dr.O.G.Ramprasad Dr.K.Dharmalingam Dr. Kim Ramasamy Dr. Bharanidharan	Ranjani Evangeline Ann Daniel
9.	Novel chemical cross-linking of the cornea for the treatment of keratoconus	EPSRC, UK and Aurolab	Dr. Venkatesh Prajna, Prof. Rachel Williams, Dr. O.G. Ramprasad, Dr. Atikah Haneef, Prof. K. Dharmalingam, Prof. Colin Willoughby, Dr. Naveen Radhakrishnan, Dr. Kishan Prajapati, Mrs. Karpagam Mr. Kannan	T.R. Divya
10.	Biomarker identification for accelerated ageing of eye in primary open angle glaucoma (POAG) and age related macular degeneration	SERB National post-doctoral fellow	Dr. K. Karuppasamy	
11.	Comparative genomics of Aspergillus flavus clinical isolates	DBT-RA Fellowship	Dr. C. Sathyapriya	
MOLECULAR GENETICS				
12.	Molecular genetics studies of Primary Angle closure Glaucoma (PACG) in south Indian population	UGC Fellowship	Dr. P. Sundaresan	Roopam Duvesh
13.	Genetic and functional approaches to understand the pathogenicity of Primary Open Angle Glaucoma (POAG)	ICMR-SRF	Dr. P. Sundaresan	Mohd Hussain Shah
14.	Genetic evaluation of genes involved in homocysteine metabolism and hyperhomocysteinemia with Pseudoexfoliation syndrome in South Indian population	AEH	Dr. P. Sundaresan	G. Prakadeeswari
15.	Molecular genetics of Macular corneal dystrophy (MCD) in Indian population	DST INSPIRE Fellowship	Dr. P. Sundaresan	M. Durga
16.	Genetics of retinal dystrophies	Aravind Eye Care System	Dr. P. Sundaresan	R.Kadarkarai Raj

17.	Genetic and transcript analysis of RB1 gene in south Indian Retinoblastoma patients	ICMR	Dr. A.Vanniarajan	K. Thirumalai Raj
18.	Establishing the genetic testing centre for childhood ocular cancer (retinoblastoma) in Aravind Medical Research Foundation	Aravind Eye Foundation	Dr. A.Vanniarajan Dr. Usha Kim Dr. R. Santhi Prof.VR. Muthukkaruppan Dr. D. Bharanidharan	A.Aloysius Abraham
19.	Understanding the molecular mechanisms of chemoresistance in retinoblastoma	CSIR-NET JRF	Dr. A. Vanniarajan	T. S. Balaji
20.	Molecular characterization of tumor progression in retinoblastoma	DST INSPIRE Fellowship	Dr. A. Vanniarajan	T. Shanthini
IMMUNOLOGY AND STEM CELL BIOLOGY				
21.	Limbal miRNAs and their potential targets associated with the maintenance of stemness	DBT	Dr .C. Gowri Priya	K. Lavanya
22.	Characterization and functional evaluation of trabecular meshwork stem cells in Glaucoma pathogenesis	SERB	Dr. C. Gowri Priya Dr. S. Senthilkumari Dr. Neethu Mohan Dr. SR.Krishnadas Prof. VR. Muthukkaruppan	R. Ashwin Rajkumar S. Yogapriya (Lady Tata Memorial Fellow)
OCULAR PHARMACOLOGY				
23.	Studying the role of Rho A – Rock signalling in conventional outflow pathway using Human Organ Culture Anterior Segment (HOCAS)	SERB	Dr. S. Senthilkumari Dr. SR. Krishnadas Dr. C. Gowri Priya	S. Ashwin Balaji
24.	IRole of miRNA in the regulation of Glucocorticoid Receptor (GR) signalling and development of New therapeutics for steroid-induced glaucoma	Wellcome-DBT /India Alliance Intermediate Fellowship (2017-2022)	Dr. S. Senthilkumari, Dr. C. Gowri Priya, Dr. D. Bharanidharan Dr. R. Sharmila	R. Haribalganesh K. Kathirvel T. Madhu Mithra
BIOINFORMATICS				
25.	Clinical exome analysis pipeline for eye disease next-generation sequencing panel	SERB	Dr. D. Bharanidharan	K. Manojkumar
26.	Comparative genomics of Methicillin-Resistant Staphylococcus aureus (MRSA) and Pseudomonas aeruginosa ocular isolates from keratitis patients with different clinical outcomes	AEH	Dr. D. Bharanidharan	K. Kathirvel
27.	An in-silico approach for identification of aberrant metabolic pathways in retinal angiogenesis towards early diagnosis and development of personalized medicine	SERB-NPDF	Dr. D. Bharanidharan	Dr. S. Umadevi

CORE RESEARCH FACILITIES

Name of the facility : 3130 – Genetic Analyser
Funding Agency : TIFAC - CORE
Contact person : Dr. P. Sundaresan,
Mr. V. Saravanan

Services rendered

3130 – Genetic Analyser is essentially used for DNA sequencing, to check polymorphisms in patients samples with comparison of controls. Department of Genetics utilizes 100% of this instrument and analyse huge number of patients and controls. Department of Microbiology is also routinely analysing DNA sequence of the bacterial genome weekly twice. We also use this Sanger sequencing for the confirmation of the data generated from Next generation sequencing assays. A number of publications are successfully generated with the data analysed through the 3130 – Genetic Analyser, out of which 4 publications for this academic year from department of genetics. AMRF is exclusively performing sequencing for the samples that are our-sourced from other institutions.

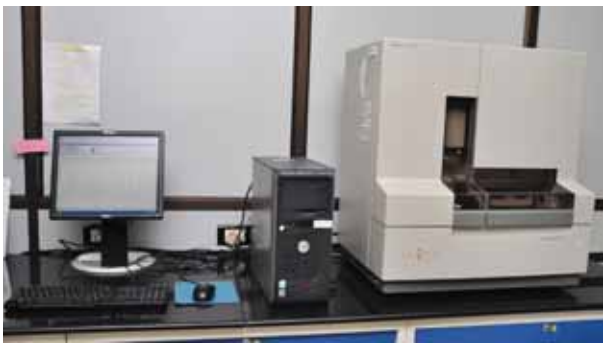

Publications

1. Decoding of tyrosinase leads to albinism in a nonidentical twin. Raj, Rajendran Kadarkarai, Prakadeeswari Gopalakrishnan, Vijayalakshmi Perumalsamy, and Periasamy Sundaresan. Journal of Clinical Neonatology. 7, no. 1 (2018): 59.
2. Genetic Analysis of CHST6 Gene in Indian Families with Macular Corneal Dystrophy. Durga Murugan, Namperumalsamy Venkatesh Prajna, Lumbini Devi, Periasamy Sundaresan. International Journal of Genetic Science. 2017;4(1): 1-10.
3. Whole mitochondrial genome analysis in South Indian patients with Leber's hereditary optic neuropathy. Saikia, Bibhuti Ballav, Sushil Kumar Dubey, Mahesh Kumar Shanmugam, and Periasamy Sundaresan. Mitochondrion 36 (2017): 21-28.
4. Identification and characterization of variants and a novel 4 bp deletion in the regulatory region of SIX6, a risk factor for primary open-angle glaucoma. Mohd Hussain Shah , Noemi Tabanera, Subbaiah Ramasamy Krishnadas , Manju R. Pillai, Paola Bovolenta & Periasamy Sundaresan. Molecular Genetics & Genomic Medicine 2017; 5(4): 323–335 doi: 10.1002/mgg3.290

Name of the facility : 7900HT Fast Real Time PCR
Funding Agency : Wellcome Trust
Contact person : Dr. P. Sundaresan,
Mr. V. Saravanan

Services Rendered

7900HT Fast Real Time PCR is essentially used for genotyping and gene expression assays. Department of Genetics utilizes 100% of this instrument and analyse huge number of patients and controls. Other departments including, Microbiology, Ocular pharmacology, Stem cell biology & Immunology and Proteomics are also routinely taking slots for this instrument in alternative days. A total of 13 publications are successfully generated with the data analysed through the Real Time PCR, out of which 6 publications for this academic year from department of genetics

Publications

1. A common variant mapping to CACNA1A is associated with susceptibility to exfoliation syndrome Aung T et al., Nat Genet. 2015 Jun;47(6):689. PMID: 25706626.

2. A common variant near TGFBR3 is associated with primary open angle glaucoma. Li Z, et al., Hum Mol Genet. 2015 Jul 1;24(13):3880-92. doi: 10.1093/hmg/ddv128.PMID:25861811.
3. Genome-wide association study identifies five new susceptibility loci for primary angle closure glaucoma. Khor CC et al., Nat Genet. 2016 May;48(5):556-62. doi: 10.1038/ng.3540. PMID: 27064256.
4. MTHFR and MTHFD1 gene polymorphisms are not associated with pseudoexfoliation syndrome in South Indian population. Prakadeeswari Gopalakrishnan. Aravind Haripriya. Periasamy Sundaresan. Int Ophthalmol.doi.10.1007/s10792-017-0498-2 Published online: 15 March 17
5. Genetic association study of exfoliation syndrome identifies a protective rare variant at LOXL1 and five new susceptibility loci. Tin Aung et al., Nat Genet. 2017 Published online 29 May 2017; PMID: 28553957doi:10.1038/ng.3875.
6. Genetic risk factors for late age-related macular degeneration in India. Anand Rajendran et al., Br J Ophthalmol 2017;0:1–5. doi:10.1136/bjophthalmol-2017-311384
7. Evaluation of primary angle closure glaucoma susceptibility loci in subjects with early stages of angle closure disease. Monisha Nongpiur et al. doi. Org / 10.1016 / j.ophtha.2017.11.016.
8. Establishment of human retinal mitoscriptome gene expression signature for diabetic retinopathy using cadaver eye. Gowthaman Govindarajan, Saumi Mathews, Karthik Srinivasan, Kim Ramasamy, Sundaresan Periyasamy. Mitochondrion (2017), doi: 10.1016/j.mito.2017.07.007
9. Identification and characterization of variants and a novel 4 bp deletion in the regulatory region of SIX6, a risk factor for primary open-angle glaucoma. Mohd Hussain Shah , Noemi Tabanera, Subbaiah Ramasamy Krishnadas , Manju R. Pillai, Paola Bovolenta & Periasamy Sundaresan. Molecular Genetics & Genomic Medicine 2017; 5(4): 323–335 doi: 10.1002/mgg3.290

Name of the facility : BIO-PLEX
Funding Agency : AUROLAB
Contact person : Dr. P. Sundaresan, Mr. V. Saravanan

Services Rendered

BIO-PLEX is used to analyse the samples including serum, aqueous humour, and vitreous humour from patients or studying the molecules involved in the disease pathophysiology. Departments such as Genetics, Microbiology and Ocular Pharmacology use this often. One publication was successfully published from the data analyzed from the aqueous humour samples of Primary Angle Closure Glaucoma (PACG), comparing the aqueous cytokine profiles between PACG patients and controls.

Publications

1. Multiplex Cytokine Analysis of Aqueous Humor from the Patients with Chronic Primary Angle Closure Glaucoma. Duvesh, Roopam, George Puthuran, Kavitha Srinivasan, Venkatesh Rengaraj, S. R. Krishnadas, Sharmila Rajendrababu, Vijayakumar Balakrishnan, Pradeep Ramulu, and Periasamy Sundaresan. Current eye research 42, no. 12 (2017): 1608-1613.

Name of the facility : NGS Facility
Funding Agency : AEF and AMRF
Contact Person : Dr. A.Vanniarajan

Services Rendered

AMRF has the complete setup required for Next Generation Sequencing (NGS) including Covaris for Library preparation, Agilent Bioanalyser for checking the quality of library preparation, Qubit and ABI real time PCR for quantifying the final libraries and Miseq for performing the NGS run.

Illumina Miseq is the bench top sequencer which includes cluster generation, paired-end fluidics and computing facility for primary analysis in a single machine. It is automated completely with the single use reagent cartridge and easy positioning of flow cell.

Miseq system can be used for a diverse applications including targeted sequencing of genes pertained to a genetic disorder, metagenomic sequencing to identify the species diversity, small genome sequencing of bacterial and fungal species, targeted gene expression analysis, ChIP Sequencing and many

more. Miseq enables up to 15 Gb of output with 25 M sequencing reads and 2x300 bp read lengths.

Almost all the departments in AMRF are utilizing the facility. So far, targeted gene sequencing for Retinoblastoma and Primary Open Angle Glaucoma (POAG), Genome sequencing of fungal species involved in keratitis, MicroRNA identification in Diabetic retinopathy were carried out with Miseq during the year. The data generated in these projects have given new findings for better understanding of the pathogenesis of various ocular disorders.

Name of the facility : LEICA TCS SP8 CONFOCAL LASER SCANNING MICROSCOPE

Funding Agency : Aravind Medical Research Foundation

Contact person : Dr. Gowri Priya Chidambaranathan

Services Rendered

Leica TCS SP8 confocal laser scanning microscope is an inverted microscope designed for optical imaging with optimal photon efficiency and high speed; facilitating optical sectioning. All optical components are matched towards increasing optical resolution using point illumination and a spatial pinhole to eliminate out of focus light in specimens by preserving fluorescence photons for image contrast and to improve cell viability in live cell

imaging. Backing up this sensitive detection are a high speed scanning system with up to 428 frames per second, large field of view of field number 22 and accelerated Z-stacking by a novel mode for the Super Z galvanometer called Galvoflow. This microscope is equipped with 4 laser ports namely UV/405, laser blue 488nm, laser green 552nm and laser red 638nm. In addition to PMT, the Leica HyD has been integrated into Leica TCS SP8 system. With its high quantum efficiency, low noise and large dynamic range, the Leica HyD is the most versatile detector in the Leica TCS SP8 confocal platform. It synergizes perfectly with the filter-free spectral detection system and the acousto-optical beam splitter (AOBS) in the gapless light detection with maximum photon efficiency. This makes the Leica TCS SP8 ideal for quantitative measurements and all-purpose imaging.

Stem Cell Biology

- Two parameter analysis (high p63/ABCG2 expression in cells with high nuclear-cytoplasmic ratio) for limbal epithelial and trabecular meshwork stem cell identification.
- Characterization of limbal stromal niche by expression analysis for various markers in comparison to corneal stromal cells.
- 3D construction of cornea and limbal tissues immunostained for the niche cell specific markers.
- Evaluation of PCO formation in lens capsular bag culture model by immunostaining for α-SMA, phalloidin, vimentin and E-cadherin.

Proteomics

- Receptor-ligand interaction between zymosan and phagocytic/non phagocytic cells.
- Assessment of phagocytosis of fungal spores in human corneal epithelial cells.
- Live/dead assay in whole corneal epithelium.
- Immunostaining of various corneal layers, cultured corneal epithelial/stromal monolayers.

Microbiology

- Host cell (human corneal epithelial cell) autophagy in response to bacterial infection.

Ocular Pharmacology

- Characterization of Human Trabecular Meshwork Cells by expression analysis.
- Evaluating the role of lutein (L) & Zeaxanthin (Z) in inhibiting the accumulation of A2E in ARPE-19 cell line using autophagy markers.

- Expression analysis of ALR and VEGF in ARPE-19 cells challenged with different glucose concentration under normoxia and hypoxia.

Publications

- Senthilkumari Srinivasan, Sharmila Rajendran, Chidambaranathan Gowripriya, and Vanniarajan Ayyasamy. Journal of Ocular Pharmacology and Therapeutics. January 2017, 33(1): 34-41.
- Kasinathan JR, Namperumalsamy VP, Veerappan M, Chidambaranathan GP. A novel method for a high enrichment of human corneal epithelial stem cells for genomic analysis. Microsc Res Tech. 2016;79(12):1165-1172.
- Saumi Mathews, Jaya Devi Chidambaram, Shruti Lanjewar, Jeena Mascarenhas, Namperumalsamy Venkatesh Prajna, Veerappan Muthukkaruppan, Gowri Priya Chidambaranathan. In vivo confocal microscopic analysis of normal human anterior limbal stroma. Cornea 2015; 34:464-70.

Name of the facility : Zeiss PALM Beam Laser Capture Microdissection System

Funding Agency : Aravind Medical Research Foundation

Contact person : Dr. Gowri Priya Chidambaranathan

This system enables laser assisted isolation of individual /group of cells from fixed sections that can be used further for genomics/proteomics. It can also be used to separate cells of interest from live culture for subculturing. The laser used for microdissection is 355 nm pulsed-laser which does not affect the quality of DNA/RNA/protein and hence the downstream processing.

This facility is currently used to enrich the corneal epithelial stem cells from a heterogenous population, in order to understand the gene expression patterns and signaling mechanisms specific to stem cells. It is possible to selectively isolate cells of our interest to get more specific information.

Publication

- Kasinathan JR, Namperumalsamy VP, Veerappan M, Chidambaranathan GP. A novel method for a high enrichment of human corneal epithelial stem cells for genomic analysis. Microsc Res Tech. 2016;79(12):1165-1172.

Name of the facility : Agilent Bioanalyzer

Funding Agency : Aravind Medical Research Foundation

Contact Person : Dr. A. Vanniarajan

Services Rendered

The Agilent Bioanalyzer is a microfluidics-based platform used to assess quantity, quality and size of DNA and RNA. The advantages of bioanlalyser over conventional methods include minimal sample requirement, faster time for analysis, high quality digital data, ready-to-use assays with pre-packed reagents. Whether it is DNA or RNA, the analysis requires only 1μl of DNA. Once the sample is loaded on to a microfluidic chip, it can analyse 12 samples in 30 minutes and separation of the nucleic acid fragments is carried out based on size using electrophoresis. The fragments will move through the channels at different speeds depending on their size and charge with smaller fragments moving more quickly than longer fragments. The analysed data can be visualized as pdf or excel formats.

Depending on the type of application, the suitable kits and chips are used. The DNA 1000 assay can be used with extracted, clean DNA to look at the size profile of a sample from 25bp to 1000bp at a concentration of 0.1-50ng/ul. The High Sensitivity assay can be used to look at DNA in the size range 50-7000bp and a concentration range of 5-500pg/ul. The quality of extracted RNA can be assessed to provide a RNA integrity number (RIN) and quantification information is also given. Two assays are available depending on the sample concentration; Nano (5-500ng/ul) or Pico (50-5000pg/μl).

Quantitative Proteomics Facility

Quantitative Proteomics is a powerful approach for unravelling the global proteome dynamic process, which is indicative of the changes in the disease state. At AMRF two different, but complementary approaches are being used for quantitation at proteome level. Selected Reaction Monitoring using a Triple Quad mass spectrometer and Label Free Quantitation using Orbitrap Mass spectrometer are used for quantifying peptides.

Two Dimension Difference Gel Electrophoresis (2D DIGE) is also used for quantitation at the level of proteins. This method also provides information about the post translational modifications of the proteins. Use of Cydyes for prestaining proteins and use of internal standards followed by scanning the same gel which carries co-separated proteins in a multi laser scanner allow accurate quantitation and avoids gel to gel variation.

Main components of the facility are:

1. Ettan IPGphor system for first dimensional separation of labeled proteins using multiple IEF strips
2. Ettan Dalt six system or shiroGEL system for second dimensional protein separation using multiplexed SDS PAGE gels
3. Typhoon trio variable mode image scanner for image scanning
4. Decyder 2D.7 and Melanie software for data analysis.

   AMRF is equipped with all the facilities and instruments mentioned above.

1. Ettan IPG phor III unit:

- An integrated high-voltage DC power supply delivering up to 10 kVolts
- Temperature control by Peltier elements
- Light exclusion during the run. Compatible with CyDye™ labeled proteins and other light sensitive stains
- IEF runs are programmed from the Ettan IPGphor 3 control panel with up to ten user-defined IEF protocols.
- Programmable functions including: rehydration time, platform temperature, current limit, voltage limit for each step, voltage gradient or step and step duration
- Ettan IPGphor 3 Control Software- records the run parameters over time and presents data as graphs and log files with a PC. Data is saved or can be exported to Microsoft® Excel

2. Vertical gel Electrophoresis unit shiroGEL vertical 20

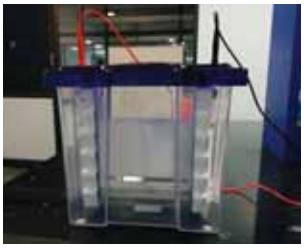

The shiroGEL vertical 20 provides application flexibility and ease of gel casting and set-up, require only four screws to set up to four 20×20 cm gels.

Glass plates with bonded spacers assure correct alignment for leak-free casting and eliminates need for manually aligning spacers

Ettan™ DALTsix

- Ettan™ DALTsix Electrophoresis System is designed to handle large second-dimension gels in a simple, efficient, and reproducible manner.
- It accommodates up to six 25.5 × 20.5 cm slab gels, either 1 mm or 1.5 mm thick, in a common tank under identical conditions.

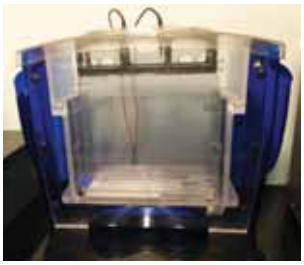

- Power is supplied to the unit by an external source such as an EPS 601 Power Supply. The unit is capable of handling 600 V, 400 mA, or 100 W.
- The heat exchanger located in the bottom of the unit must be connected to a circulating water bath for temperature control.

3. Typhoon 9400 trio variable mode image scanner

Amersham Typhoon trio variable mode image scanner is a new generation of laser scanners that provide with sensitive detection, high image resolution, and a very broad linear dynamic range. These imaging systems support multiple imaging modes, including phosphor imaging, red/green/blue (RGB) and near infrared fluorescence, as well as optical densitometry (OD) of proteins in stained gels.

Features:

- Versatility: use one system to image multifluorescent-, radioisotope-labeled, and colorimetric samples on gels, membranes, etc.

- Accurate quantitation: detect signals from as low as 3 pg of protein and differences across a dynamic range with greater than 5 orders of magnitude
- High resolution: resolve fine details in the sample with a pixel resolution of as low as 10 µm.
- 2-D DIGE imaging: simultaneously image two 2-D DIGE gels for differential expression studies
- High speed: a 24 x 25 cm gel can be scanned in less than two minutes at 100 µm resolution without compromising sensitivity
- High sample throughput: large scanning area of 40 × 46 cm enables to simultaneously image up to 20 gels or blots, measuring 10 × 8 cm in size.
- Generates a multi-channel image which will be compatible to analyze in the Decyder 2D software or Melanie software

Lasers: It houses three main lasers that includes 488 nm 20mw Blue, 532 nm 20mw Green, and 633 nm 10mw Red with emission filter sets: Cy2, R6G, Cy3, Fluorescein, and TRITC

GE Typhoon 9400 trio variable mode image scanner

5. Image analysis software

DeCyder 2D™

DeCyder 2D™ 2D software is an automated image analysis software suite which enables detection, quantitation, matching and analysis of Ettan DIGE system gels. The difference in the protein level can be accurately quantified and statistically analyzed in DeCyder 2D software by employing the internal standard. The novel co-detection algorithm exploits the identical spot patterns generated when multiple samples are resolved on the same gel.

Melanie software

Melanie is a comprehensive software solution for visualization, matching, detection, quantitation, and analysis of 2-D DIGE and other 2-D gel images.

Features

- High degree of flexibility, from image display choices through normalization options
- Use for 2D-DIGE, conventional 2-D gel analysis, Western blots, and other multiplex protein applications; 2-D DIGE applications requires purchase of 2-D DIGE package, or upgrade from Classic to DIGE
- Detect real differences in protein expression with high objectivity, sensitivity, and confidence
- 100% spot matching and advanced normalization options to extend the range of applications
- Specific statistical support for many one- and two-factor analyses, improving detection of true differences
- Choose between a node-locked license (a license fixed to one PC) or a floating license (a license that can be shared among PCs connected to a network license server).

Applications in proteomics:

Mainly used in the discovery phase to identify the biomarkers for various eye diseases to quantitate the differentially expressed proteins and to look for change in the proteoform level across the different stages of the disease.

- Diabetic retinopathy- Using this approach the difference in the proteoforms of complement factor B during disease progression.
- Fungal keratitis the change in the proteoform level of Zinc Alpha 2 Glycoprotein (ZAG) in different stages of infection (Early, intermediate and late) was identified and quantitated.
- It was also used to analyze the differentially expressed proteins in human corneal epithelial cellls during using in vitro infection model.

Fluorescence images of different protein samples:

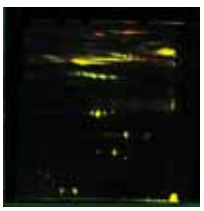

Serum Proteome (Control Vs PDR)

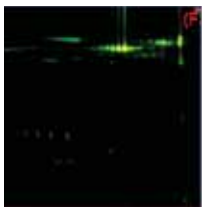

Tear Proteome (Control Vs Infection)

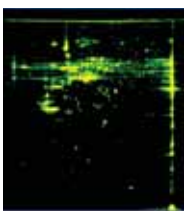

Human corneal epithelial Cell proteome (Control Vs treated)

Mass Spectrometry Facility

High resolution LC-MS/MS platform is needed for all proteomics studies. Mass spectrometry facility at Aravind Medical Research Foundation has Orbitrap Velos Pro mass spectrometer with ETD module. This facility helps researchers at AMRF as well as other institutions to carryout MS based proteomics studies.

Facility

The Facility is equipped with two high-performance mass spectrometers, both connected to Ultra high-pressure nanoLC system.

1.Easy-nLC 1000 Liquid Chromatograph

- A fully integrated nano-LC system that works up to 1000bar (15000psi.)
- Narrow column ID to increase analyte and improve detection sensitivity
- Seamless integration with state-of-the-art mass spectrometers

2. Orbitrap Velos ProTM Hybrid Ion Trap-Orbitrap Mass Spectrometer

A combined technology of Orbitrap Velos ProTM and OrbitrapTM mass analyzer delivers elevated performance

Orbitrap Velos ProTM Hybrid Ion Trap-Orbitrap Mass Spectrometer

- Higher mass resolution and higher scan speed
- Advanced signal processing for higher resolution
- Innovative pre-amplifier electronics improve sensitivity
- Improved ion optics for efficient ion injection
- increased robustness
- Very high resolving power-up to 240,000 FWHM
- Multiple fragmentation techniques-CID, HCD and ETD—provide versatility and complementary data
- Parallel MS and MSn capability speeds analyses

Applications

- Very high resolution and complementary fragmentation modes facilitate top-down protein identification and characterization
- Electron Transfer Dissociation option preserves labile side chains while fragmenting the peptide backbone for improved analysis of PTMs
- Fast scanning combined with high resolution and high spectral quality yields more protein identifications in a single analysis
- Very high resolution and selectivity in both full-scan MS and MSn modes enhance relative quantification results from stable isotope labeling or isobaric mass tagging experiments

3. TSQ Quantum Ultra™ triple quadrupole mass spectrometer

This MS allows quantification of target proteins with outstanding accuracy using the principle of Multiple Reaction Monitoring. It provides higher sensitivity and specificity without sacrificing versatility.

Specifications:

- Heated Electrospray Ionization (HESI-II) Probe as Ion source
- HyperQuadTM Mass filter reduces noise and increases sensitivity
- Mass Range:10–3000 Da
- High-resolution selected reaction monitoring
- Quantification of multiple target compounds in a single run

TSQ Quantum Ultra™ triple quadrupole mass spectrometer

4. Data Analysis

A dedicated computational facility for the analysis of Orbitrap MS generated high throughput data is also available along with additional support from AMRF Biocomputing Centre.

This facility includes

- One server and three workstations to handle computationally intensive workloads.
- Three dedicated network storage devices are available for storing raw as well as analyzed MS data

Proteomics Services Offered	What is performed in the facility
In-solution digestion	In-solution protein digest Zip-tip purification Nano-LC-MS/MS analysis Database search and report of results
In-gel digestion	In-gel protein digest Extraction of peptides Zip-tip purification Nano-LC-MS/MS analysis Database search and report of results
Peptide sequencing and Protein Identification	Zip-tip purification Nano-LC-MS/MS analysis Database search and report of results
Custom database search with MASCOT and SEQUEST	Create a custom database with your specific protein sequences to be used for protein ID or modification search
De novo peptide sequencing using PEAKS studio	De novo peptide identification of proteins from species whose genome are not available
Label-free quantification	LFQ based on spectral counting and intensity
Search for additional, custom or non-strand PTMs modifications	Searches performed using user specified

Service Description

5. Softwares

- Proteome Discoverer 1.4 - Identification of proteins using workflow combined with in built database and Mascot server
- PEAKS studio 7 – Protein Identification integrating database search and de novo sequencing
- PINPOINT 1.4 - To analyze and quantify from MRM data
- MASCOT 2.4 - database search engine for the identification of proteins

In-house Applications

- Identification of fungal exoproteome and mycelial proteome
- Identification of proteins in tear samples collected from fungal keratitis patients
- Identifications of proteins in serum from patients at different stages of Diabetic Retinopathy
- Quantification of Complement proteins in tear samples using MRM methodology
- Identification of cross-linked peptides from cross linker treated human and porcine corneal stroma

External Application

As an extended service, we perform mass spectrometry analysis for other Institutes and universities is being performed. More than 500 samples were run and analyzed for outside researchers.

Data Processing, Results and Storage

At the end of the analysis, the user will be provided with the instrument generated RAW data (raw format), analyzed data (.msf and .xlsx format) along with the sample analysis report (.pdf). Depending on the size, data will be sent to the user by email or copied onto a CD or DVD at a minimal fee. All the data will be archived into the facilities Network attached storage and stored for three months.

Publications:

- Aspergillus flavus induced alterations in tear protein profile reveal pathogen-induced host response to fungal infection. Jeyalakshmi Kandhavelu, Naveen Luke Demonte, Venkatesh Prajna Namperumalsamy, Lalitha Prajna, Chitra Thangavel, Jeya Maheshwari Jayapal, Dharmalingam Kuppamuthu. Journal of Proteomics 152 (2017) 13–21.
- Quantitative profiling of tear proteome reveals down regulation of Zinc-α2 glycoprotein in Aspergillus flavus keratitis patients. Niranjana Parthiban, Jayapal JeyaMaheshwari, Namperumalsamy Venkatesh Prajna, Prajna

Lalitha, Kuppamuthu Dharmalingam. Molecular Vision submitted

- Aspergillus flavus induced alterations in tear proteome: Understanding the pathogen induced Host response to fungal infection. Jeyalakshmi Kandhavelu Naveen Luke Demonte , Venkatesh Prajna Namperumalsamy, Lalitha Prajna, Chitra Thangavel, Jeya Maheshwari Jayapal, Dharmalingam Kuppamuthu. Data in Brief (2016)888–894

Name of the Facility : Human Organ Cultured Anterior Segment (HOCAS) Facility for Trabecular Meshwork Studies

Funding Agency : Aravind Eye Foundation (AEF), New York

Contact person : Dr. S. Senthilkumari, Scientist, Department of Ocular Pharmacology

Services Rendered

- Hands-on training on Dissection, HOCAS set up, Drug treatment protocol and data analysis.
- Being used to establish mechanical stress model and steroid-induced ocular hypertension model to investigate the role of Rho A/ROCK signaling (SERB Project) and micro RNA in understanding the pathogenesis of POAG and steroid-induced glaucoma respectively as a part of research projects funded by Indian Funding agencies (RhoA/ROCK signaling –SERB Funding; miRNA in steroid-glaucoma – Wellcome-DBT/India Alliance Project).

Publications:

- Srinivasan Senthilkumari, Ashwinbalaji Soundararajan, Subbiah Ramaswami Krishnadas and Veerappan Muthukkaruppan. Establishment of Human Organ Cultured Anterior Segment, an Ex vivo Model System for Studying the Trabecular Meshwork Outflow Facility in Human Eyes, Indian Journal of Ophthalmology, 2017 (Under submission).

Name of the Facility : High Performance Liquid Chromatography (HPLC) for bio-analysis of Drugs.

Funding Agency : Aravind Medical Research Foundation

Contact person : Dr. S. Senthilkumari, Scientist, Department of Ocular Pharmacology

Services Rendered

- Investigated the ocular pharmacokinetics of voriconazole in aqueous humor of cataract patients (AMRF funded project)
- Estimated the levels of ascorbic acid in aqueous humor, lens and plasma of cataract patients to explore the genetic factors influencing ascorbic acid concentrations (AEH funded project)
- Estimated vitamin A in plasma of pateints with vernal conjunctivitis (AEH funded collaborative study)

- Estimated moxifloxacin, prednisolone, voriconazole, cefazolin and bevacizumab to investigate the human amniotic membrane (HAM) drug reservoir function (AEH funded project)
- Quantified plasma carotenoids (lutein, zeaxanthin, beta carotene and lycopene) as a part of IND-MACAER study funded by Indian Council of Medical Research

Publications

- Yelchuri ML, Madhavi B, Gohil N, Sajeev HS, Venkatesh Prajna N, Srinivasan S. In Vitro Evaluation of the Drug Reservoir Function of Human Amniotic Membrane Using Moxifloxacin as a Model Drug. Cornea. 2017 May;36(5):594-599.

Name of the Facility : AMRF Biocomputing Center (ABC)

Funding Agency : Aravind Medical Research Foundation (AMRF), Madurai.

Science and Engineering Research Board (SERB), Govt. of India.

Department of Biotechnology (DBT), Govt. of India

Contact person : Dr. D. Bharanidharan, Scientist-Bioinformatics,

The AMRF Biocomputing Center (ABC) provides a core computational facility with a reliable infrastructure and framework equipped with Dell T630 Server (With Ubuntu 14.04) and HP DL580R07 (E7) CTO Server, three Dell workstations and five Intel i7-3370 3.5GHz workstations. It comprises of LINUX and Windows based servers and workstations to support interdisciplinary and computational research by developing and maintain computing facilities including data storage, database development and maintenance, algorithm development, analysis software tools, hardware support. It is a multidisciplinary research environment that provides to customize data analysis tailored to the needs of individual research projects across all the research groups and extend this service to others on mutually acceptable terms. In addition, it helps to train manpower by way of workshops and short training courses.

Services Rendered

- Next-generation sequence data processing and analysis: The resource has developed processing and analysis pipelines for illumine and ion data such as
- Clinical exome analysis pipeline for eye disease next-generation sequencing panel
- Exome/Targeted data analysis to detect and filter clinical variants from Next-generation sequencing clinical data of Primary Open Angle Glaucoma patients

- Comparative bacterial and fungal genomics of ocular isolates from keratitis patients to find genome wide differences and mutations and genes associated with drug resistance mechanism and virulence
- Transcriptome analysis of predicting target genes associated with the maintenance of stemness using next-generation RNA sequencing (RNA-seq) data.
- In-house Bioinformatics Pipeline to Identify Pathogenic Variants of Retinoblastoma (RB).
- MicroRNAs profiling and their regulatory role in microbial keratitis
- RNA-seq analysis of saprophyte and corneal isolates of A.flavus at two different growth temperatures
- 16s Metagenomics. The input to the NGS pipeline is either raw reads from the sequencing machines or mapped reads from alignment software.
- Microarray data processing and analysis: This includes background correction, normalization, summarization, quality control, detecting differentially expressed genes, and correlation of gene expression with phenotypes or clinical variables.
- miRNA and mRNA expression analysis of uveal melanoma patients
- Bioinformatics: The resource is available to help investigators with bioinformatics analysis such as pathway and gene function enrichment analysis and gene network analysis.
- A Bioinformatics approach to understand the molecular mechanisms of genetic eye disorders caused by non-synonymous single nucleotide variants (nsSNVs)
- An in silico approach of gene expression level analysis to quantify the aberrance of metabolic pathways in retinal angiogenesis towards early diagnosis and development of personalized medicine
- Database: Services include design and implementation of interactive web applications as well as the underlying database back-ends. Support is available for investigators with problems concerning data acquisition, management, and analysis.
- miRNA database for eye
- Understanding the Molecular Mechanisms of Indian Genetic Eye Diseases: A Bioinformatics Approach and Database Development

- Training: Hands-on training on Mass Spec data analysis and NGS data analysis is during the clinical proteomics workshop and NGS workshop.

Publications

- Hemadevi, B. Vidyarani, M. Lalitha, P. Bharanidharan, D*. (2015) Human Corneal MicroRNA Expression Profile in Fungal Keratitis, Invest Ophthalmol Vis Sci.56:7939–7946.
- Kannan T, Aloysius A, Bharanidharan D, Namrata G, Usha K, Veerappan M and Ayyasamy V. (2015) A stepwise strategy for rapid and cost-effective RB1screening in Indian retinoblastoma patients, J Hum Genet. 60:547-52.
- Bharanidharan D*, Logambiga P, Thirumalai Raj K, Aloysius A A, Usha K, Veerappan M and Ayyasamy V*. (2015) Targeted next generation sequencing of RB1gene for the molecular diagnosis of Retinoblastoma. BMC Cancer. 15:320.

Data in public repository for open access

- Exoproteome of Aspergillus flavus corneal isolates and saprophytes, (2015) Selvam RM, Nithya R, Devi PN, Shree RS, Nila MV, Demonte NL, Thangavel C, Maheshwari JJ, Lalitha P, Prajna NV, Dharmalingam K, ProteomeXchange ID: PXD001296

Name of the facility : Tensile strength analyzer

Funding Agency : Aurolab

Contact person : Mrs. Karpagam; Dr. O.G. Ramprasad

Services rendered

The tensile strength analyzer is an equipment to assess the stiffness and the tensile strength of a material. The material of interest is cut using a dog-bone shaped punch, clamped into the machine and pulled apart with a constant force to determine the stiffness and the maximum load the material can withstand at the break-point (known as tensile strength). Originally the equipment was designed to test the stiffness of the acrylic hydrophilic materials used for the manufacture of intra-ocular lens, polycryl absorbable sutures and other materials. Subsequently, customized clamps and dog-bone punches were designed for use with biological tissues.

The tensile strength analyzer has been used to analyze the stiffness and tensile strength of the cadaver cornea and the diseased keratoconus cornea before and after treatment with a novel chemical cross-linker. The equipment has also been used to determine the tensile strength of scleral tissues. The equipment can be used to determine the tensile strength of any biological tissue with the customized punches and clamps.

(A) Tensile strength analyzer

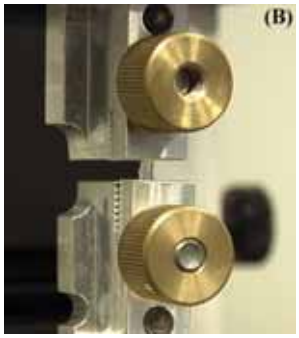

(B) Customized clamps to hold biological tissue

(C) Dog-bone punches to cut the tissue